International School for Advanced Studies - SISSA

Neurobiology Sector

Transient oxidative stress evokes early changes in the functional properties of neonatal rat hypoglossal motoneurons *in vitro*

Thesis submitted for the degree of

"Doctor Philosophiae"

Candidate:

Francesca Nani

Supervisor:

Prof. Andrea Nistri

SISSA, Via Bonomea 265, 34136 Trieste, Italy

Note

The work described in this thesis was carried out at the International School for Advanced Studies, Trieste, between November 2006 and July 2010. All work reported arises from my own experiments and data analysis (electrophysiology) and in collaboration with Alessandra Cifra (immunohistochemistry). Part of the data reported in the present thesis has been published in the following articles:

Cifra, A.[1], Nani, F.[2], Sharifullina, E. & Nistri, A. ([1], [2]: these authors equally contributed to the present study, 2009) A repertoire of rhythmic bursting produced by hypoglossal motoneurons in physiological and pathological conditions. Philos Trans R Soc Lond B Biol Sci., 364, 2493-500.

Nani, F., Cifra, A. & Nistri, A. (2010) Transient oxidative stress evokes early changes in the functional properties of neonatal rat hypoglossal motoneurons in vitro. Eur J Neurosci., 31, 951-66.

Contents

Abbreviations

AHP, afterhyperpolarization;

ALS, amyotrophic lateral sclerosis;

AMPA, α-amino-3-hydroxy-5-methyl-4-isoxazoleproprionic acid;

APV, D-amino-phosphonovalerate;

ARE, antioxidant-response element;

ATF-3, activating transcription factor 3;

BCL2, B-cell lymphoma 2;

BiP, binding immunoglobulin protein;

CHMP2B, charged multivesicular body protein 2B

CNQX, 6-cyano-7-nitroquinoxaline-2,3-dione;

CSF, cerebrospinal fluid;

CytC, cytochrome c;

DHR 123, dihydrorhodamine 123;

DMRC; dorsal medullary reticular column;

dsDNA, double strand DNA;

EAAT2, excitatory amino acid transporter 2;

ER, endoplasmic reticulum;

FUS / TLS, fused-in-sarcoma / translated-in-liposarcoma;

GABA, γ-aminobutyric acid;

GAPDH, glyceraldehyde 3-phosphate dehydrogenase;

GC, guanylate cyclase;

GFAP, glial fibrillary acidic protein;

GLT-1, glutamate transporter-1;

GluR2, glutamate receptor subunit 2;

GSH / GSSG, glutathione reduced and oxidized form;

GST, glutathione S-transferase;

HCN, hyperpolarization-activated cyclic nucleotide-gated channels;

HM, hypoglossal motoneuron;

H_2O_2, hydrogen peroxide;

HO-1, heme oxygenase 1;

IP3R, inositol-1,4,5-trisphosphate receptor;

I_h, hyperpolarization-activated cationic current;

I_{peak}, maximum current amplitude;

$I_{res,}$ residual current;

ITPR2, inositol 1,4,5-triphosphate receptor 2;

mEPSC, miniature excitatory postsynaptic current;

mIPSC, miniature inhibitory postsynaptic current;

NaNP, sodium nitroprusside;

NF-H neurofilament-heavy;

NF-L, neurofilament-light;

NMDA, N-methyl-D-aspartate;

NO, nitric oxide;

NOS, nitric oxide synthase;

NQO1, NAD(P)H:quinone oxidoreductase 1;

Nox, NADPH oxidases;

Nrf2, nuclear erythroid 2-related factor 2;

NTS; nucleus of the solitary tract;

8-OHdG, 8-hydroxy-2′-deoxyguanosine;

$O_2{\cdot}^-$, superoxide radical anion;

${\cdot}OH$, hydroxyl radical;

$ONOO^-$, peroxynitrite;

P1-P5, postnatal day 0-5;

PDI, protein disulfide isomerase;

PI, propidium iodide;

PIC, persistent inward current;

PIC(Ca), persistent calcium current;

PIC(Na), persistent sodium current;

PKA, protein kinase A;

r, correlation coefficient;

Rho 123, rhodamine 123;

R_{in}, cell input resistance;

RNS, reactive nitrogen species;

ROS, reactive oxygen species;

SNAP, S-nitroso-N-acetyl-DL-penicillamine;

SOD1, superoxide dismutase 1;

sPSC, spontaneous postsynaptic current;

TASK, TWIK-Related Acid-Sensitive K^+ channel;

TDP-43, TAR DNA-binding protein 43;

TOM, translocator outer membrane;

τSD, strength-duration time constant;

TTX, tetrodotoxin;

UPR, unfolded protein response;

VAPB, vesicle-associated membrane protein B;

V_h, holding potential under voltage clamp mode;

V_m, membrane potential under current clamp mode;

w.o., washout;

XO, xanthine oxidase.

Abstract

Oxidative stress of motoneurons is believed to be an important contributor to neurodegeneration underlying the familial (and perhaps even the sporadic) form of amyotrophic lateral sclerosis (ALS). This concept has generated numerous rodent genetic models with inborn oxidative stress to mimic the clinical condition. ALS is, however, a predominantly sporadic disorder probably triggered by environmental causes that, upon repeated exposure, ultimately evoke motoneuron degeneration. Thus, it is interesting to understand how wildtype motoneurons react to strong oxidative stress since this response might cast light on the presymptomatic disease stage. The present study used, as a model, hypoglossal motoneurons from the rat brainstem slice to investigate how hydrogen peroxide could affect synaptic transmission and intrinsic motoneuron excitability in relation to their survival. Hydrogen peroxide (1 mM; 30 min) induced an inward current (or membrane depolarization) accompanied by an increase in input resistance, augmented firing and depressed spontaneous synaptic events. Despite enhanced intracellular oxidative processes, there was no early death of motoneurons although most cells became immunopositive for ATF-3, a stress related transcription factor. No astroglia damage was observed. In the presence of hydrogen peroxide, voltage clamp experiments indicated increased frequency of excitatory and inhibitory miniature events, and reduced voltage-gated persistent currents of motoneurons. The global effect of this transient oxidative challenge was to depress the input flow from the premotoneurons to motoneurons that became more excitable due to a combination of enhanced input resistance and impaired spike afterhyperpolarization. Our data, therefore, show previously unreported changes in motoneuron activity associated with cell distress caused by a transient oxidative insult.

Furthermore, as a way of comparison with hydrogen peroxide effects, preliminary experiments were started to characterize changes in motoneuron electrophysiological properties subsequent to application of a nitrosative agent, namely the nitric oxide donor sodium nitroprusside (500 μM; 30 min). These data outlined an action of NO distinct from the one of hydrogen peroxide, indicating that the cellular mechanisms underlying oxidative and nitrosative damage are likely to be different.

Introduction

Amyotrophic lateral sclerosis (ALS) is among the most common adult-onset neurodegenerative diseases. ALS typically develops between 50 and 60 years of age as a relentless, progressive neuromuscular failure, caused by degeneration of both upper motoneurons in the motor cortex and lower motoneurons connecting the spinal cord and brainstem to skeletal muscle fibers, leading to muscle denervation and atrophy. Initial symptoms often present in one motoneuron population, but will spread to contiguous motoneuron groups. Although variants of the disease may apparently affect a discrete motoneuron population, such as only lower motoneurons, upper motoneurons, or bulbar motoneurons (innervating muscles that control speech, chewing, and swallowing), signs of both upper and lower motoneuron dysfunction develop in the majority of patients as the disease progresses. Certain motoneuron populations are much less vulnerable, specifically those in the upper brainstem nuclei that control eye movements and those in Onuf's nucleus in the sacral spinal cord controlling the pelvic floor muscles. The rate of disease progression varies between individuals and can be influenced by the site of onset, but is usually rapid, with an average survival of only 2-3 years from symptom onset. The major cause of death is respiratory failure. ALS pathology is characterized by loss of motoneurons with ubiquitinated inclusions, abnormal mitochondria, and neurofilament aggregates in surviving motoneurons, and glial activation. Riluzole, the only drug currently licensed as a neuroprotective agent for ALS, extends life expectancy by only approximately 3 months (Leigh, 2007).

1. Causes of ALS

The disease cause is unknown in the majority of ALS cases, which are described as being sporadic (SALS), although 5-10 % of cases are genetic and are classified as familial (FALS). The etiology of SALS is largely unknown, and the worldwide incidence of disease is fairly uniform at around 1-2 / 100,000 in most populations (Kurtzke, 1982). The exceptions to this are the Western Pacific island of Guam and the Kii peninsula of Japan, where the incidence has been much higher, possibly linked to an environmental toxin such as β-methylamino-L-alanine (Cox *et al.*, 2003). The prevalence of ALS has also been reported to be increased among Gulf War veterans (Horner *et al.*, 2003; Kasarskis *et al.*, 2009) and in some groups of athletes (Chiò *et al.*, 2005). SALS and FALS are clinically indistinguishable and do not usually develop until middle or later life, so identification of genetic cases is not

straightforward, as a clear family history needs to be documented. Mutations in several genes have now been identified as leading to ALS, and additional loci have also been linked to the disease (Valdmanis & Rouleau, 2008). The first gene to be identified as being mutated in ALS, which accounts for 10-20 % of autosomal dominant FALS cases, was copper / zinc superoxide dismutase (Cu / Zn SOD, SOD1; Rosen *et al.*, 1993). Other genes, mutations of which can lead to adult-onset ALS, include fused-in-sarcoma / translated-in-liposarcoma (FUS / TLS; Kwiatkowski *et al.*, 2009; Vance *et al.*, 2009), TAR DNA-binding protein (TDP-43; Kabashi *et al.*, 2008; Sreedharan *et al.*, 2008), charged multivesicular body protein 2B (CHMP2B; Parkinson *et al.*, 2006), vesicle-associated membrane protein (synaptobrevin-associated protein) B (VAPB; Nishimura *et al.*, 2004), and angiogenin (Greenway *et al.*, 2006), although all of these are less common than SOD1 mutations. Over 140 mutations in the 153 amino acids of the SOD1 protein have been described to date and these are spread throughout all five exons, as well as a small number in untranslated regions (Orrell, 2000; Fig. 1).

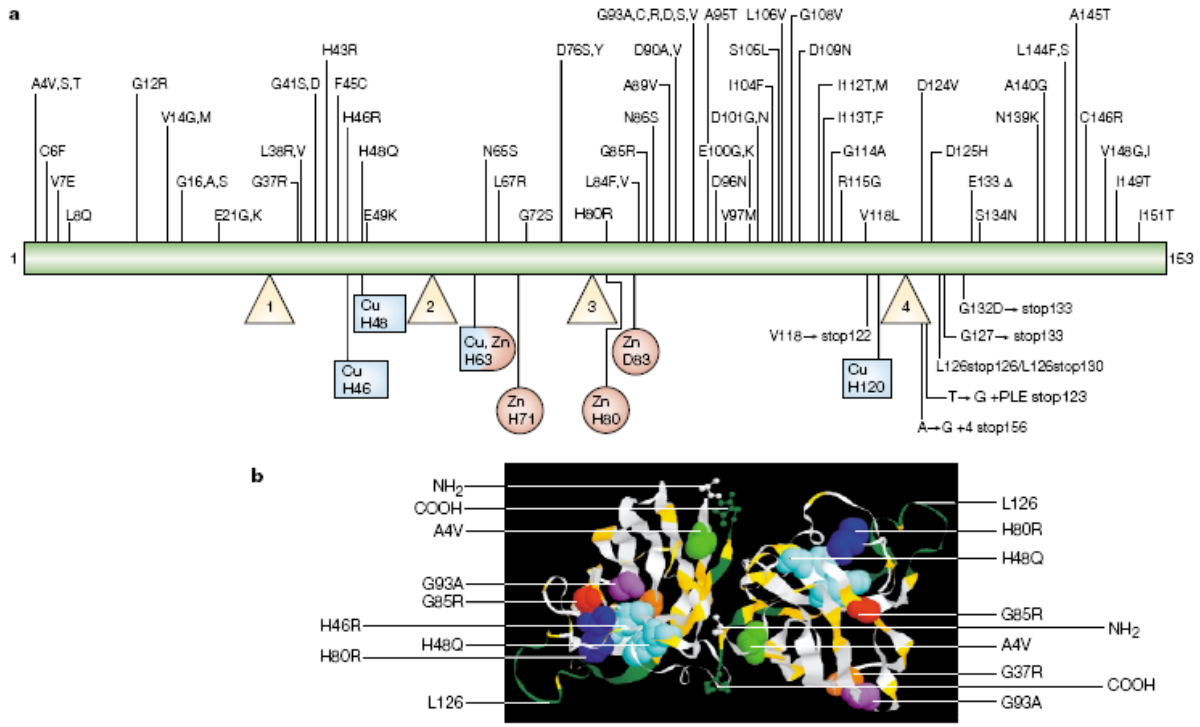

Fig. 1. ALS-causing mutations lie throughout the SOD1 polypeptide. (a) Mutations in the 153-amino-acid superoxide dismutase 1 (SOD1) polypeptide that are known to cause ALS. (b) The positions of these mutations in the three-dimensional structure of crystallized human SOD1 were highlighted using Rasmol (R. Sayle, Biomolecular Structures Group, GlaxoWellcome Research & Development). Mutations are scattered throughout the protein: at turns of the β-barrel, within β-sheets of the β-barrel, within the active site channel, at the dimer interface, and at copper-coordinating residues in the active site. Some mutated

positions are marked with spacing-filling models of the amino-acid side chains. The positions of others are simply coloured yellow in the polypeptide chain. The 20 amino acids of the carboxyl terminus are truncated in several mutants and are coloured in green. The remaining polypeptide backbone is grey (adapted from Cleveland & Rothstein, 2001).

Given the diversity of the physiological functions affected by mutations in these genes, it is generally assumed that the disease classified as "ALS" is the result of defects in a variety of cellular mechanisms. Identification of SOD1 mutations has enabled development of animal and cell culture models, from which much of our understanding of the mechanisms of neurodegeneration in ALS has emerged. These include oxidative stress, excitotoxicity caused by dysregulation of glutamate signaling, mitochondrial dysfunction, endoplasmic reticulum stress, protein aggregation, disruption of the neurofilament network and intracellular trafficking along microtubules, involvement of non-neuronal cells neighboring motoneurons, and defects in RNA processing. The degeneration leads to motoneuron death through a caspase-dependent programmed cell death pathway resembling apoptosis (Sathasivam *et al.*, 2001; Fig. 2).

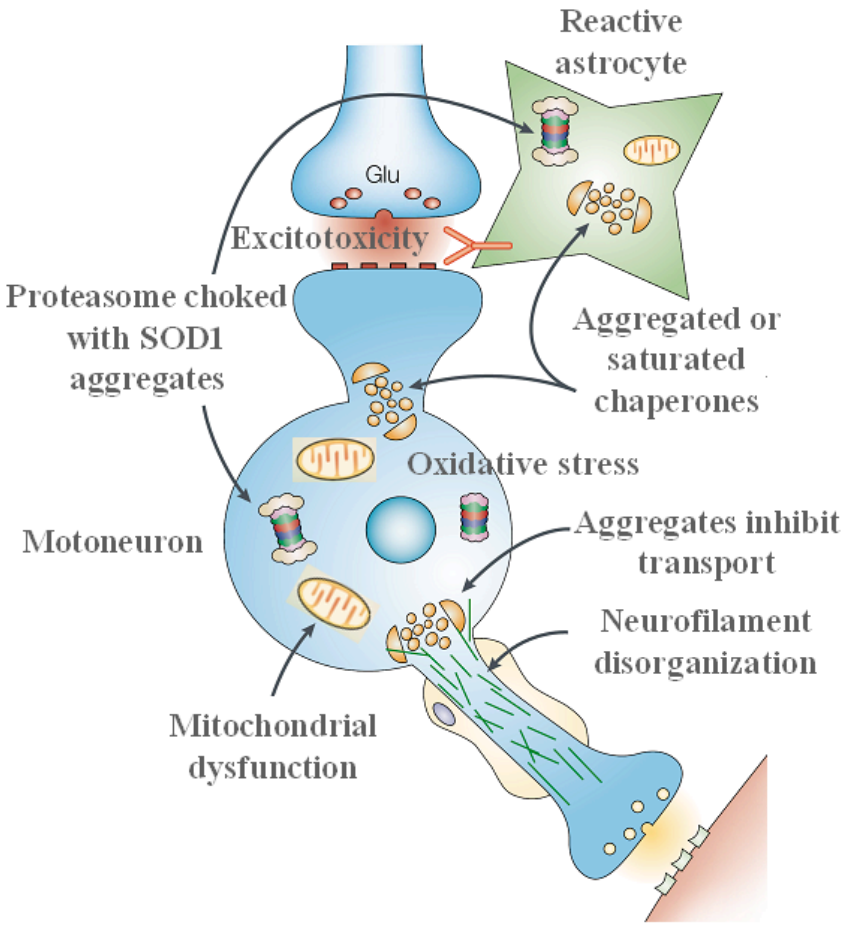

Fig. 2. Schematic representation of putative major mechanisms responsible for ALS neurodegeneration (adapted from Cleveland & Rothstein, 2001).

2. ALS animal models

Mutations of SOD1 are one of the proven causes of ALS in humans, at least in its familial form (Rosen *et al*., 1993; Gurney *et al*., 1994; Ripps *et al*., 1995; Wong *et al*., 1995; Prudencio *et al*., 2009). More than 140 mutations of this enzyme, mostly involving single amino acids replacements, have been associated with cases of FALS (Boillée *et al*., 2006; Bergemalm *et al*., 2006). Murine models incorporating a human mutated hSOD1 gene are, thus, important tools to study the mechanisms involved in FALS pathology (Gurney *et al*., 1994; Cleveland & Rothstein, 2001; Boillée *et al*., 2006). Because FALS and SALS cases are clinically similar, progress in elucidating the mechanisms underlying FALS may provide insight into both forms of the disease. Most work has focused on the $SOD1^{G93A}$ mouse model (high expressor line) overexpressing the dominant missense G93A mutation (Gly93 to Ala amino acid substitution) of Cu / Zn superoxide dismutase human gene (Gurney *et al*., 1994). These mice develop a disease with a relatively short course and a pathology mainly characterized by severe vacuolar degeneration of motoneurons and their processes. A similar vacuolar pathology is displayed by mice expressing high levels of $SOD1^{G37R}$ mutants (Wong *et al*., 1995). However, recent work (Bergemalm *et al*., 2006) has shown that high levels of hSOD1 expression can cause artificial loading of SOD1 enzyme in mitochondria and cause effects potentially misleading for an understanding of human ALS pathology. Other models expressing a lower copy number of the mutant hSOD1 gene and surviving longer include the $SOD1^{G93A}$ low expressor mice, which survive 6-7 months (Dal Canto & Gurney, 1997) and the $SOD1^{G85R}$ transgenic mice expressing the G85R mutation with GLY85 to arginine amino acid substitution (Bruijn *et al*., 1997; 1998). The homozygous $SOD1^{G85R}$ (line 148) survives 7.5-8 months (Bruijn *et al*., 1997) and the heterozygous $SOD1^{G85R}$ survives 10-12 months (Williamson & Cleveland, 1999). In these animals, anterior horn cell depletion, atrophy, astrocytosis, axonal swellings, and the presence of numerous ubiquitinated Lewy-like bodies are the main pathological features, while vacuolar pathology is minimal. These mutants, with ALS symptoms more resembling human FALS, may be preferable models for the study of this pathogenesis (Jonsson *et al*., 2004; Bergemalm *et al*., 2006). Behavioral tests on a strain of $SOD1^{G85R}$ homozygous mice (line 148) have shown delayed development of reflex responses during the first postnatal week (Amendola *et al*., 2004; Durand *et al*., 2006), together with an abnormal dendritic branching increasing the surface area of the mutant motoneurons (Amendola *et al*., 2007; Amendola & Durand, 2008) at the same age. In this

mutant line, astrocytes seem to be the primary target leading to motoneuron degeneration (Bruijn *et al*., 1997). However, some types of experimental manipulations have been difficult in ALS mice because of their innate size limitations. It has been almost impossible, for example, to analyze cerebrospinal fluid (CSF) from the ALS mice, even at single time points. It has also been very difficult to use therapies that involve repeated administration of compounds into the CSF. There is only a single report of pump-mediated delivery of drugs to the CSF of the ALS mice, and that approach was intraventricular rather than intrathecal (Li *et al*., 2000); it is likely that intrathecal administration will produce significantly better therapeutic levels of compounds at the spinal cord level than will the intraventricular approach (Gurney *et al*., 2000). It has also been difficult to obtain sufficient tissue to perform extensive biochemical analyzes, such as investigations of posttranscriptional modifications of proteins like SOD1 itself during disease progression. For these reasons, rat models of ALS have been developed by expressing a human SOD1 transgene (Nagai *et al*., 2001; Howland *et al*., 2002; Aoki *et al*., 2005). Rats that express a human SOD1 transgene with two different ALS-associated mutations (G93A and H46R) develop striking motoneuron degeneration and paralysis. As in the human disease and transgenic ALS mice, pathological analysis demonstrates selective loss of motoneurons in the spinal cords of these transgenic rats. In spinal cord tissues, this is accompanied by activation of apoptotic genes triggered by the mutant SOD1 protein *in vitro* and *in vivo*. These animals provide additional support for the proposition that motoneuron death in SOD1-related ALS reflects one or more acquired, neurotoxic properties of the mutant SOD1 protein (Nagai *et al*., 2001). In $SOD1^{G93A}$ rat, motoneuron disease depends on high levels of mutant SOD1 expression, increasing from 8-fold over endogenous SOD1 in the spinal cord of young presymptomatic rats to 16-fold in end-stage animals. Disease onset in these rats is early, ≈ 115 days, and disease progression is very rapid thereafter with affected rats reaching end-stage on average within 11 days. Pathological abnormalities include vacuoles initially in the lumbar spinal cord and subsequently in more cervical areas, along with inclusion bodies that stain for SOD1, Hsp70, neurofilaments, and ubiquitin. Vacuolization and gliosis are evident before clinical onset of disease and before motoneuron death in the spinal cord and brainstem. Focal loss of the glutamate excitatory amino acid transporter 2 (EAAT2) in the ventral horn of the spinal cord coincides with gliosis, but it appears before motoneuron / axon degeneration. At end-stage disease, gliosis increases and EAAT2 loss in the ventral horn exceeds 90 %, suggesting a role for this protein in the events leading to cell death in ALS (Howland *et al*., 2002). According

to Lladó *et al*. (2006), facial and hypoglossal motoneurons in the mutant SOD1^{G93A} rats (Howland *et al*., 2002) appear to be spared, especially when compared with the 45 % loss of C3-C5 cervical motoneurons. The loss of trigeminal motoneurons is also very modest (12 %). Interestingly, Haenggeli and Kato (2002) have observed a significant loss of motoneurons in the trigeminal, facial, and hypoglossal motor nuclei with sparing of the motoneurons in the oculomotor / trochlear nuclei when studying the SOD1^{G93A} mouse. They have pointed out that these findings are consistent with those seen in human ALS (DePaul *et al*., 1988). This suggests that the rat model differs not only from the murine counterpart, but also from some cases of human ALS. One possible explanation for these differences is that the rapidity of motor decline from onset of disease to end-stage is significantly shorter in the rat and thus the sparing of cranial nuclei may be more apparent than real since the disease progresses from hindlimb to forelimb paresis and to respiratory decline too rapidly for the cranial nuclei to undergo a more delayed degeneration. The presence of vacuolar pathology observed within the neuropil of the cranial nuclei suggests that the typical SOD1^{G93A} pathology is already present in the region, even if motoneurons have not yet degenerated (Lladó *et al*., 2006).

3. Evidence for oxidative stress in ALS

Oxidative stress arises from an imbalance between the production of reactive oxygen species (ROS) and the ability of the system to remove or repair the damage. Cellular ROS arise as by-products of aerobic metabolism (Coyle & Puttfarcken, 1993; Lenaz, 1998; Halliwell & Gutteridge, 1999), mostly due to leakage of electrons from the mitochondrial respiratory chain, resulting in incomplete reduction of molecular oxygen during oxidative phosphorylation, to produce the superoxide radical anion ($O_2^{\cdot -}$) and hydrogen peroxide (H_2O_2). A small proportion of cellular ROS is produced by other cellular oxidative enzymes, including xanthine oxidase in the cytoplasm and the oxidase activity of the cytochrome P450 system in the endoplasmic reticulum. Free radicals such as superoxide and nitric oxide ($NO^{\cdot}$) are also produced as second messengers, particularly by immune cells. Neither superoxide nor hydrogen peroxide is highly reactive, but each one undergoes further reaction to produce more potent oxidants. Superoxide reacts rapidly with nitric oxide, a weak oxidant produced by nitric oxide synthase (NOS), to produce peroxynitrite ($ONOO^-$; Pryor & Squadrito, 1995; Beckman & Koppenol, 1996), whereas hydrogen peroxide slowly decomposes to the highly

reactive hydroxyl radical (·OH) in a process that can be catalyzed by reduced metal ions such as Fe^{2+} in the Fenton reaction (Fig. 3).

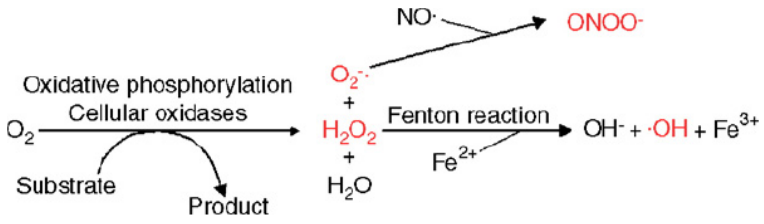

Fig. 3. Production of reactive oxygen species. Incomplete reduction of molecular oxygen during oxidative phosphorylation and other oxidative reactions leads to production of superoxide radicals ($O_2^{\cdot -}$) and hydrogen peroxide (H_2O_2). Reaction between superoxide and nitric oxide (NO) produces peroxynitrite ($ONOO^-$). Hydrogen peroxide is converted to hydroxyl radical (·OH) by cytosolic transition metal cations in the Fenton reaction. ROS are shown in red (adapted from Barber *et al.*, 2006).

Both peroxynitrite and hydroxyl radicals are highly reactive oxidizing agents, capable of damaging proteins, lipids, and DNA. Such a damage includes changing protein conformation, altering cellular membrane dynamics by oxidation of unsaturated fatty acids, and alterations in DNA and RNA species (Fig. 4).

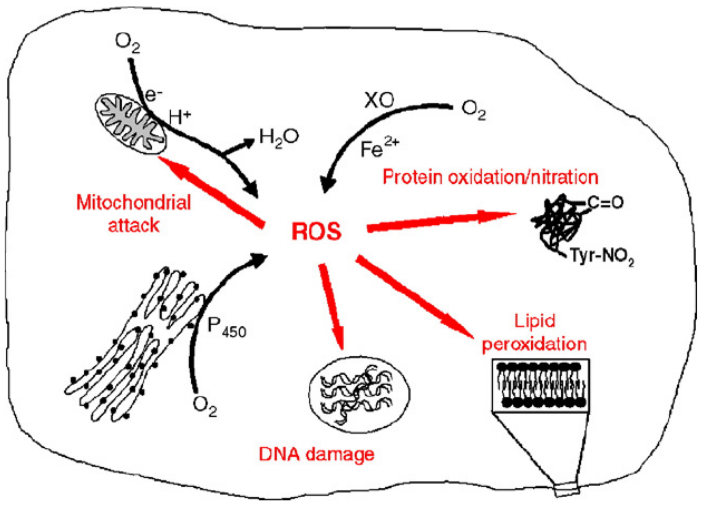

Fig. 4. Sources of reactive oxygen species and their targets. ROS are produced during oxidative phosphorylation in mitochondria, by oxidative enzymes including cytochrome P450 in the endoplasmic reticulum, and by xanthine oxidase (XO) and reduced metal ions in the cytosol. Cellular targets attacked by ROS include DNA, proteins, membrane lipids, and mitochondria (adapted from Barber *et al.*, 2006).

Multiple pathological studies have reported evidence of increased oxidative stress in ALS postmortem tissue compared to control samples. Elevated protein carbonyl levels have been

shown in the spinal cord (Shaw *et al.*, 1995) and motor cortex (Ferrante *et al.*, 1997) from SALS cases, and increased 3-nitrotyrosine levels, a marker for peroxynitrite-mediated damage, are found within spinal cord motoneurons in both SOD1-FALS and SALS patients (Abe *et al.*, 1995; Beal *et al.*, 1997). Immunoreactivity to the brain and endothelial forms of NOS, but not the inducible form, is also elevated in ALS motoneurons relative to controls (Abe *et al.*, 1997), suggesting alterations in reactive nitrogen species (RNS) as well as ROS. Markers for lipid oxidation are detected in spinal cord from SALS patients, but are absent in control spinal cords (Shibata *et al.*, 2001). Levels of 8-hydroxy-2′-deoxyguanosine (8-OHdG), a marker of oxidized DNA, are elevated in whole cervical spinal cord from ALS patients (Fitzmaurice *et al.*, 1996) and are most prominent within the ventral horn (Ferrante *et al.*, 1997). Studies using CSF from ALS patients enable measurement of oxidative stress markers at earlier disease stages, rather than simply looking at the end-stage. Such studies have reported elevated levels of 8-OHdG (Bogdanov *et al.*, 2000; Ihara *et al.*, 2005), 4-hydroxynonenal (a marker of lipid peroxidation; Smith *et al.*, 1998; Simpson *et al.*, 2004), and ascorbate free radical (Ihara *et al.*, 2005) in CSF samples from ALS patients. Increased 3-nitrotyrosine levels have also been measured in ALS patient CSF (Tohgi *et al.*, 1999), although a subsequent study has shown 3-nitrotyrosine to be elevated in CSF from a minority of ALS patients only, and the mean level is not significantly different from that found in control CSF samples (Ryberg *et al.*, 2004). Transgenic mouse and cell culture models of ALS based on mutant SOD1 recapitulate the oxidative damage to protein, lipid, and DNA observed in the human disease (Ferrante *et al.*, 1997b; Andrus *et al.*, 1998; Liu *et al.*, 1998; Liu *et al.*, 1999; Cookson *et al.*, 2002; Poon *et al.*, 2005; Casoni *et al.*, 2005; Zimmerman *et al.*, 2007; Barber *et al.*, 2009), with mutant SOD1 being one of the most severely oxidized proteins identified (Andrus *et al.*, 1998).

4. Sources of oxidative stress in ALS

Since the upstream cause of the disease is unknown, researchers are limited to working on the pathogenethic mechanisms implicated in disease progression. This has led to a debate as to whether oxidative stress is the primary cause of degeneration or whether it is merely a consequence of some other toxic insult. One of the few clearly identified risk factors for developing ALS is age, with few cases being diagnosed before the age of 50. ROS production is known to increase with age, primarily due to increased leakage from the mitochondrial respiratory chain, and is believed to be a major cause of aging (Beal, 2002;

Lenaz *et al*., 2002; Genova *et al*., 2004). Although this is unlikely to be the sole cause of disease initiation, in some cases it may be what tips the homeostatic control mechanisms from coping with a toxic insult into a cycle of cellular injuries that result in motoneuron degeneration. The identification of SOD1 mutations has, therefore, revealed a clear association between oxidative stress and disease onset. Several mechanisms for mutant SOD1 toxicity have been proposed based on altered dismutase activity: (1) loss of dismutase function leading to increased levels of superoxide, which can react with nitric oxide to produce peroxynitrite (Beckman *et al*., 1993; Deng *et al*., 1993); (2) a dominant negative mechanism in which the mutant SOD1 protein not only is inactive, but also inhibits the function of normal SOD1 expressed by the normal allele (Rosen *et al*., 1993); or (3) increased SOD1 activity leading to increased hydrogen peroxide and hydroxyl radical levels (Rosen *et al*., 1993). However, subsequent investigations have revealed that the mechanism for mutant SOD1 toxicity is not so simple. Although some mutations do reduce the dismutase activity of SOD1 (such as A4V and G85R; Borchelt *et al.*, 1994), other mutants (such as G37R and G93A) retain full dismutase activity (Borchelt *et al.*, 1994; Yim *et al.*, 1996). Additionally, a SOD1 knockout mouse does not develop ALS (Reaume *et al.*, 1996), and increasing or decreasing levels of wild-type SOD1 also has no effect on mutant SOD1-related ALS (Bruijn *et al.*, 1998). It is, therefore, now widely accepted that loss of SOD1 dismutase activity is not sufficient to cause disease and that the mutated SOD1 is toxic through an unknown gain of function. A variety of aberrant oxidative reactions catalyzed by mutant SOD1 have been proposed to contribute to this new toxic function (Fig. 5). These generally assume that mutated SOD1 has a more open conformation than the wild-type protein, enabling substrates other than superoxide to enter the active site and react with the copper and zinc ions contained within. Normally, SOD1 catalyzes dismutation of superoxide radicals to hydrogen peroxide and oxygen in a two-step redox reaction involving reduction and reoxidization of the copper ion in the active site of the dimeric protein. However, SOD1 has also been reported to act as a peroxidase, either catalyzing the reverse of its normal dismutase reaction or using the hydrogen peroxide produced in the dismutation as a substrate to produce hydroxyl radicals through the Fenton reaction (Yim *et al.*, 1990; Yim *et al.*, 1993).

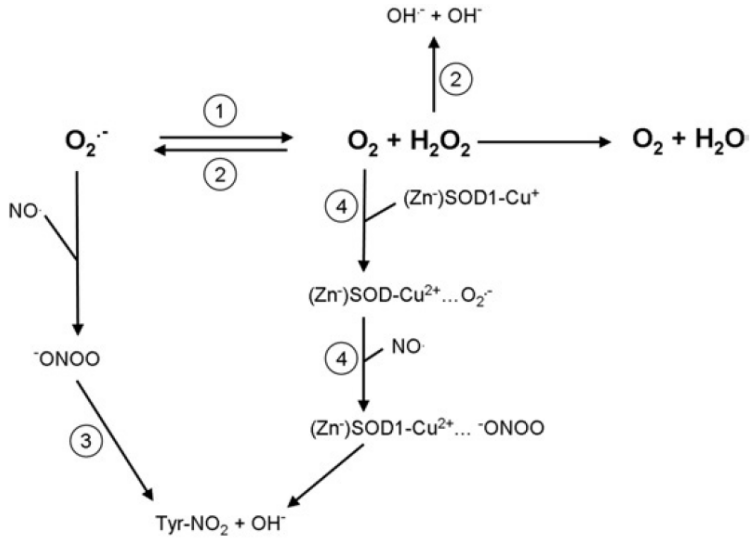

Fig. 5. Summary of SOD1 activity. (1) Normal dismutase activity of SOD1, converting superoxide into oxygen and hydrogen peroxide. (2) Peroxidase activity catalyzing the reverse of the dismutase reaction or using the hydrogen peroxide produced in the dismutation as a substrate to produce hydroxyl radicals through the Fenton reaction. (3) Superoxide reacts with nitric oxide to produce peroxynitrite, which is used by SOD1 to cause nitration of tyrosine residues within proteins. (4) Zinc-deficient SOD1 is reduced by reducing agents other than superoxide (e.g., ascorbate and glutathione). The reduced SOD1-Cu^{+} can produce superoxide in the reverse of its usual dismutase reaction, which reacts with nitric oxide within the active site to produce peroxynitrite, which then causes tyrosine nitration (adapted from Barber & Shaw, 2010).

The ALS-causing mutants $SOD1^{A4V}$ and $SOD1^{G93A}$ are reported to have enhanced peroxidase activity both *in vitro* and *in vivo* (Wiedau-Pazos *et al.*, 1996; Roe *et al.*, 2002), although another study has found no differences between the peroxidase activity of wild-type SOD1 and the same SOD1 mutants (Singh *et al.*, 1998), casting doubt on the contribution of peroxidase activity to mutant SOD1-mediated ALS. Alternatively, many ALS-associated SOD1 mutants have been reported to show altered zinc binding (Smith & Lee, 2007), and the geometry of zinc-deficient SOD1 allows reducing agents other than superoxide (for example, ascorbate and glutathione) to react rapidly with the oxidized Cu^{2+} at the active site (Lyons *et al.*, 1996; Crow *et al.*, 1997; Roberts *et al.*, 2007). It has been proposed that the reduced SOD1-Cu^{+} can produce superoxide in the reverse of its usual dismutase reaction, which reacts with nitric oxide within the active site to produce peroxynitrite (Estevez *et al.*, 1999), which then causes tyrosine nitration. In support of this, zinc deficiency in $SOD1^{G93A}$ mice accelerates disease progression, whereas moderate zinc supplementation delays death (Ermilova *et al.*, 2005). However, if peroxynitrite contributed significantly to disease progression, it would be predicted that decreasing nitric oxide level, which is required for

production of peroxynitrite, would alter the disease course. Deletion of either neuronal or inducible nitric oxide synthase has been reported to have no effect on disease progression of mutant SOD1 mice (Facchinetti *et al.*, 1999; Son *et al.*, 2001; Bruijn *et al.*, 2004), casting doubt on the role of zinc deficiency in mutant SOD1 pathogenesis. Other studies have shown that enzymatically inactive SOD1 is also capable of causing motoneuron degeneration; depleting copper loading into SOD1 by deletion of the copper chaperone for SOD1 leads to marked reduction of SOD1 activity, but has no effect on disease onset, progression, or pathology of $SOD1^{G93A}$, $SOD1^{G37R}$, or $SOD1^{G85R}$ mutant mice (Subramaniam *et al.*, 2002). Similarly, abolishing the copper-binding site by mutating the four histidine residues that hold the copper ion in the active site (including the two disease-causing mutations H46R and H48Q, which have previously been described in patients) produces a completely inactive protein, but still causes motoneuron disease similar to other mouse models of ALS (Wang *et al.*, 2003). This suggests that mutant SOD1 may induce oxidative stress via an unknown mechanism beyond its own catalytic activity.

Microarray studies of motoneuronal cells expressing mutant SOD1 report down-regulation of genes involved in the antioxidant response, including the transcription factor Nrf2 (nuclear erythroid 2-related factor 2), several members of the glutathione S-transferase family, and two peroxiredoxins (Kirby *et al.*, 2005). Reduced Nrf2 messenger RNA (mRNA) and protein expression has more recently been reported in spinal cord neurons from ALS patients (Sarlette *et al.*, 2008). Activation of Nrf2 leads to its translocation from the cytoplasm to the nucleus, where it interacts with the antioxidant-response element (ARE) enhancer sequence to increase expression of proteins involved in antioxidant defense systems (Nguyen *et al.*, 2009; Fig. 6). Nrf2 is not only involved in inducible gene expression in response to elevated oxidative stress, but is also responsible for low-level constitutive activation of the ARE, driving the basal expression of antioxidant enzymes in unstressed conditions (Nguyen *et al.*, 2009). The promoter region of the Nrf2 gene itself contains an ARE sequence, so Nrf2 may regulate its own expression levels (Kwak *et al.*, 2002); activation of Nrf2 leads to increased Nrf2 production, thereby enlarging the cytosolic pool of Nrf2 available for future activation. Although it is currently unclear how Nrf2 expression comes to be down-regulated in ALS patients, it should be noted that cellular Nrf2 levels decline by over 50% in old rats (24 months) relative to young rats (3 months; Suh *et al.*, 2004). Given that increased age is one of the major known risk factors for developing ALS, it seems conceivable that the mechanism(s) involved in the age-related down-regulation of Nrf2 may also contribute to the

down-regulation observed in ALS patients. Down-regulation of Nrf2 expression in ALS may reduce the cell's ability to remove ROS generated through normal cellular metabolism, resulting in a gradual increase in oxidative stress over time. These findings suggest that increasing Nrf2 activity may represent a novel therapeutic goal.

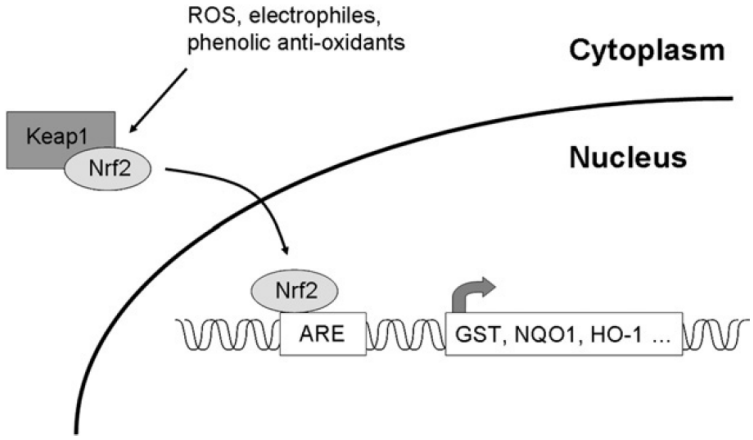

Fig. 6. Nrf2-ARE signaling pathway. Nrf2 is held in the cytoplasm by Keap1. Upon activation, Keap1 releases Nrf2, which translocates to the nucleus and binds to the ARE, thereby increasing expression of antioxidant proteins such as glutathione S-transferase (GST), NAD(P)H:quinone oxidoreductase 1 (NQO1), and heme oxygenase 1 (HO-1). Reduced Nrf2 mRNA and protein expression in motoneurons may contribute to the increased oxidative stress observed in ALS (adapted from Barber & Shaw, 2010).

A novel mechanism through which mutant SOD1 might lead to ALS via microglia has recently been described (Harraz *et al.*, 2008; Boillée & Cleveland, 2008). Although expression of mutant SOD1 restricted to microglia is not sufficient to induce motoneuron degeneration in mice, wild-type microglia slows motoneuron loss and disease progression in mice expressing mutant SOD1, suggesting that microglia may not contribute to disease onset, but does influence disease progression (Beers *et al.*, 2006; Boillée *et al.*, 2006). A mechanism for the role of microglial mutant SOD1 has been reported, whereby mutant SOD1 increases microglial superoxide production by NADPH oxidases (Nox). Nox enzymes are transmembrane proteins that, upon activation, reduce oxygen to superoxide (Bedard & Krause, 2007). They have important roles in host defense, inflammation, cellular signaling, gene expression, cell growth and senescence, and cell death. However, increased Nox activity can be pathogenic, and Nox2 is up-regulated in both SALS patients and $SOD1^{G93A}$ mutant mice, and deletion of either Nox1 or Nox2 extends survival in $SOD1^{G93A}$ mice (Wu *et al.*, 2006; Marden *et al.*, 2007). SOD1 has recently been reported to stabilize Rac1-GTP in the activated Nox2 complex, enabling the Nox2 complex to produce superoxide and other

ROS derived from superoxide (Fig. 7). Mutant SOD1 is found to lock Rac1 in its active, GTP-bound form, thereby prolonging Nox2 activation and increasing ROS production, which in turn causes damage to nearby neurons (Harraz *et al.*, 2008; Boillée & Cleveland, 2008). Although this mechanism neatly fits the available data for a toxic gain of function in mutant SOD1 exerting neurotoxic effects through microglia, it should be noted that enzymatically inactive demetallated SOD1 is incapable of binding Rac1, suggesting that this mechanism may not be common to all ALS-causing SOD1 mutations.

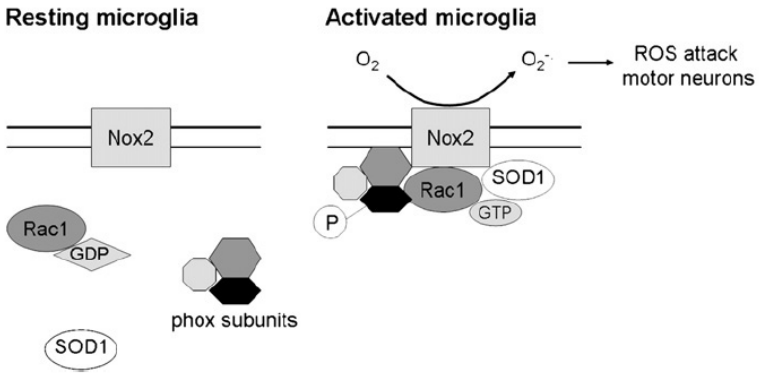

Fig. 7. Role of SOD1 in ROS production by Nox2 in activated microglial cells. In resting microglia, inactive Nox2 is membrane bound and phox subunits, Rac1-GDP, and SOD1 are all cytosolic. In activated microglia, Nox2 becomes activated by phosphorylated phox subunits and Rac1-GTP, resulting in production of superoxide. SOD1 has recently been shown to stabilize Rac1-GTP in the activated complex, and mutant SOD1 locks Rac1 in its active, GTP-bound form, thereby prolonging Nox2 activation and increasing ROS production, which in turn causes damage to nearby neurons (adapted from Barber & Shaw, 2010).

5. Cross talk between oxidative stress and other pathogenic mechanisms

The pathogenic processes involved in ALS are complex, multifactorial, and incompletely understood. What is clear is that motoneuron death occurs not as the result of a single insult, but rather through a combination of mechanisms including not only oxidative stress, but also excitotoxicity, mitochondrial dysfunction, endoplasmic reticulum stress, protein aggregation, cytoskeletal dysfunction, involvement of non-neuronal cells, and defects in RNA processing and trafficking. Given the complexity of the disease it is therefore not surprising that dissecting cause and effect is not a simple matter. Oxidative stress, whether as a primary cause of disease or a secondary consequence, has been implicated in many of these processes (Fig. 8).

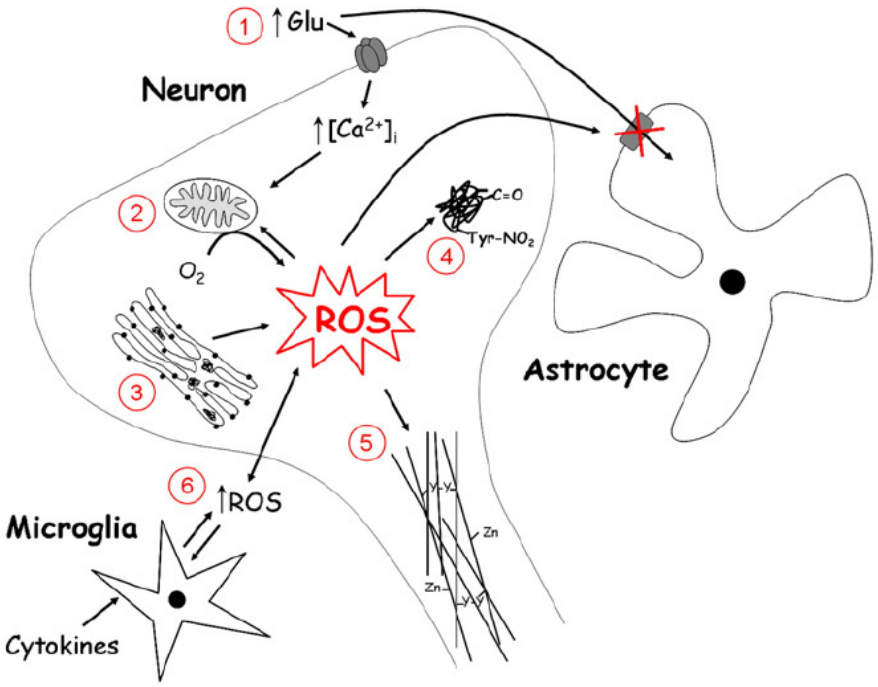

Fig. 8. Oxidative stress can exacerbate other neurodegenerative mechanisms in ALS. (1) Glutamate excitotoxicity increases intracellular calcium levels, which are buffered by mitochondria leading to increased ROS production. ROS can then inhibit glutamate uptake into glial cells, thereby increasing extracellular glutamate levels. (2) The high energy demands of the motoneuron are met by mitochondria, but the leaky respiratory chain means that ROS are also produced. (3) Prolonged activation of the unfolded protein response in the endoplasmic reticulum increases ROS production. (4) Aberrant oxidative reactions catalyzed by mSOD1 increase production of the highly reactive peroxynitrite and hydroxyl radicals, causing nitration and aggregation of proteins including mSOD1 itself. (5) ROS can attack neurofilament subunits, causing dityrosine cross-link formation and aggregation of neurofilament subunits. Zinc binding to neurofilaments could deplete zinc binding to mSOD1, leading to aberrant SOD1 activity and ROS production. (6) ROS can also cross the cell membrane and activate microglia, which respond by releasing cytokines and further ROS. The numbering is for illustrative purposes only and does not imply any particular order (adapted from Barber & Shaw, 2010).

5.1 Glutamate-mediated excitotoxicity

Over the past decade, studies have suggested a potential role for glutamate excitotoxicity in the pathogenesis of ALS. Glutamate is the major excitatory neurotransmitter released from presynpatic nerve terminals, with subsequent diffusion across the synaptic cleft and activation of specific postsynaptic receptors, particularly the ionotropic N-methyl-D-aspartate (NMDA) receptors and α-amino-3-hydroxy-5-methyl-4-isoxazoleproprionic acid (AMPA) receptors. The excitatory signal is terminated upon removal of glutamate from the synaptic cleft by specific glutamate reuptake transporters located on both neurons and astrocytes (Heath & Shaw, 2002). Excitotoxicity occurs when the balance between release

and reuptake of glutamate is disturbed, resulting in increased synaptic glutamate concentrations and excessive stimulation of glutamate receptors (Heath & Shaw, 2002). A significant reduction in the expression of EAAT2, the main astrocytic glutamate transporter, is reported in the motor cortex and spinal cord of ALS patients, with oxidative reactions inactivating EAAT2 (Rothstein et *al*., 1995). Reduced expression of GLT-1 (glutamate transporter-1, equivalent to human EAAT2) and decreased function of the Na^+-dependent glutamate transporters on astrocytes have also been reported in the transgenic SOD1 mouse models (Bruijn *et al.*, 1997). Recently, activation of caspase-1, which normally inhibits the EAAT2 transporter, is found in the SOD1 mouse model prior to onset of motoneuron degeneration and clinical features of ALS (Gibb *et al.*, 2007). However, the loss of EAAT2 appears to be a delayed event in motoneuron degeneration rather than being a primary cause. Other mechanisms, particularly SOD1 aggregation and caspase-3 activation, may seem to be more important (Bruijn *et al.*, 1997; Guo *et al.*, 2003).

Turning to postsynaptic processes, increased expression of the NMDA receptor, permeable to influx of Na^+ and Ca^{2+}, along with expression of AMPA receptors containing an unedited GluR2 subunit, have been reported in ALS (Williams *et al*., 1997; Van Damme *et al*., 2002). The GluR2 subunit regulates AMPA receptors Ca^{2+} permeability and absence of this subunit increases Ca^{2+} permeability of these receptors (Hollmann *et al*., 1991). Moreover, the clinical benefit of riluzole, an inhibitor of glutamate release, in ALS patients lends further support for glutamate-mediated excitotoxicity. A number of cell-specific features of motoneurones may render them vulnerable to glutamate toxicity. First, motoneurones preferentially express AMPA receptors lacking the functional GluR2 subunit and thereby rendering them more permeable to Ca^{2+} influx (Williams *et al*., 1997; Van Damme *et al*., 2002). Secondly, motoneurones vulnerable to degeneration lack the intracellular expression of Ca^{2+} binding proteins parvalbumin and calbindin, both required to buffer intracellular Ca^{2+}. Recently, increased expression of the inositol 1,4,5-triphosphate receptor 2 (ITPR2) gene is reported in ALS (van Es *et al.*, 2007). The ITPR2 is involved in glutamate-mediated neurotransmission, with stimulation of glutamate receptors resulting in binding of inositol 1,4,5-triphosphate to ITPR2, which subsequently increases intracellular calcium, and ultimately leads to apoptosis.

Regarding the cross talk between oxidative stress and excitotoxicity, exposure to ROS has been demonstrated to be sufficient to reduce glutamate uptake through glutamate transporters on both glial and neuronal cells (Volterra *et al.*, 1994; Trotti *et al.*, 1996, 1998; Rao *et al.*, 2003). Furthermore, increased calcium uptake into motoneuron mitochondria, following

AMPA or kainate application, triggers increased ROS generation (Carriedo *et al.*, 2000). AMPA / kainate-treated motoneurons release these ROS into the extracellular milieu at concentrations sufficient to induce oxidation and disrupt glutamate uptake in neighboring astrocytes, thus creating a vicious cycle of increasing oxidative stress and excitotoxicity that ultimately leads to motoneuron degeneration (Rao *et al.*, 2003; Rao & Weiss, 2004).

5.2 Mitochondrial dysfunction

Numerous studies have focused on the role of the mitochondrion in the pathogenesis of ALS. Evidence of mitochondrial dysfunction in ALS patients includes clusters of abnormal mitochondria and morphological defects identified within mitochondria of skeletal muscles and intramuscular nerves in human SALS cases (Afifi *et al.*, 1966; Atsumi, 1981). In such cases biochemical analyses have delineated defects in the respiratory chain complexes I and IV in muscle (Wiedemann *et al.*, 1998), and elevated levels of mitochondrial calcium (Siklos *et al.*, 1996) in muscle and spinal cord. In ALS mice, the main morphological evidence for mitochondrial pathology is the presence of vacuolated mitochondria (for example, in the G93A and G37R transgenic lines). In the $SOD1^{G93A}$ mice, mitochondrial vacuoles derived from a detachment between the inner and the outer membrane (Higgins *et al.*, 2003) appear early, and drastically increase in number and volume as the disease progresses (Kong & Xu, 1998; Bendotti *et al.*, 2001; Sasaki *et al.*, 2004).

In vitro and *in vivo* studies further point to mitochondrial defects in ALS mice. The expression of mutant SOD1 in neuronal cell lines or in cultured primary motoneurons depolarizes mitochondria (Jung *et al.*, 2002; Rizzardini *et al.*, 2006), impairs calcium homeostasis (Damiano *et al.*, 2006) and reduces ATP production (Menzies *et al.*, 2002). Similarly, $SOD1^{G93A}$ mice show reduced respiratory chain activity and reduced ATP synthesis that increase in severity with disease progression. Whether mitochondrial dysfunction and pathology represent primary or secondary pathological events is unknown, as mitochondrial abnormalities can both result from and cause oxidative toxicity. In either circumstance, the pathological mitochondria could mediate cell death by releasing calcium into the cytoplasm, producing inadequate levels of ATP and triggering apoptosis (Fig. 9 a). It is likely that the mitochondrial function modifies the course of motoneuron degeneration. In ALS mice, inhibition of manganese superoxide dismutase (a mitochondrial dismutase) accelerates disease progression. Conversely, the disease is slowed by interventions that improve mitochondrial function - for example, creatine, which inhibits the opening of the

mitochondrial transition pore, and minocycline, which blocks the egress of cytochrome c (Klivenyi *et al.*, 1999; Zhu *et al.*, 2002). Several observations have indicated that mutant SOD1 could directly damage mitochondria. It is evident that a fraction of SOD1 is localized to the mitochondrion (Higgins *et al.*, 2002; Mattiazzi *et al.*, 2002; Okado-Matsumoto & Fridovich, 2002; Pasinelli *et al.*, 2004; Liu *et al.*, 2004). *In vitro* studies of differentially targeted SOD1 reveal that mutant SOD1 more potently triggers cell death when localized to mitochondria where it forms intra-mitochondrial protein aggregates (Takeuchi *et al.*, 2002; Fig. 9 b).

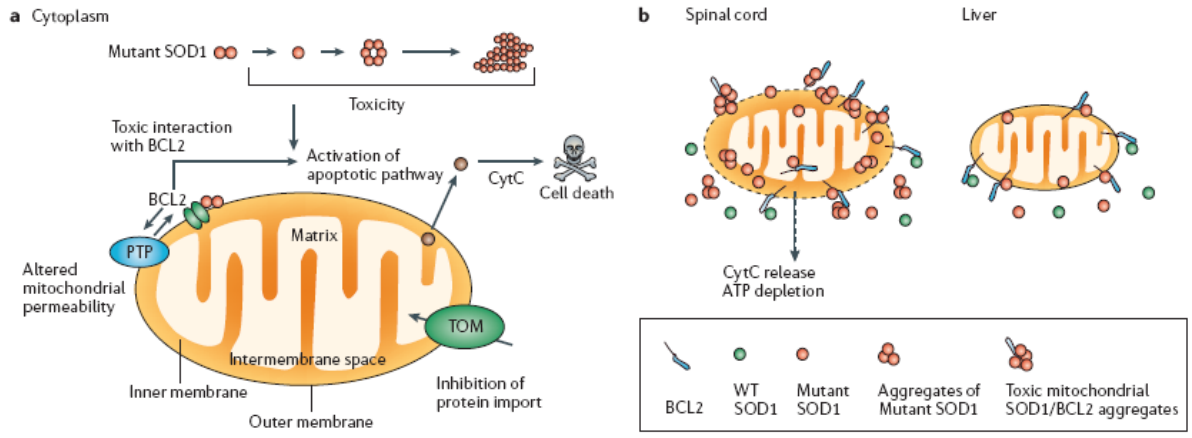

Fig. 9. The mitochondrion as a target for mutant SOD1. Long considered a cytoplasmic protein, SOD1 also localizes to the mitochondrion, although its precise localization is not fully defined. (a) Mutant SOD1 forms insoluble aggregates that could directly damage the mitochondrion through: swelling, with expansion and increased permeability of the outer membrane and intermembrane space, leading to release of cytochrome c (CytC) and caspase activation; inhibition of the translocator outer membrane (TOM) complex, preventing mitochondrial protein import; and aberrant interactions with mitochondrial proteins such as BCL2. (b) Aggregates of mutant SOD1 and BCL2 are found specifically in spinal cord but not liver mitochondria, a finding that might relate to the motoneuronal specificity of mutant SOD1 phenotypes. Codeposition of mutant SOD1 with BCL2 might eliminate BCL2 function, disrupt the mitochondrial membrane, deplete energy, deregulate mitochondrial bioenergetics and activate the mitochondrial apoptotic pathway (WT, wildtype; adapted from Pasinelli & Brown, 2006).

Several interlocking mechanisms explain how mutant SOD1 impairs mitochondria from within. In SOD1^{G93A} mice, mutant SOD1 colocalizes with cytochrome c and the peroxisomal membranes associated with the vacuoles (Higgins *et al.*, 2003). Therefore, mutant SOD1 could be involved in fusing the peroxisomes and the outer mitochondrial membrane, a process that could form pores in the mitochondrial membrane allowing for the release of cytochrome c and the initiation of an apoptotic cascade. A second hypothesis is that mutant SOD1 is selectively recruited to the outer mitochondrial membrane, where it forms

aggregates that slowly disrupt the protein translocation machinery (the translocator outer membrane complex, TOM) of the mitochondrion and limits the import of functional proteins into the mitochondrion (Liu *et al.*, 2004). Two studies suggest that mutant SOD1 is selectively recruited to mitochondria in affected tissues only (Pasinelli *et al.*, 2004; Liu *et al.*, 2004). It has, therefore, been proposed that the selective loss of TOM function in spinal cord mitochondria might form the basis for the tissue specificity of ALS. Finally, mutant SOD1 aggregates could damage the mitochondrion through abnormal interaction with other mitochondrial proteins such the anti-apoptotic protein BCL2 (Pasinelli *et al.*, 2004). A recent study challenges the notion of a toxic mitochondrial mutant SOD1, suggesting that mitochondrial loading of mutant SOD1 is simply the result of overexpression of the mutant SOD1 that normally would not be associated with mitochondria (Bergemalm *et al.*, 2006).

5.3 Endoplasmic reticulum stress and unfolded protein response

The endoplasmic reticulum (ER) is the site of translation, folding, and transport of membrane proteins and secreted proteins. In normal cells, approximately 30 % of newly synthesized proteins are misfolded (Schubert *et al*., 2000), some of these proteins are refolded to have correct structures, assisted by ER chaperones such as the binding immunoglobulin protein BiP, whereas the other remain misfolded, accumulate in ER, and cause ER stress (Ellgaard *et al*., 1999). Under such ER stress condition, an adaptive self-defense response named unfolded protein response (UPR) is triggered to decrease the load of misfolded proteins. Several cellular conditions such as high demand for protein secretion (Gass *et al*., 2002; Lipson *et al*., 2006), viral infection (Isler *et al*., 2005), deprivation of nutrient / oxygen (Lee, 1992; Feldman *et al*., 2005), and missense mutations (Bartoszewski *et al*., 2008; Ito & Suzuki, 2009) enhance protein misfolding and lead to severe ER stress and overwhelming accumulation of unfolded or misfolded proteins that causes fatal ER stress. In ALS pathogenesis, the ER stress theory has recently emerged. Studies with tissue samples from ALS patients and *in vivo* experiments indicate the involvement of ER stress in ALS (Kikuchi *et al*., 2006; Nagata *et al*., 2007). In the spinal cord neurons of SALS patients and $SOD1^{G93A}$ mice, levels of ER stress-related proteins are upregulated (Kikuchi *et al*., 2006; Nagata *et al*., 2007). ER-stress responses have been reported to be selectively up-regulated in vulnerable motoneuron populations, at presymptomatic ages, in three different mutant SOD1 transgenic mouse models (Saxena *et al*., 2009). Furthermore, mutations in vesicle-associated membrane protein-associated protein B (VAPB), which has a key role in the UPR, have been shown to

lead to ALS in a small proportion of FALS cases (Nishimura *et al*., 2004). Another intriguing hypothesis is that exacerbation of ER stress may be part of the toxic gain of function of mutant SOD1. Indeed, mutant, but not wild-type, SOD1 forms highmolecular-weight aggregates and interacts with BiP in the ER of spinal cord motoneurons (Kikuchi *et al*., 2006), and mutant SOD1 interacts with the protein Derlin-1 (involved in the ER-associated protein degradation pathway) in mouse neuronal tissue, leading to ER stress-mediated cell death through apoptosis-stimulating kinase-1 (Nishitoh *et al*., 2008).

In case of sustained ER stress (for instance, accumulation of misfolded proteins; see above), the ER itself can become a source of oxidative stress. During disulfide bond formation (part of the protein folding function of the ER), electrons are passed from thiol groups on the protein substrates to Ero1 (the protein Ero1, together with protein disulfide isomerase, PDI, is essential, in eukaryotic cells, for the disulfide bond formation supported by ER) and finally to molecular oxygen, resulting in the generation of ROS (Tu & Weissman, 2004). Unstable disulfide bonds are reduced by glutathione in a reaction also catalyzed by Ero1, thereby both depleting cellular reserves of reduced glutathione and increasing the number of thiol groups available for disulfide bond formation with the concomitant increase in ROS (Cuozzo & Kaiser, 1999). Activation of the UPR increases Ero1 expression, which may explain why sustained ER stress and prolonged activation of the UPR lead to increased production of ROS (Haynes *et al*., 2004).

5.4 Protein aggregation

The presence of protein aggregates is a pathological feature common to many neurodegenerative diseases, including ALS, although whether they play a role in disease pathogenesis, or are harmless by-products, or represent a defense mechanism by sequestration of harmful intracellular proteins is not known (Caughey & Lansbury, 2003; Ross & Poirier, 2004, 2005). A variety of protein aggregates has been described in ALS, the most common of which is the ubiquitinated inclusion, so named because they immunostain positively for ubiquitin (Leigh *et al.*, 1988; Wood *et al.*, 2003). One of the major protein constituents of ubiquitinated inclusions in ALS is TDP-43 (Neumann *et al.*, 2006; Arai *et al.*, 2006). Mutant SOD1 is also a major constituent of inclusions in SOD1-linked FALS cases (Shibata *et al.*, 1996, 1996b; Chou *et al.*, 1996) and is found in inclusions in mutant SOD1 transgenic mice (Bruijn *et al.*, 1997, 1998; Johnston *et al.*, 2000; Watanabe *et al.*, 2001) and cell culture models (Durham *et al.*, 1997; Lee *et al.*, 2002). Oxidative damage to both mutant

and wild-type SOD1 causes dissociation of SOD1 dimers to monomers and subsequent aggregation (Rakhit *et al.*, 2004). Because aberrant oxidative reactions catalyzed by metal-bound SOD1 mutants cause oxidative damage to SOD1 itself (Hodgson & Fridovich, 1975; Yim *et al.*, 1990; Andrus *et al.*, 1998), it has been proposed that such oxidative damage could lead to aggregation of mutant SOD1 (Valentine & Hart, 2003). Alternatively, SOD1 mutants with reduced metal ion binding or demetallated wild-type SOD1 are less stable than metallated SOD1 (Rodriguez *et al.*, 2002) and show increased propensity to aggregate (Rakhit *et al.*, 2002). A general mechanism for SOD1 oligomerization has recently been proposed that applies to many SOD1 mutations of various natures distributed along the length of the protein where the apo-SOD1, before it is metallated, is susceptible to oligomerization (Banci *et al.*, 2008).

5.5 Cytoskeletal dysfunction

The neuronal intermediate filament network is composed largely of neurofilaments and is responsible for maintaining cell shape and axonal caliber. Abnormal neurofilament accumulations are a pathological feature observed in spinal cord motoneurons of human ALS cases (Hirano *et al.*, 1984, 1984b; Fig. 10 a, b) and mutant SOD1 transgenic mice (Gurney *et al.*, 1994; Tu *et al.*, 1996; Morrison *et al.*, 1996; Zhang *et al.*, 1997; Dal Canto & Gurney, 1997; Fig. 10 c, d). Reduced expression of neurofilament-light (NF-L), causing changes in the stoichiometry of neurofilament subunits, has been reported in sporadic and familial ALS cases, $SOD1^{G93A}$ transgenic mice, and a cell culture model of ALS (Bergeron *et al.*, 1994; Zhang *et al.*, 1997; Wong *et al.*, 2000; Menzies *et al.*, 2002b; Fig. 10 e). Mutant, but not wild-type, SOD1 has been reported to bind directly to the 3′ untranslated region of NFL mRNA, leading to destabilization and increased degradation of mRNA (Ge *et al.*, 2005). NF-L is required for assembly of medium and heavy neurofilament subunits, so changes in its expression may disrupt neurofilament assembly and trigger aggregation. ROS produced by SOD1 have also been reported to attack NF-L subunits as the peroxidase activity of SOD1 causes dityrosine cross-link formation and aggregation of NF-L subunits (Kim *et al.*, 2004). SOD1-catalyzed peroxynitrite production selectively nitrates NF-L tyrosine residues in brain homogenates to inhibit the normal assembly of unmodified neurofilament subunits (Crow *et al.*, 1997b). The zinc-binding affinity of NF-L is sufficient to potentially remove zinc from both wild-type and mutant SOD1, particularly those mutants with reduced zinc binding, thereby increasing the peroxynitrite-mediated tyrosine nitration activity catalyzed by SOD1

(Crow *et al.*, 1997). In this way, ROS produced by mutant SOD1, and particularly mutants with reduced zinc binding, may lead to disruption of the neuronal cytoskeleton.

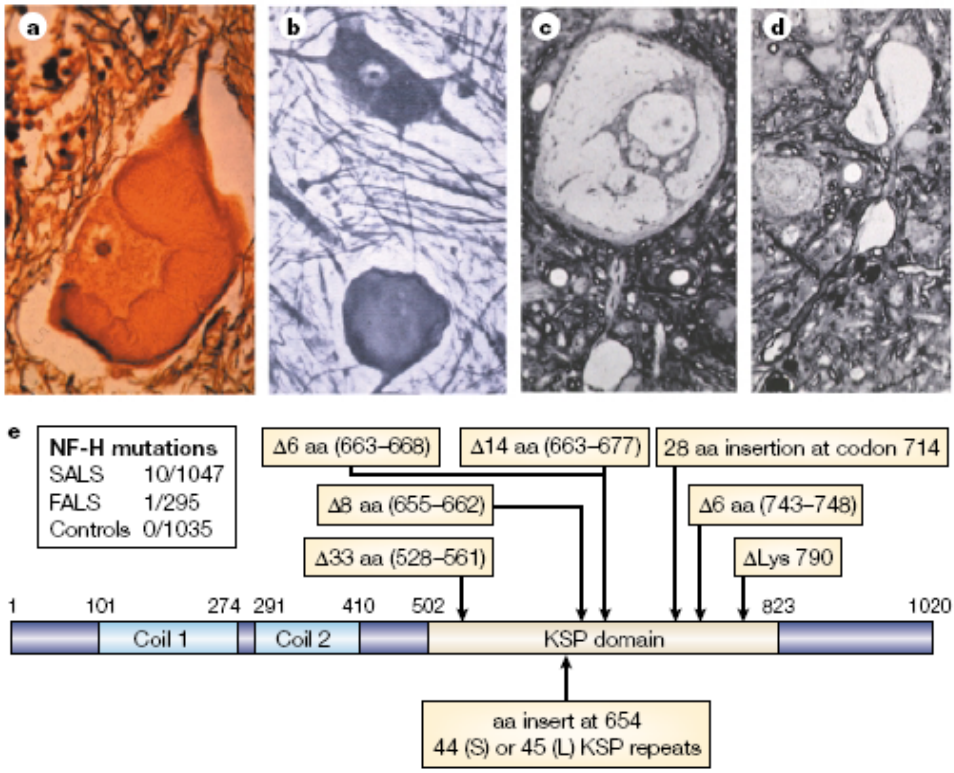

Fig. 10. Neurofilament involvement in motoneuron disease. (a, b) Aberrant accumulation of neurofilaments is a common feature in motoneuron cell bodies and axonal swellings of sporadic ALS. (a) Silver staining reveals swirling masses of neurofilaments swelling a motoneuron cell body in the spinal cord of a sporadic ALS patient. (b) A spheroidal swelling comprising masses of tangled neurofilaments in a proximal axonal segment of a spinal motoneuron from a sporadic ALS patient. Note that the cell body of this neuron appears to be normal. (c, d) Disorganized neurofilaments in the cell body (c) and spheroidal axonal swellings (c, d) of a mouse that has developed motoneuron disease by expressing a point mutation (NF-LL394P) in the neurofilament light polypeptide (NF-L) gene. (e) Deletions or insertions identified in the KSP (lysine-serine-proline) repeat domain of the neurofilament heavy polypeptide (NF-H) gene from SALS and FALS patients (adapted from Cleveland & Rothstein, 2001).

5.6 Involvement of non-neuronal cells

The concept that non-neuronal cells could affect the viability of motoneurons stems from the observation that substantial activation of microglial and astroglial cells in ALS is one of earliest microscopic manifestations of this disease (Ince *et al.*, 1996). Nonetheless, it has been difficult to obtain decisive data to test this hypothesis or to discern whether the activation of astrogliosis or microgliosis is detrimental or beneficial. Experiments with mice have shown that the specific expression of mutant SOD1 in motoneurons or glia fails to trigger motoneuron degeneration (Gong *et al.*, 2000; Pramatarova *et al.*, 2001). With the

caveat that the levels of expression of mutant SOD1 in the targeted cells might have been insufficient to induce a phenotype, these experiments favour the view that motoneuron death in transgenic ALS mice is not cell autonomous. Analyses of chimeric mice with mixed populations of cells expressing either endogenous or transgenic mutant SOD1 are consistent with this view (Clement *et al.*, 2003). In these mice, motoneurons expressing transgenic G93A or G37R SOD1 fail to degenerate if they are adjacent to large numbers of supporting cells (such as astrocytes and glia) without the mutant protein. Reciprocally, motoneurons without the transgene demonstrate pathology if surrounded by non-neuronal cells with the mutant SOD1 transgene. The minimal sets of mutant-expressing cell types required for the development of motoneuron degeneration are still poorly defined. Recent studies with deletable transgenes have documented that expression of the mutant SOD1 transgene in microglia accelerates the late phase of murine ALS (Boillée *et al.*, 2006). Parallel studies suggest that expression of the mutant SOD1 transgene within the macrophage lineage (presumably encompassing microglial cells) is not required for the ALS phenotype (Wang *et al.*, 2005). ROS released from damaged motoneurons have been found to disrupt glutamate uptake into neighboring astrocytes, thereby leading to higher extracellular glutamate levels and increased excitotoxicity (Rao *et al.*, 2003). ROS could also activate glial cells, resulting in release of further ROS, reactive nitrogen species, and proinflammatory cytokines that activate neighboring glial cells (Banati *et al.*, 1993) and could be neurotoxic (Giulian, 1993; Koutsilieri *et al.*, 2002; Zhao *et al.*, 2004;). Glial involvement may therefore be one way in which motoneuron degeneration, which often starts focally, spreads to contiguous motoneuron populations (Brooks *et al.*, 1995).

5.7 Defects in RNA processing and trafficking

Only recently RNA processing has become implicated in the pathogenesis of ALS, with the discovery of mutations in two genes with RNA / DNA-binding functions, TDP-43 (Kabashi *et al*., 2008; Sreedharan *et al*., 2008; Fig. 11 A) and FUS / TLS (Kwiatkowski *et al*., 2009; Vance *et al*., 2009; Fig. 11 B), being identified in FALS patients (Lagier-Tourenne & Cleveland, 2009). ALS-causing mutations in both genes result in the translocation of mutant proteins from the nucleus to the cytoplasm, where they form inclusions. Whether these cytoplasmic inclusions are toxic or act to sequester protein remains unclear. Whether oxidative stress contributes to this process is also unknown. However, oxidation of mRNA has been identified in ALS patients and in transgenic mice expressing a variety of FALS-

linked SOD1 mutations (Chang *et al.*, 2008). In mutant SOD1^{G93A} mice, increased mRNA oxidation is observed in spinal cord motoneurons and oligodendrocytes at presymptomatic ages. Some mRNA transcripts are more vulnerable to oxidation than others, with RNA species encoding proteins involved in mitochondrial electron transport and protein biosynthesis, folding, and degradation and SOD1 itself being more highly oxidized. Although treatment with the antioxidant vitamin E does not alter survival of SOD1^{G93A} mice, it reduces mRNA oxidation, delays disease onset (defined by motor and pathological indications), and improves motor performance during the disease (Chang *et al.*, 2008).

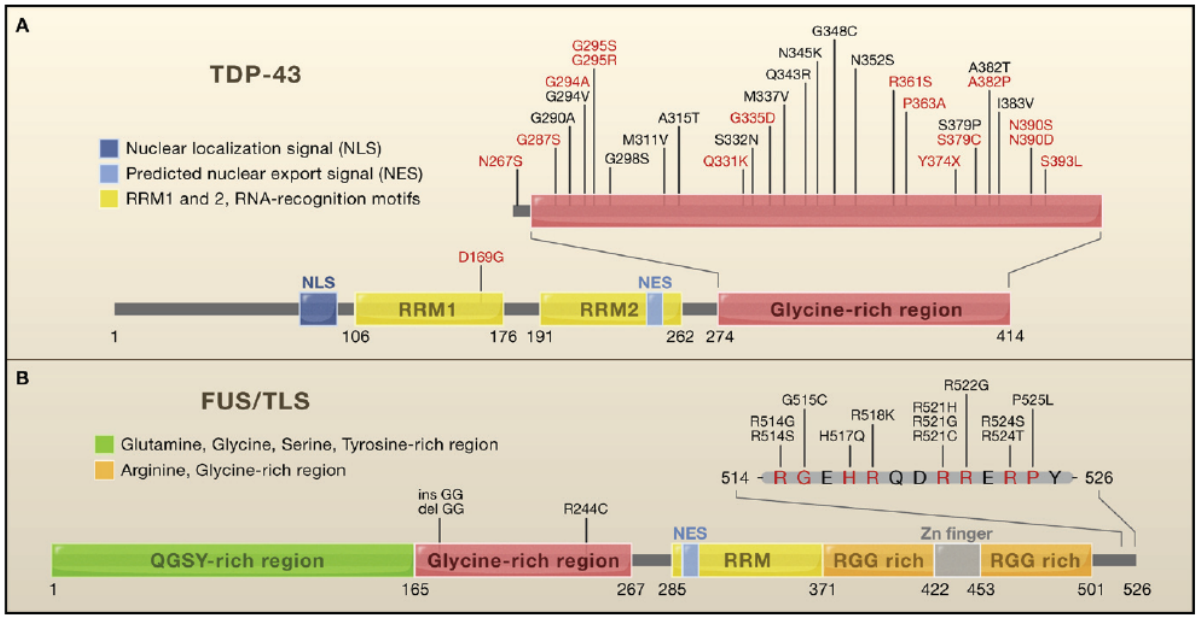

Fig. 11. TDP-43 and FUS / TLS Mutations in ALS. (A) Thirty dominant mutations in TDP-43 have been identified in sporadic (red) and familial (black) ALS patients, with most lying in the C-terminal glycine-rich region of TDP-43. All are missense mutations, except for the truncating mutation TDP-43Y374X. (B) Fourteen mutations in FUS / TLS have been identified in familial ALS cases, with most lying in the final 13 amino acids of this protein (R514S and G515S are found in cis; adapted from Lagier-Tourenne & Cleveland, 2009).

6. Persistent Na^+ conductances in ALS

6.1 Hyperexcitability and persistent Na^+ conductances in ALS patients

From a clinical perspective, cortical hyperexcitability, together with muscle cramps and fasciculations are inevitable features of both familial and sporadic forms of ALS (Roth, 1984; Miller & Layzer, 2005). Studies of axonal excitability undertaken in ALS patients establish that strength-duration time constant (τSD) is increased (Mogyoros *et al.*, 1996). τSD is a measure of the rate at which the threshold current for a target potential declines as the stimulus duration increases (Bostock, 1983; Bostock & Rothwell, 1997). Computer

modelling of the behaviour of human motor axon suggests that τSD reflects persistent Na^+ conductances which constitute approximately 1 % of total Na^+ current in motor axons (Bostock & Rothwell, 1997). Specifically, increasing the fraction of the persistent Na^+ current by means of membrane depolarization prolongs τSD. Over the last years, techniques have been developed to assess τSD in a clinical setting using a computerized threshold tacking protocol (Kiernan *et al.*, 2000). Widespread abnormalities in axonal ion channel function, including reduction of slow and fast K^+ channel conductances combined with upregulation of persistent Na^+ conductances (Vucic & Kiernan, 2006; Tamura *et al.*, 2006), have been reported in SALS and proposed as a likely mechanism underlying the generation of the ectopic activity of motor axons leading to cramps and fasciculations (Mogyoros *et al.*, 1996; Kiernan & Burke, 2004; Vucic & Kiernan, 2006). Whether such changes are intrinsic to the process of axonal degeneration, or develop as an epiphenomenon, remains to be clarified. In addition to underlying the generation of such ectopic axonal activity, abnormalities of axonal ion channel function, in particular upregulation of persistent Na^+ conductances, has been associated with the process of axonal degeneration (Kanai *et al.*, 2003). Further, in SALS patients, cortical hyperexcitability is correlated with upregulation of persistent Na^+ conductances (Vucic & Kiernan, 2006b), thereby suggesting a 'dying forward' process, which proposes that cortico-motoneurons drive death of anterior horn cells (Eisen *et al.*, 1992). The notion of a dying forward process as a potential mechanism of neurodegeneration in ALS is further supported by finding that cortical hyperexcitability precedes the onset of FALS (Vucic *et al.*, 2008). In addition, a recent report by Vucic and Kiernan (2010) has documented an increase in the τSD in FALS patients (Fig. 12). The upregulation of persistent Na^+ conductances, expressed as τSD, correlates with peripheral markers of disease burden such as the decreased amplitude of the compound muscle action potential, and the Neurophysiological Index that also includes the frequency and latency of a series of electrical responses of skeletal muscle (de Carvalho & Swash, 2000). Furthermore, the τSD is also correlated with measures of cortical excitability, like the short interval intracortical inhibition (Vucic & Kiernan, 2010). In summary, the proposed increase in persistent Na^+ conductances appears to be linked to the process of axonal degeneration and cortical hyperexcitability.

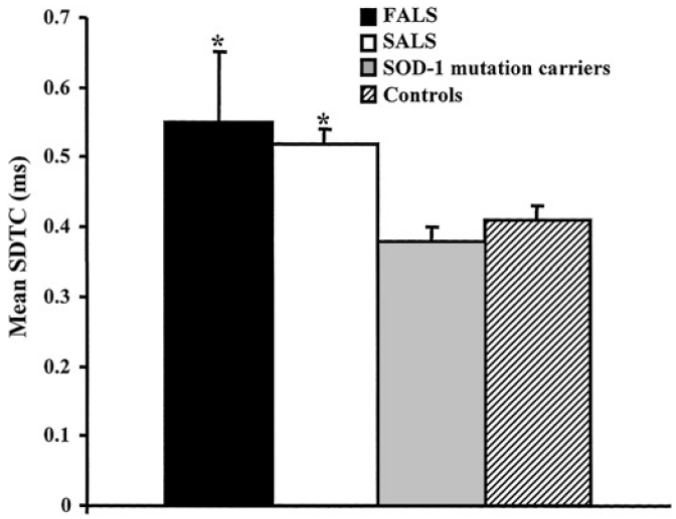

Fig. 12. Mean data illustrating that the strength-duration time constant (τSD) was significantly increased in both familial amyotrophic lateral sclerosis patients (FALS) and sporadic amyotrophic lateral sclerosis (SALS) patients when compared with asymptomatic superoxide dismutase-1 (SOD-1) gene mutation carriers and controls (*$p<0.05$; adapted from Vucic & Kiernan, 2010).

6.2 Persistent Na^+ conductances and electrophysiological properties in ALS animal models

The findings concerning persistent Na^+ conductances in human ALS patients are consistent with recent studies reporting upregulation of persistent Na^+ current in the transgenic $SOD1^{G93A}$ mouse model (Kuo *et al*., 2005; van Zundert *et al*., 2008; Pieri *et al*., 2009). Specifically, using patch-clamp techniques, augmented persistent Na^+ conductances are reported in presymptomatic cortical, brainstem and spinal motoneurons of the $SOD1^{G93A}$ model (Kuo *et al*., 2005; van Zundert *et al*., 2008; Pieri *et al*., 2009). Furthermore, these studies have examined the passive membrane properties and the pattern of motoneuron repetitive firing, demonstrating that, while the former are similar in control and G93A motoneurons, the firing frequency increases significantly in the G93A motoneurons, because of their higher persistent sodium current (Kuo *et al*., 2005; van Zundert *et al*., 2008; Pieri *et al*., 2009). Nonetheless, the electrophysiological phenotype is complex, as demonstrated by the work by Pambo-Pambo *et al.* (2009). This study compares the properties of control mouse motoneurons in the second postnatal week to those of two different SOD1 mutant lines, the $SOD1^{G93A}$ low expressor line and the $SOD1^{G85R}$ line. The authors show that very early changes in excitability occur in SOD1 mutant motoneurons. The $SOD1^{G93A}$ low expressor line displays specific differences not found in other mutant lines including a more depolarized membrane potential, larger spike width, and slower spike rise slope. After

injecting current pulses, $SOD1^{G93A}$ low expressor cells are hyperexcitable. Low expressor mutants show reduced total persistent inward currents compared with control motoneurons. The differences observed between these mutants could be due to the diverse toxic properties of the mutated SOD1 proteins (Prudencio *et al.*, 2009) and / or to different timing of developmental processes interacting with compensation mechanisms.

7. Hypoglossal nucleus

The hypoglossal nucleus (XII cranial nucleus) is located in the medulla oblongata close to the midline immediately beneath the base of the fourth ventricle (Fig. 13). It innervates the tongue intrinsic and extrinsic muscles. The extrinsic muscles have bone attachment, and include hypoglossus, styloglossus, geniohyloid and genioglossus muscles, whose activity control protrusion, retraction and elevation of the tongue. Intrinsic muscles are not attached to the bone and are located within the body of the tongue. They are composed of vertical, transversal, superior and inferior longitudinal muscles that alter the shape of the tongue. In the rat, the ventrolateral subdivision of XII nucleus innervates the tongue protractor muscles, while the dorsal part innervates retractor muscles, and the motoneurons of the middle third of the XII nucleus innervate tongue intrinsic muscle (Aldes, 1995; McClung & Goldberg, 1999, 2000; Sokoloff, 2000). Such XII nucleus organization allows the fine control of various tongue movements, including mastication, sucking, swallowing, controlling respiration and others oral behaviours (Lowe, 1980).

At least 90 % of neurons within the hypoglossal nucleus are motoneurons, while the remaining ones are interneurons (Viana *et al.,* 1990). Hypoglossal motoneurons (HMs) are large (25-50 μm), multipolar cells, whereas interneurons are smaller (10-20 μm), round to oval shaped neurons. Motoneurons spread their dendrites extensively within the XII nucleus and the neighboring reticular formation, while the interneurons have few dendritic processes and are located at the ventrolateral or dorsolateral borders of the nucleus. Axons of the HMs exit the hypoglossal nucleus, penetrate the *dura mater* and coalesces to form the hypoglossal nerve (XII cranial nerve) in the hypoglossal canal (Fig. 13). The XII nerve then runs to the floor of the mouth, where its fibers are distributed to intrinsic and extrinsic muscles of the tongue.

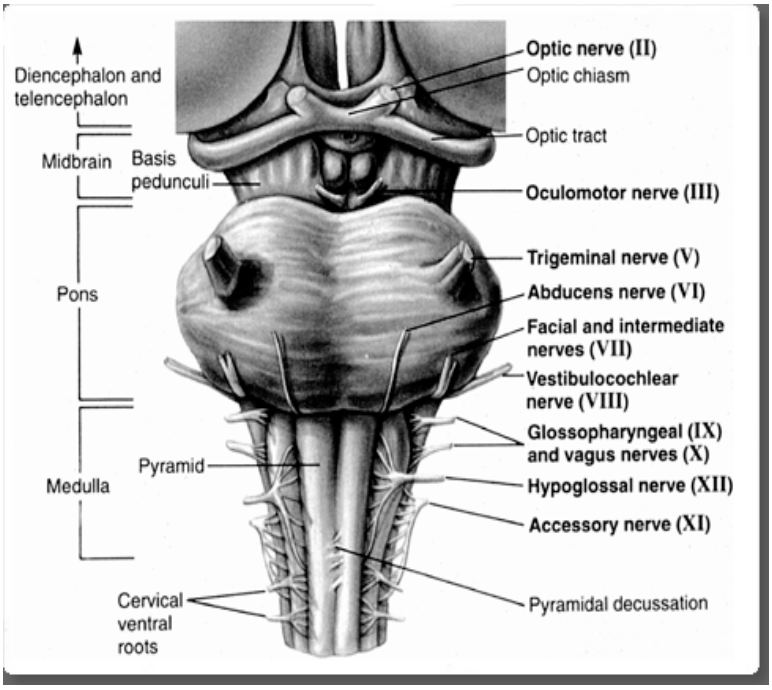

Fig. 13. Ventral view of human brainstem. The brainstem is composed of three major divisions: medulla, pons, and midbrain. The hypoglossal nerve (XII cranial nerve) originates in the medulla (adapted from Kandel *et al.,* 1991).

The XII nucleus receives innervation from the reticular formation, other brainstem centers and higher centers of the brain (Borke *et al.,* 1983; Dobbins & Feldman, 1995). The primary source of the inputs to the XII nucleus arises from the caudal reticular formation immediately ventral to the nucleus of the solitary tract (NTS), which is termed dorsal medullary reticular column (DMRC; Cunningham & Sawchenko, 2000; Fig. 14). Projections from the DMRC are largely bilateral, distributed to both dorsal and ventral subdivisions of XII nucleus, and, therefore, can simultaneously innervate both tongue protractor and retractor muscles. This arrangment shows an independent, albeit coordinated activation of antagonist muscles of the tongue (Dobbins & Feldman, 1995; Fay & Norgren, 1997; Cunningham & Sawchenko, 2000). Human XII nucleus receives cortico-nuclear fibers from the pre-central gyrus of both cerebral hemispheres; however, no direct cortical connections to orofacial motor nuclei, including the XII nucleus, have been shown in rats (Travers & Norgren, 1983). Thus, voluntary motor commands in rat must pass through various relay stations.

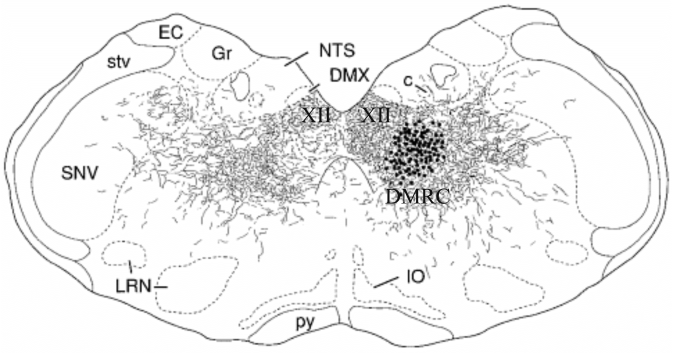

Fig. 14. Schematic representation of XII nucleus innervation. Anterograde labeling shows that hypoglossal nuclei (XII) receive inputs from dorsomedial reticular column (DMRC), where labeling dye was injected. DMRC innervates both contralateral and ipsilateral XII nuclei. Abbreviations: NTS, nucleus tractus solitarius; DMX, dorsal motor nucleus of the vagus nerve; Gr, gracile nucleus; EC, external cuneate nucleus; stv, spinal tract of the trigeminal nucleus; SNV, spinal trigeminal nucleus; LRN, lateral reticular nucleus; py, pyramidal tract; IO, inferior olive (modified from Cunningham & Sawchenko, 2000).

Excitatory premotoneurons in the XII nucleus are glutamatergic, while the inhibitory ones are GABAergic and glycinergic (Rekling *et al.,* 2000). *In vitro* recordings from neonatal rats show that HMs express both NMDA and non-NMDA receptors at synaptic sites (O'Brien *et al.,* 1997). However, *in vivo* recording from adult rats (Ouardouz & Durand, 1994) and recordings from HM embryonic organotypic cultures (Launey *et al.,* 1999) suggest that NMDA receptors are not directly involved in synaptic transmission, and could be located either extrasynaptically or at silent synapses. The neurotransmitters GABA and glycine operate by activating Cl^- channels. GABA receptors mainly belong to $GABA_A$ class and are reversibly blocked by bicuculline, while glycine receptors are blocked by strychnine (Barnard *et al.,* 1993; Kuhse *et al.,* 1995; Donato & Nistri, 2000). On brainstem motoneurons, $GABA_A$ and glycine receptors are present on the same neuron, and HMs receive both GABAergic and glycinergic synaptic inputs (O'Brien & Berger, 1999). On hypoglossal motoneurons, however, glycinergic events are significantly faster and larger in amplitude than GABAergic currents, and occur at higher frequency (Donato & Nistri, 2000).

7.1 Hypoglossal nucleus: a model for studying oxidative stress in relation to ALS

Hypoglossal motoneurons are among the most strongly damaged neurons in ALS (Krieger *et al.,* 1994; Lips & Keller, 1999). It has been suggested that HM vulnerability could be due to their characteristic intracellular Ca^{2+} homeostasis (Ladewig *et al.,* 2003), expression of Ca^{2+} permeable AMPA channels (Del Cano *et al.,* 1999), or impaired glutamate uptake

(Sharifullina & Nistri, 2006). HM dysfunction, resulting in dysarthria and dysphagia, is often a very early symptom of ALS (Medina *et al.*, 1996; Shaw & Ince, 1997), and initial bulbar symptoms are diagnosed on the basis of the patient's ability to speak and manage food and drinks (Kühnlein *et al*., 2008).

Current theories of ALS propose that motoneuron damage may result from oxidative stress as indicated by the host (>140) of SOD-1 mutations implicated in the genetic forms of the disease that, however, are only 10 % of all clinical cases and have generated a large number of mouse genetic models (Vucic & Kiernan, 2009). Since the vast majority of ALS cases are sporadic, presumably implying an environmental toxic agent (Cleveland & Rothstein, 2001), and oxidative stress has also been implicated as a major player, even in the absence of mutated SOD1 (Shaw *et al.*, 1995; Ferrante *et al.*, 1997; Bogdanov *et al.*, 2000; Ihara *et al.*, 2005), wildtype HMs are an appropriate model for studying the consequences of a free-radical challenge.

The present study used HMs from the neonatal rat brainstem to investigate how hydrogen peroxide and nitric oxide could affect synaptic transmission and intrinsic motoneuron excitability in relation to survival. We wished to find out if even a transient oxidative stress might be sufficient to trigger off electrophysiological alterations accompanied by expression of the ATF-3 transcription factor typical of motoneuron distress (Tsujino *et al*., 2000; Hai & Hartman, 2001; Vlug *et al*., 2005) and the S100B protoplasmic astrocytic marker, known to be associated with brain damage and degenerative brain disease (Migheli *et al.*, 1999; Rothermundt *et al.*; 2003; Blackburn *et al.*, 2009). Both ATF-3 and S100B have a Janus-like function: the former subserves either damage repair or degeneration depending on the nature of the insult (Tsujino *et al*., 2000; Nakagomi *et al*., 2003; Vlug *et al*., 2005); the latter can exert beneficial (neurotrophic) or detrimental (neurotoxic) effects on surrounding glia and neurons depending on its concentration (Rothermundt *et al.*, 2003).

The hypoglossal nucleus have been extensively studied to clarify the basic pathogenethic mechanisms of ALS and to understand its selective vulnerability. Funk's laboratory has characterized the differential expression of calcium binding proteins, of Group I metabotropic glutamate receptors, of GluR2 AMPA Receptor Subunit, and of voltage-activated Ca^{2+} channels in motoneurons at low and high risk for degeneration in ALS (Laslo *et al*., 2000, 2001, 2001b; Miles *et al*., 2004), indicating how the nucleus hypoglossus is at very high risk of neurodegeneration. $SOD1^{G93A}$ neonatal and adult hypoglossal motoneurons have also been studied to elucidate Ca^{2+} homeostasis (von Lewinski *et al*., 2008; Jaiswal &

Keller, 2009). These authors have reported low Ca^{2+} buffering capabilities in such vulnerable motoneurons, and considered it a significant risk factor for degeneration (von Lewinski *et al*., 2008; Jaiswal & Keller, 2009). Changes in HM activity of neonatal brainstem slice preparations have been investigated using as a source of tissue both wild-type and $SOD1^{G93A}$ mice, demonstrating higher excitability of the mutant neurons even at presymptomatic stage (van Zundert *et al*., 2008).

8. Hydrogen peroxide

Hydrogen peroxide is a reactive oxygen species and is generated as a by-product of aerobic metabolism in cells, due to molecular oxygen partial reduction. ROS, together with RNS, are disruptive to cells redox state if not detoxified. Indeed, over-production and/or under-detoxification of ROS / RNS, or even normal demands for these reactive species may cause oxidative / nitrosative stress. Among all organs in the body, the brain is particularly prone to oxidative stress-induced damage because of the high oxygen demand of this organ, the abundance of redox-active metals (iron and copper), the high levels of oxidizable polyunsaturated fatty acids, and the fact that neurons are post-mitotic cells with relatively restricted replenishment by progenitor cells during the lifespan of an organism. ROS / RNS-induced oxidative stress to the brain has been implicated in normal aging and in various neurodegenerative disorders, including ALS, Parkinson's disease, Alzheimer's disease, and ischemia-reperfusion injury (Beckman *et al*., 1990; Ames & Shigenaga, 1992; Dreher & Junod, 1995; Golino *et al*., 1996; Lewen *et al*., 2000; Chandra *et al*., 2000).

Over millions of years of evolution, cells have developed a multitude of anti-oxidant mechanisms to cope with the potential damaging effects of ROS and RNS. These mechanisms include anti-oxidant enzymes (such as superoxide dismutase, catalase, glutathione peroxidase, and the thioredoxins), as well as non-protein antioxidants (such as glutathione, GSH; α-tocopherol, vitamin E; ascorbic acid, vitamin C; bilirubin, and coenzyme Q10). Glutathione is a major non-protein antioxidant in cells and the ratio of its reduced and oxidized form (GSH / GSSG) is an indicator of cellular redox status (Schafer & Buettner, 2001; Jones, 2002). The combination of anti-oxidant proteins and smaller molecules offers a versatile and flexible system to control intracellular levels of ROS / RNS. The high efficiency of this system in cells, including neurons, is maintained through the diverse subcellular localization of the antioxidants, their biochemical properties, and the differential inducibility of anti-oxidant enzymes at both transcriptional and translational

levels. Although cellular antioxidants are highly efficient in maintaining redox homeostasis, such anti-oxidant defenses do not completely eradicate ROS / RNS from the intracellular environment. Nor would such eradication be desirable as ROS / RNS are essential components of a repertoire of signals on which neurons depend to respond to internal and external, environmental and developmental cues (Gutierrez *et al*., 2006). Numerous neurotransmitter systems are sensitive to ROS, including adrenergic (Kvaltinova *et al*., 1993), dopaminergic (Joseph *et al*., 1998), serotonergic (Muakkassah-Kelly *et al*., 1982) and GABAergic (Schwartz, 1988; Sah & Schwartz-Bloom, 1999) systems. The effects of ROS on neurotransmission can occur via various mechanisms (van der Want *et al*., 1992). For example, ROS may interact with neurotransmitter receptors and ion transport proteins such as channels, pumps, and transporters, leading to changes in receptor activity and ionic homeostasis. In addition, ROS can alter ligand-receptor interactions or ion transport indirectly via actions within the lipid environment of cell membranes. Among the most important signaling pathways modulated by H_2O_2 are those involving kinase and phosphatase enzymes (Denu & Tanner, 1998; Nakamura *et al*., 1993; Klann *et al*., 1998; Whisler *et al*., 1995). For GABAergic neurotransmission, ROS have been shown to increase release (and decrease uptake) of GABA in a variety of neuronal preparations (Rego *et al*., 1996; Saransaari & Oja, 1998; Sah & Schwartz-Bloom, 1999). A recent study indicated that H_2O_2 increased GABAergic mIPSCs through presynaptic inositol-1,4,5-trisphosphate receptor (IP3R)-sensitive Ca^{2+} release mechanism (Takahashi *et al.*, 2007). Furthermore, ROS / RNS signals can influence synaptic plasticity (Kamsler & Segal, 2004, 2007; Serrano & Klann, 2004; Kishida & Klann, 2007). This pathway contains redox-sensitive proteins that can undergo reversible oxidation / reduction and thus modulate their function based on the cellular redox status (Kohr *et al*., 1994; Suzuki *et al*., 1997; Forman *et al*., 2002; Lipton *et al*., 2002; Hidalgo, 2005; Janssen-Heininger *et al*., 2008). This modulation can be conferred by ROS / RNS either directly or indirectly through other redox-sensitive molecules such as glutathione or thioredoxins. Many of these proteins contain redox-sensitive cysteine residues that may be oxidized to either sulfenic acid or disulfide bonds, thus producing changes in structural and functional states of the respective proteins (Denu & Tanner, 1998; Droge, 2003; Piotukh *et al*., 2007). The downstream effects are, for example, the activation / deactivation of a variety of effectors, such as kinases, phosphatases and transcription factors (e.g., Nrf2 and NF-κB; Arrigo, 1999).

9. Nitric oxide

Nitric oxide (NO) is a crucial signaling molecule in cardiovascular (Ignarro *et al*., 1987; Palmer *et al*., 1987), reproductive (Hurt *et al*., 2006), immune (Bogdan, 2001), and central nervous systems (CNS; Bredt *et al*., 1990; Bon & Garthwaite, 2003; Garthwaite, 2008). NO exhibits properties ideally suited for a transcellular messenger: being highly soluble and mobile (unimpeded by cell membranes), widely synthesized and of limited lifetime. It acts via a well-characterized NO-cGMP pathway (Southam & Garthwaite, 1993), although S-nitrosylation of proteins, generation of ROS, and regulation of cellular respiration also contribute to physiological and pathological roles (Ahern *et al*., 2002).

In mammals, NO is synthesized by nitric oxide synthases (NOS) through the conversion of L-arginine to NO and L-citrulline. NOS are complex proteins found constitutively in two isoforms, neuronal (nNOS) and endothelial (eNOS). The third, inducible, type (iNOS) is rarely present normally but can be expressed in numerous cell types (prototypically in macrophages, mainly in microglia of the CNS) when subjected to immunological challenge. NOS have distinct functional and structural features (reviewed by Alderton *et al*., 2001; Stuehr *et al*., 2004). nNOS is activated by Ca^{2+} complexed with calmodulin and has a wide but uneven distribution in the mammalian brain (Bredt *et al*., 1991; Vincent & Kimura, 1992). Although nNOS is the most abundant isoform generally found in the central and peripheral nervous systems, it is widely expressed in the neocortex, cerebellum, and hippocampus, and is closely associated with NMDA receptors (Brenman *et al*., 1996) and synaptic plasticity (Hopper & Garthwaite, 2006; Jacoby *et al*., 2001; Son *et al*., 1996).

NO mediates its effect by activating guanylate cyclases (GC) for the production of cGMP, a well-known second messenger (Reynolds & Burstyn, 2000). GC is an αβ-heterodimer of which there are two known isoforms, α1β1 and α2β1 (Denninger & Marletta, 1999; Koesling *et al*., 2004). Although widespread, the two NO effector isoforms have a diverse cellular distribution in the brain (Budworth *et al*., 1999; Gibb & Garthwaite, 2001; Mergia *et al*., 2003; Szabadits *et al*., 2007) and, at the subcellular level, may also have different locations because the α2β1 effector is enriched in synapses (Russwurm *et al*., 2001), while the other isoform, α1β1, may be cytosolic in part, but there is evidence that it may become plasma membrane-associated under conditions of raised intracellular Ca^{2+} (Zabel *et al*., 2002) or exposure to cannabinoids (Jones *et al*., 2008). NO also reacts with cysteine residues on target proteins to form nitrosothiols that mediate signal transduction. S-nitrosylation is a reversible process facilitated by an acid-base amino acid motif within the protein structure

(Stamler *et al*., 1997; Stamler *et al*., 2001). However, deregulation of S-nitrosylation due to increased nitrosative stress can contribute to the pathogenesis of various neurodegenerative diseases like ALS. Schonhoff *et al*. (2006) have demonstrated that selective depletion of nitrosothiols is prominent in the spinal cord of G93A and G85R mutant SOD1 transgenic mice. The mechanism of how the depletion of nitrosothiols can contribute to motoneurons degeneration in ALS is not known, but this report suggests it to be related to decreased levels of S-nitrosylated glyceraldehyde 3-phosphate dehydrogenase (GAPDH). Since S-nitrosylation of GAPDH is known to regulate its translocation to the nucleus, a process critical for cell survival, it is hypothesized that decreased S-nitrosylation of GAPDH can contribute to the demise of motoneurons in ALS.

Aims of the study

The present study aimed at addressing the following scientific questions:

- What is the effect of oxidative stress, for example induced by H_2O_2, on excitatory & inhibitory synaptic transmission and excitability of HMs?
- What is the nucleus hypoglossus response to H_2O_2 in terms of intracellular generation of reactive oxygen species, cell survival & neuronal / astroglial distress?
- What are the electrophysiological changes induced by sodium nitroprusside (NaNP), a NO donor, on HMs and how does this effect compares with those evoked by H_2O_2?

Materials & Methods

1. Slice preparation

All experiments were carried out in accordance with the regulations of the Italian Animal Welfare act (DL 27/1/92 n.116) following the European Community directives no. 86/609 93/88 (Italian Ministry of Health authorization for the local animal care facility in Trieste D 69 / 98-B), and approved by the local authority veterinary service. As full details of the experimental methods have been published earlier (Quitadamo *et al.*, 2005; Lamanauskas & Nistri, 2006, 2008), only a brief account is provided hereafter. Brainstem slices (250 μm thick) from neonatal (P1-P5 day old) urethane - anaesthetized Wistar rats were cut in ice-cold, oxygenated (95% O_2/5% CO_2) Krebs solution, containing (in mM): NaCl, 130; KCl, 3; NaH_2PO_4, 1.5; $CaCl_2$, 1; $MgCl_2$, 5; $NaHCO_3$, 25; glucose, 100 (pH 7.4; 300-320 mOsm). After 40 min recovery at 32 ºC and 1 h at room temperature, they were used for recording.

2. Electrophysiological recordings

HMs were identified within the nucleus hypoglossus with an infrared video-camera (Fig. 15 A, B). All cell recordings were obtained, at ambient temperature, under whole-cell patch-clamp conditions. For voltage clamp experiments, patch electrodes had 3-4 MΩ resistance, whereas for current clamp experiments they had 8-10 MΩ resistance. Cells were clamped at values between -60 and -70 mV holding potential (V_h), as close as possible to initial resting potential. Cells were used for analysis when series resistance increases did not exceed 10%. Voltage-activated currents were measured in response to slow (either 21 mV/s or 42 mV/s) triangular voltage-clamp commands from -80 mV to +20 mV and back (Lamanauskaus & Nistri, 2008) in accordance with the studies by Schwindt & Crill (1980). In current clamp mode, neurons were kept at their initial resting level of membrane potential (V_m) while the bridge was routinely balanced throughout the experiment. Intracellular DC currents (200-500 pA; 500 ms) were injected into HMs to study firing properties and afterhyperpolarization (AHP) amplitude. Voltage and current pulse generation and data acquisition were performed using pClamp 10.0 software (Axon Instruments, Molecular Devices, Sunnyvale, CA, USA). Patch pipettes were filled with intracellular solution containing (in mM): CsCl, 130; NaCl, 5; $MgCl_2$, 2; $CaCl_2$, 1; HEPES, 10; EGTA, 10; ATP-Mg, 2; sucrose, 2 (pH 7.2 with CsOH; 280-300 mOsm) for voltage clamp experiments. Intracellular CsCl, that minimized the leak

current of the recorded cell, was used to enable larger changes in V_h. For current clamp experiments, 130 mM KCl always replaced CsCl.

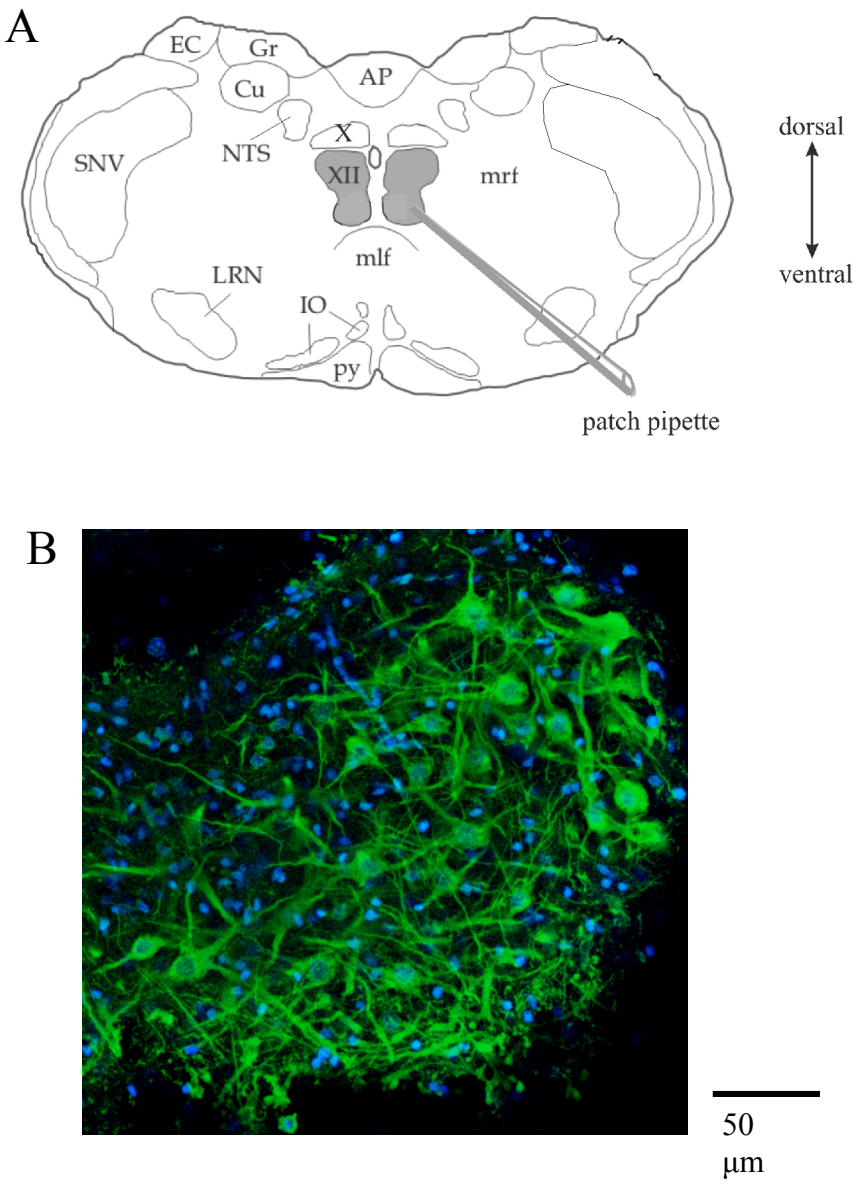

Fig. 15. HM identification within the brainstem slice. (A) Schematic representation of a brainstem slice. Recordings were done via patch pipette. The following structures can be identified: AP, area postrema; Cu, cuneate nucleus; EC, external cuneate nucleus; Gr, gracile nucleus; IO, inferior olive; LRN, lateral reticular nucleus; mlf, medial longitudinal fasciculus; mrf, medullary reticular formation; NTS, nucleus of the tractus solitarius; SNV, spinal trigeminal nucleus; py, pyramidal tract; X, vagal nucleus; XII, hypoglossal nucleus. (B) Confocal image of a hypoglossal nucleus labeled with the motoneuron marker SMI 32 (Jacob *et al.*, 2005; Raoul *et al.*, 2005; green pseudocolour) and Hoechst 33342 DNA staining (blue pseudocolour). Single motoneurons could be easily identified within the XII nucleus.

3. Solutions and drugs

Slices were superfused (2-3 mL/min) with a gassed solution containing (in mM): NaCl, 130; KCl, 3; NaH_2PO_4, 1.5; $CaCl_2$, 1.5; $MgCl_2$, 1; $NaHCO_3$, 25; glucose, 10 (pH 7.4; 300–320 mOsm). The following drugs were used: 6-cyano-7-nitroquinoxaline-2,3-dione (CNQX), D-amino-phosphonovalerate (APV), bicuculline methiodide (bicuculline) and strychnine hydrochloride (strychnine) purchased from Tocris (Bristol, UK); $MgCl_2$, H_2O_2 and sodium nitroprusside dehydrate (NaNP) were from Sigma (Milan, Italy). Tetrodotoxin (TTX) was obtained from Latoxan (Valence, France), thapsigargin from Calbiochem (Merck Chemicals, Darmstadt, Germany). Drugs were applied by superfusion. Since the focus of the present study was on the toxic activity of free oxygen radicals, as a routine, H_2O_2 was applied at 1 mM concentration because this dose was previously shown to produce neurotoxicity of *in vitro* spinal neurons (Taccola *et al.*, 2008). Similar effects were seen in preliminary experiments with 0.5 mM H_2O_2. We checked that 1 mM H_2O_2 did not vary the pH of the superfusing solution (observed pH change switching from control Krebs to H_2O_2 containing solution was from 7.38 to 7.40).

To investigate nitrosative stress effects on HMs, we perfused brainstem slices with 500 μM NaNP, a NO donor. Indeed, near-micromolar NO concentrations are associated with toxicity and cell death (Dawson *et al*., 1993; Liu & Martin, 2001; Hall *et al*., 2009), and, in the case of NaNP, Southam and Garthwaite (1991) estimate that a range from 1 μM to 10 mM in the perfusate corresponds to a concentration near the tissue ranging from 0.1 nM to 1 μM. Accordingly, the dose of 500 μM used in the present work should correspond to a concentration in the recording chamber of 0.05 μM.

4. Data analysis

In voltage clamp experiments, cell input resistance (R_{in}) was calculated by measuring the current response to 10 mV hyperpolarizing steps from V_h. In current clamp experiments, R_{in} was calculated by measuring the voltage response to -50 pA current injections (Pagnotta *et al.*, 2005; Quitadamo *et al.*, 2005). Spontaneous and miniature, excitatory and inhibitory, postsynaptic currents (sPSCs, mIPSCs and mEPSCs) were detected using the template search software Clampfit 10.0 (Axon Instruments). Cumulative probability plots of synaptic events were constructed with SigmaPlot 9.01 software (Jandel Scientific, San Rafael, CA, USA).

Decay-time was calculated by exponential fitting of the decay phase of captured single events. In accordance with the standard protocols used by Ptak *et al.* (2005), Enomoto *et al.* (2006), Aracri *et al.* (2006) and Magistretti *et al.* (2006), persistent inward currents (PICs) were evoked by injecting triangular voltage commands at the rate of either 21 mV ⁄ s or 42 mV ⁄ s. The voltage-activated inward current was obtained after subtracting the passive leak current (Cramer *et al.*, 2007; Theiss *et al.*, 2007), extrapolated from linear regression fits to the I-V curve at membrane voltages between -80 and -60 mV. The inward current area was also measured as the area below the trace baseline after leak correction. SigmaPlot 9.01 software was used for linear regression analysis including the quantification of the time dependence of firing frequency. Gradual changes in spike firing following a long current pulse injection were investigated by Sawczuk *et al.* (1995) who used HMs of rat brainstem slices in control solution to show multiphasic decay in the firing frequency after the initial high rate. In analogy with these studies we examined changes in spike firing rate before and after application of H_2O_2 by fitting a cubic polynomial function to the plot of the interspike intervals *versus* the spike sequence in the train (see Fig. 22 D) as shown by the following equations:

Control: $y_1 = 0.0148 + 0.0189x - 0.0029x^2 + 0.0001x^3$ with $r = 0.8528$, and

H_2O_2: $y_2 = 0.0084 + 0.0035x - 0.0002x^2 + 3.92*10^{-6}x^3$ with $r = 0.8999$.

We then calculated the difference integral for the first 13 spikes in the plot and normalized the result with respect to control to give the % change. It is noteworthy that this analysis was performed with data obtained under non steady-state conditions because of the developing toxic action of H_2O_2 on HMs. Because H_2O_2 application was transient to mimic a temporary oxidative stress and it induced ongoing changes in baseline membrane potential and neuronal properties under non steady-state conditions, it was not feasible to perform standard tests of HM firing responses to varying amplitudes of injected current. CorelDraw (Vector Capital, San Francisco, CA, USA) was used for graphical data presentation.

5. Intracellular measurement of reactive oxygen species (ROS) generation

Generation of intracellular free oxygen radicals was evaluated with dihydrorhodamine 123 (DHR 123; Molecular Probes, Invitrogen, Milan, Italy; Sánchez-Carbente *et al.*, 2005; Jiang *et al.*, 2006). At room temperature, continuously oxygenated, thin slices (250 μm thick) were first incubated in Krebs solution or 1 mM H_2O_2 for 30 min, then treated with 5 μM DHR 123 and the cell-permeable DNA dye Hoechst 33342 (10 mg ⁄ ml stock from Molecular Probes,

Invitrogen; final dilution was 1:1000) in Krebs solution for 20 min. Slices were finally washed, transferred to a glass chamber containing Krebs solution (without fixation) and examined with a TCS SP2 Leica confocal microscope (×40). Hoechst 33342, used to counterstained slices, is a cell-permeable dye that, once bound to dsDNA, emits blue fluorescence. For fluorescence imaging of rhodamine 123 (Rho 123, the oxidized form of DHR 123), slices were visualized by excitation at 514 nm and emission at 530-610 nm. For each slice side and for both hypoglossal nuclei, a 40 μm z-stack (corresponding to one HMs plane) was acquired (5 μm step size); ImageJ software (version 1.43 j, Wayne Rasband, National Institutes of Health, USA) was used to create a 3D reconstruction of every hypoglossal nucleus in order to detect Hoechst 33342 and Rho 123 signal positive voxels. To avoid background noise, an automatic threshold was set for both Rho 123 signal and Hoechst 33342 signal. Data are expressed as ratio of Rho 123 signal positive voxels versus Hoechst 33342 signal positive voxels.

6. Viability assay

At room temperature, continuously oxygenated, thin slices (250 μm thick) were first incubated in Krebs solution or 1 mM H_2O_2 for 30 min or 1 h, then treated with propidium iodide (PI; 1 mg/ml stock from Sigma, Milan, Italy; final dilution was 1:3000) and Hoechst 33342 (10 mg/ml stock; final dilution was 1:1000) in Krebs solution for 45 min. Slices were finally washed, transferred to a glass chamber containing Krebs solution (without fixation) and examined with a TCS SP2 Leica confocal microscope (×40). Hoechst 33342 provided the global number of cells (surviving plus damaged) in each tissue section. PI was used to investigate the number of cells killed by H_2O_2 treatment since it is a cell-impermeable DNA dye which can bind DNA and emits red fluorescence when cell and nuclear membranes have been damaged (Jones & Senft, 1985**)**. For each slice side and for both hypoglossal nuclei, a 40 μm z-stack was acquired (5 μm step size); Leica confocal software was used to create a 2D average projection of each images series along z axis. An in house-written ImageJ software macro was used to count PI and Hoechst positive cells. Images were first converted into binary images with the nuclei coloured in black over a white background. Thereafter, only nuclei of specified size and circularity were analyzed and measurements relative to particles count were displayed. Data are expressed as ratio of PI positive cells versus Hoechst positive cells.

7. Immunohistochemistry

Brainstems removed from P3-P5 rats were cut in two thick (500 μm) slices comprising the nucleus hypoglossus in ice-cold, oxygenated Krebs solution; slices were incubated (under continuous oxygenation) either in Krebs solution or in 1 mM H_2O_2 for 30 min at room temperature, and rinsed. Treated and untreated slices were always processed in parallel to minimize bias. Slices were fixed either immediately for SMI 32 and S100 at the end of H_2O_2 application, or rinsed and kept for 1 h in Krebs solution for ATF-3 staining. To investigate the hypoglossal nucleus expression of neuronal nitric oxide synthase (nNOS) and guanylate cyclase (GC), brainstems removed from P3-P5 rats were immediately fixed. The fixative medium was phosphate-buffered saline (PBS) containing 4% paraformaldehyde (24 h at 4°C) followed by 30% sucrose PBS for cryoprotection (24 h at 4°C). Cryostat tissue sections (30 μm) were collected sequentially and treated with blocking solution (1% fetal calf serum, 5% bovine serum albumin, 0.3% Triton X-100 in PBS) for 1 h at room temperature. Slices were then incubated overnight at 4°C with primary antibodies against SMI 32 (mouse monoclonal, 1:200 dilution, Covance Research Products Inc., Berkeley, CA, USA), ATF-3 (rabbit polyclonal, 1:500 dilution, Santa Cruz Biotechnology, Santa Cruz, CA, USA), S100 (rabbit polyclonal, 1:100 dilution; Dako, Glostrup, Denmark), nNOS (rabbit polyclonal, 1 μg / ml diluition; Invitrogen, Camarillo, CA, USA), GC β1 subunit antibody (rabbit polyclonal, 1:100 dilution; Abcam, Cambridge, UK). β1 subunit is common to the two known GC isoforms, namely α1β1 and α2β1 (Denninger & Marletta, 1999; Koesling *et al*., 2004). AlexaFluor 488 and 594 were used as secondary antibodies (1:500 dilution; Molecular Probes, Invitrogen, Milan, Italy) for 2 h at room temperature. Omission of the primary antibodies did not produce any signal. The use and specificity of SMI 32 and S100 antibodies are detailed in a recent report from our lab (Kuzhandaivel *et al*., 2010). The use of SMI 32 to stain rat motoneurons has been recently validated (Taccola *et al*., 2008; Mazzone *et al*., 2010). Anti-S100 targets the S100B calcium binding protein found in the cytoplasm and nuclei of astrocytes and ependymal cells (Cocchia, 1981; Donato, 2003). In the adult rat brain, both fibrous and protoplasmic astrocytes express S100B (Cocchia, 1981; Didier *et al*., 1986), but only the former express high amount of glial fibrillary acidic protein (GFAP), an intermediate filament protein characteristic for white matter astrocytes (Eng, 1985; Didier *et al*., 1986). According to Miller & Raff (1984), fibrous and protoplasmic astrocytes represent

distint classes of glial cells: the former are located primarily in the white matter, while the latter are found mainly in the gray matter and appear at least one week before fibrous astrocytes. In accordance with this notion, in the P4 rat nucleus hypoglossus, we could observe only very few GFAP (tested with mouse monoclonal anti-GFAP; 1:400; Sigma, Milan, Italy) positive astrocytes in the gray matter (Fig. 16 A) against a strong, diffuse labeling of S100B positive astrocytes (see Results, Fig. 26). To confirm that this observation was a typical characteristic of motor nuclei, we also investigated the presence of GFAP and S100B positive cells in the ventral horn area of the P4 rat spinal cord (Fig. 16 B, C), demonstrating a distribution of such cells analogous to the one in the nucleus hypoglossus. On the basis of the aforementioned considerations, in this report we considered S100B positive cells as protoplasmic astrocytes.

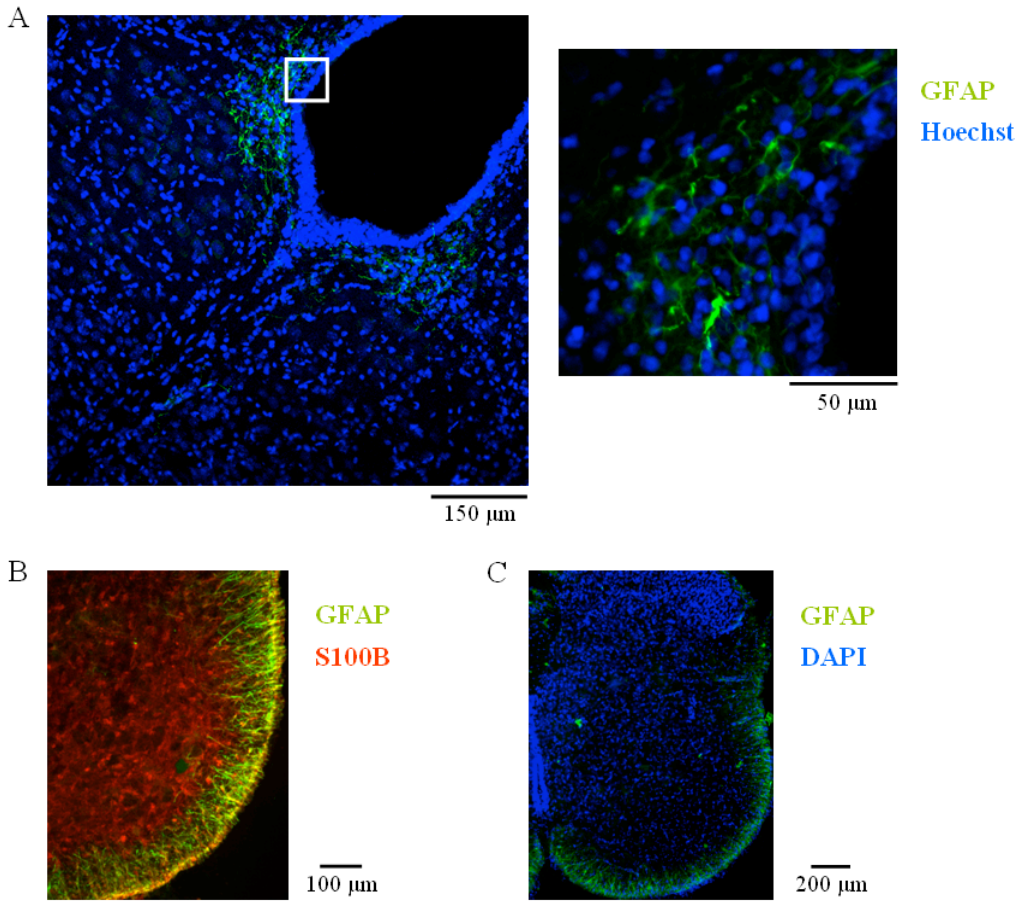

Fig. 16. Astrocyte population in the P4 rat nucleus hypoglossus and spinal cord. (A) Example of a confocal image (20x) of hypoglossal nuclei labeled with GFAP (fibrous astrocyte marker; green pseudocolor) and Hoechst 33342 (blue pseudocolour). The inset (higher magnification) shows how GFAP labeling is limited to the central canal profile. (B) Example of GFAP (green pseudocolor) and S100B (protoplasmic astrocytic marker; red pseudocolor) immunoreactivity of the spinal cord ventral horn (fluorescence microscopy

image, 10x). (C) Histological example of GFAP (green pseudocolor) and DAPI (blue pseudocolor) staining of cells in the rat spinal cord (fluorescence microscopy image, 5x).

After the incubation with the secondary antibody, slices were rinsed and stained with Hoechst 33342. Slices were mounted with Vectashield (Vector Laboratories Burlingame, CA, USA) to avoid photobleaching, and visualized with the confocal microscope (×10; ×20; ×40). For quantifying S100B immunoreactivity, sections were analyzed with ImageJ software. Only astrocytes that showed S-100B staining co-localizing with Hoechst 33342 were counted. CellCounter software (Glance Vision Technologies s.r.l., Trieste, Italy) was used to count SMI 32 immunopositive HMs. CellCounter is a tool for automatic classification and counting of cells; the parameters like cell diameter and signal intensity threshold can be automatically estimated in the sample. Concerning SMI 32 stained images, average parameters setting was: cell diameter, 19.07 μm; intensity threshold, 0.371. The number of SMI 32 positive neurons was similar in untreated and treated brainstem slices (see results). Because the confocal settings used for image acquisition were the same for treated and untreated slices, the average SMI 32 staining intensity was assumed to be identical for treated and untreated slices. Co-staining of ATF-3 and SMI 32 was analyzed on the basis of their covariance. In probability theory and statistics, covariance is a measure of how much two variables change together. Covariance can assume any value between $-\infty$ and $+\infty$. If covariance is positive, the two variables change concordantly; if covariance is negative, the two variables change in an opposite way; finally, two variables whose covariance is zero are called uncorrelated. In our samples, for each images pair of ATF-3 and SMI 32 staining, a function converted red green blue images (I) to graded gray levels (I_g). Thereafter, the average intensity value of every image was subtracted from each pixel intensity ("I_g - average I_g"). The covariance (C) value was the scalar product of the two images ("I_{1g} - average I_{1g}" for ATF-3 and "I_{2g} - average I_{2g}" for SMI 32) divided by the image pixel number according to the equation:

$$C = \langle (I_{1g} - \text{average } I_{1g}), (I_{2g} - \text{average } I_{2g}) \rangle / \text{image pixel number}$$

When the covariance value was significantly higher than control, this indicated stronger ATF-3 staining intensity because the SMI 32 fluorescence remained similar.

Covariance between ATF-3 staining and SMI 32 staining was analyzed by means of a MATLAB 7.1 software macro kindly provided by Dr. Walter Vanzella (Glance Vision Technologies).

8. Statistics

Results were expressed as means ± SEM; n refers to the number of cells or animals, as indicated. For statistical calculations, we used SigmaStat 3.11 (Systat Software, Chicago, IL, USA): in particular, data distribution was first processed with a normality test and, then, with the Student's *t*-test (power of performed test with alpha = 0.050) or the Mann-Whitney test used for parametric or for non-parametric data (for the latter, *T* represents the Mann-Whitney T statistic value, which is the sum of the ranks in the smaller sample group or from the first selected group when both groups are of the same size. This value was compared to the population of all possible rankings in order to determine the occurrence of T). For paired comparison of non-parametric data, Wilcoxon Sign Rank test was applied; the Wilcoxon test statistic W was computed by ranking all the differences before and after the treatment based on their absolute value, then attaching the signs of the difference to the corresponding ranks. The signed ranks were then summed and compared. Concerning association analysis, statistical significance was assessed with the Pearson Product Moment Correlation Coefficient. The Kolmogorov-Smirnov test was used to assess statistical significance for probability distribution. Two groups of data were considered statistically different if $P \leq 0.05$.

Results

1. H_2O_2: an oxidative challenge to HMs

1.1 Application of H_2O_2 induced changes in HM electrophysiological characteristics

Bath-applied H_2O_2 (1 mM; 30 min) increased HM input resistance that, on average, rose from 383±32 MΩ to 408±37 MΩ when measured on the same neurons before and after application (Student's *t*-test, t_5 = 3.922, P = 0.011, n = 6). Fig. 17 A shows, for each cell, normalized data for such a input resistance change that on average was 6±1 % (Wilcoxon Signed Rank Test, W = -21.00, P = 0.031, n = 6). This effect could not be reversed even after prolonged (30 min) washout in four cells, while it was reversible in two of them. Comparable tests run for analogous length of time did not indicate a gradual rise in input resistance under control conditions. The example of Fig. 17 A (inset) indicates that the slope of the linear plot of the current/voltage relation is decreased with extrapolated crossover at -93 mV. The rise in input resistance was accompanied by the onset of an inward current reaching its maximum at ≥ 15 min (-98.3±25.5 pA I_{peak} *versus* -53.3±10.2 pA baseline, Student's *t*-test, t_5 = -2.773, P = 0.039, n = 6; Fig. 17 B) corresponding to a 76±19 % change. Even if the current increase tended to fade towards the end of H_2O_2 application, the inward current amplitude (residual current; I_{res}) was still significantly augmented (61±21 %) when compared to control condition (-88.7±21.7 I_{res} *versus* -53.3±10.2 pA, Student's *t*-test, t_5 = -2.576, P = 0.050, n = 6; Fig. 17 B) with poor recovery on washout (-85.0±22.6 pA). Furthermore, 1 mM H_2O_2 induced global depression of spontaneous postsynaptic currents frequency (0.58±0.15 Hz *versus* 1.75±0.49 Hz control, Student's *t*-test, t_5 = -3.403, * P = 0.019, n = 6), that persisted even after washout (0.41±0.19 Hz, Student's *t*-test, t_5 = -3.784, # P = 0.013, n = 6; see histograms & sample traces in Fig. 1 C). Conversely, there was no significant change in event amplitude caused by H_2O_2 (-48.5±5.3 control *versus* -33.8±5.9 pA in H_2O_2 solution; Student's *t*-test, t_5 = 2.192, P = 0.080, n = 6).

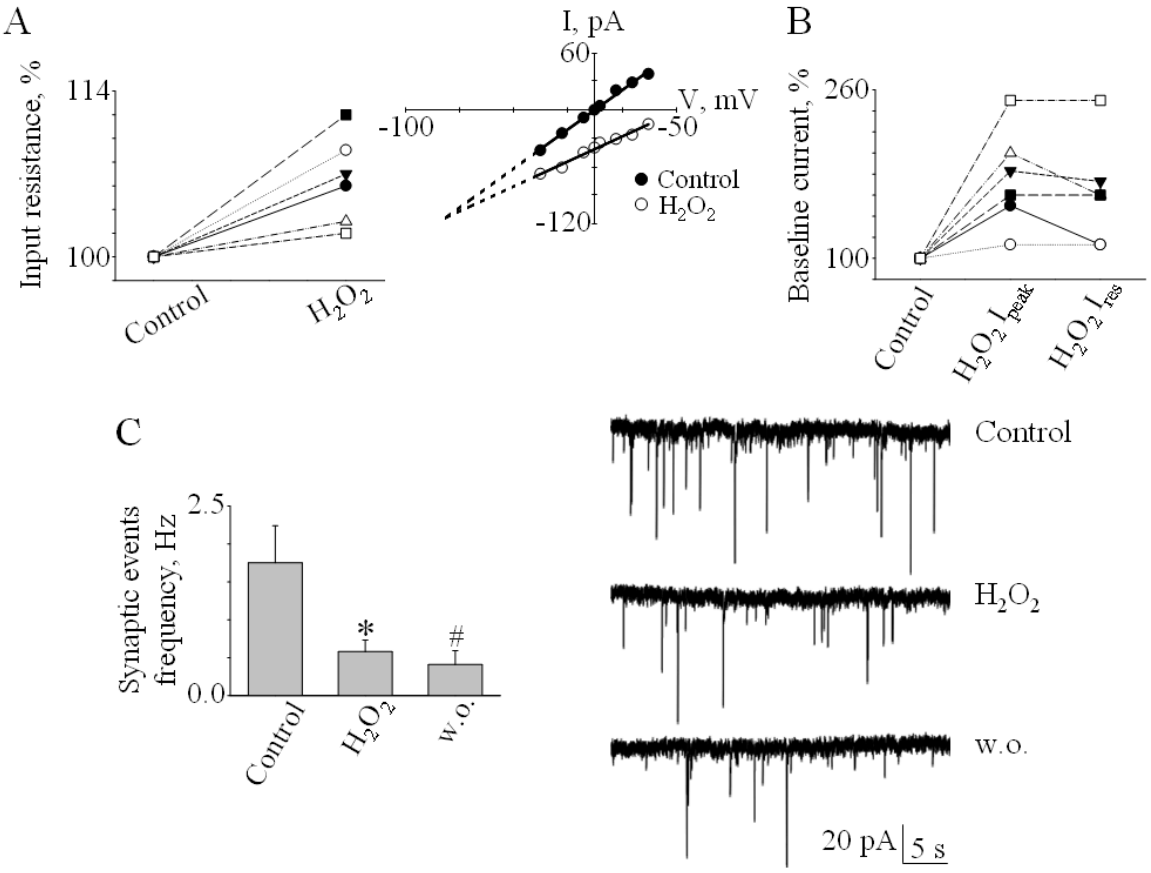

Fig. 17. HM electrophysiological characteristics after application of 1 mM H_2O_2. (A) Increased input resistance observed in voltage-clamp configuration after H_2O_2 application (Student's *t*-test, t_5 = 3.922, P = 0.011, n = 6; 6±1 %, Wilcoxon Signed Rank Test, W = -21.00, P = 0.031, n = 6). Each line represents an individual neuron. Inset shows example of current / voltage plot in control (filled circles) or during application of H_2O_2 (open circles). Note decreased slope of the linear portion of the plot with extrapolated crossover at -93 mV. (B) H_2O_2 caused an inward current reaching its maximum value at ≥ 15 min (H_2O_2 I_{peak}, 76±19 %, n = 6), the effect was maintained for the length of H_2O_2 bath application (residual current following H_2O_2, I_{res}, 61±21 %, n = 6). Each line represents an individual neuron. (C) Fall in spontaneous synaptic events frequency after application of H_2O_2 (Student's *t*-test, t_5 = -3.403, * P = 0.019, n = 6). This effect was not reversible even after prolonged washout (Student's *t*-test, t_5 = -3.784, # P = 0.013, n = 6). Inset (right) shows example of depression of synaptic event frequency by H_2O_2 with poor recovery on washout. w.o., washout.

1.2 Relative contribution by excitatory and inhibitory synaptic transmission to the effects of H_2O_2

Synaptic depression evoked by H_2O_2 might have had a complex origin which we attempted to investigate by studying whether H_2O_2 modulated release of the excitatory transmitter glutamate (O'Brien *et al.*, 1997; Essin *et al.*, 2002) or of the inhibitory transmitters GABA and glycine (Donato & Nistri, 2000). To explore any direct action, we blocked

premotoneuron activity with TTX and looked at the effects of H_2O_2 on motoneuron intrinsic properties and release mechanisms. Table 1 shows that, although TTX per se did not change control input resistance (Student's *t*-test, $t_4 = 0.706$, $P = 0.519$, $n = 5$), it slightly reduced the baseline holding current (Student's *t*-test, $t_4 = 4.921$, * $P = 0.004$, $n = 5$) indicating a tonic contribution by synaptic transmitter release to the baseline current.

Table 1. Average change in input resistance and baseline current induced by application of TTX

Input resistance, MΩ	
Control	183±19
TTX	191±25
Statistics	Student's *t*-test, $t_4 = 0.706$, $P = 0.519$, $n = 5$
Baseline current, pA	
Control	-94.2±19.2
TTX	-51.7±14.1 *
Statistics	Student's *t*-test, $t_4 = 4.921$, * $P = 0.004$, $n = 5$

Fig. 18 A, B illustrates the persistence of the effect of H_2O_2 on input resistance (293±35 MΩ *versus* 208±20 MΩ TTX, Student's *t*-test, $t_5 = 3.176$, * $P = 0.025$, $n = 6$) and baseline holding current (-91.6±15.3 pA I_{peak} *versus* -56.6±14.0 pA TTX, Student's *t*-test, $t_5 = -3.130$, # $P = 0.026$, $n = 6$; -77.5±15.9 pA I_{res}, Student's *t*-test, $t_5 = -2.751$, □ $P = 0.040$, $n = 6$) after blocking ionotropic glutamate receptors with APV (50 μM) and CNQX (10 μM). Unexpectedly, H_2O_2 significantly enhanced mIPSC frequency (3.19±0.59 Hz *versus* 1.55±0.26 Hz TTX, Student's *t*-test, $t_5 = 3.383$, ♦ $P = 0.015$, $n = 6$; Fig. 18 C) without changing their amplitude (-34.3±4.8 pA *versus* -28.6±2.4 pA TTX, Student's *t*-test, $t_5 = -1.200$, $P = 0.275$, $n = 6$; Fig. 18 D).

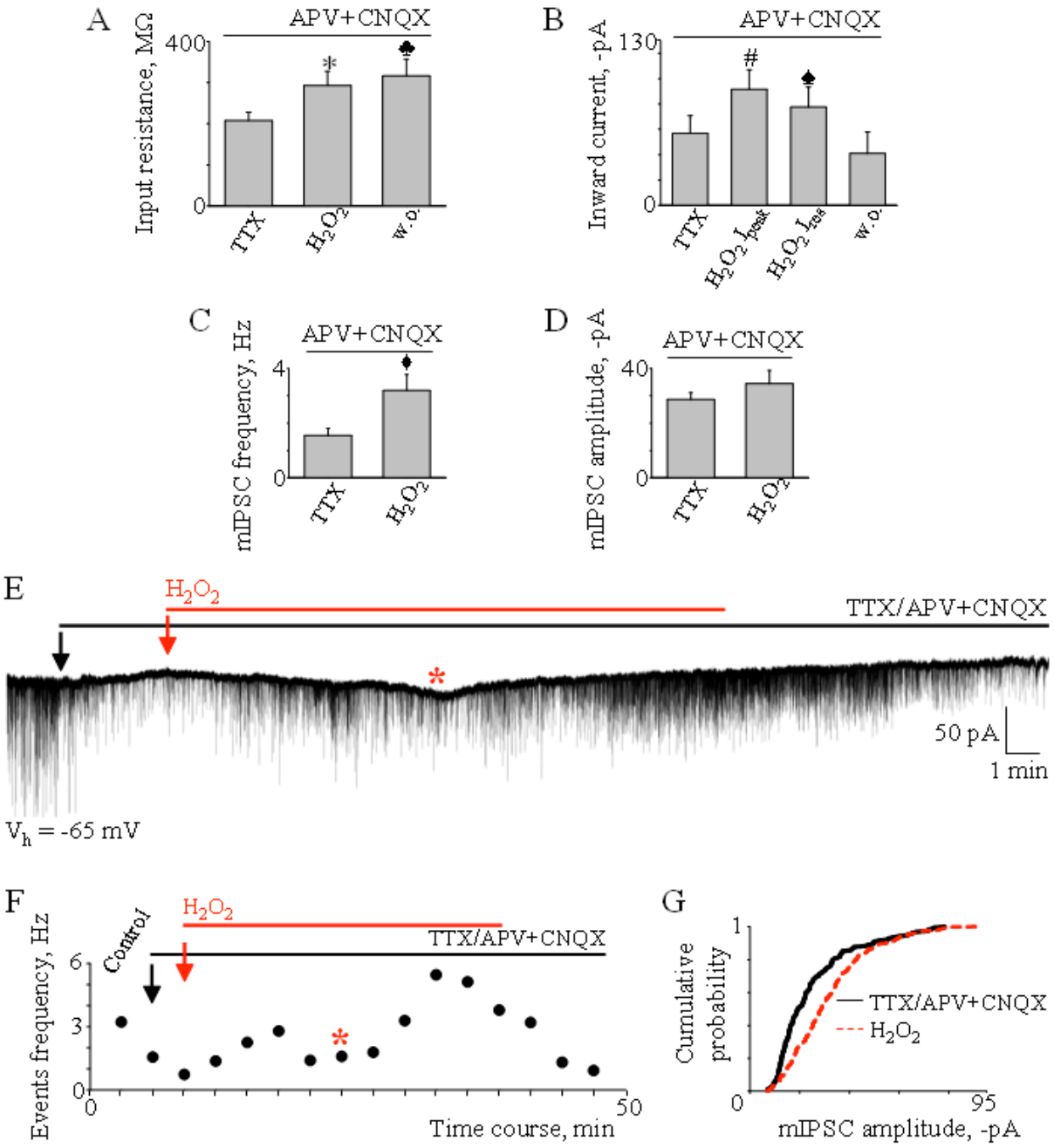

Fig. 18. H_2O_2-induced electrophysiological changes were insensitive to glutamatergic blockers. (A) In the presence of d-amino-phosphonovalerate (APV; 50 μM) and 6-cyano-7-nitroquinoxaline-2,3-dione (CNQX; 10 μM), H_2O_2 increased HM input resistance, an effect not reversible even after prolonged washout (Student's *t*-test, t_5 = 3.176, * P = 0.025 for H_2O_2 vs. control; t_5 = 2.664, ♣ P = 0.045 for w.o. vs. control, n = 6). (B) APV and CNQX did not alter the effect of H_2O_2 on inward current amplitude that rose during the application, reached a maximum value (H_2O_2 I_{peak}, Student's *t*-test, t_5 = -3.130, # P = 0.026, n = 6), and persisted for the duration of the treatment (H_2O_2 I_{res}; Student's *t*-test, t_5 = -2.751, ♠ P = 0.040, n = 6). (C) H_2O_2 significantly increased miniature inhibitory postsynaptic current (mIPSC) frequency (Student's *t*-test, t_5 = 3.383, ♦ P = 0.015, n = 6). (D) mIPSC amplitude did not change following H_2O_2 (Student's *t*-test, t_5 = -1.200, P = 0.275, n = 6). (E) Time course of changes in HM holding current (V_h = -65 mV). Tetrodotoxin (TTX) / APV / CNQX application caused a slight outward current (filled arrow); note slowly developing inward

current following H_2O_2 superfusion (red arrow) that reached its maximum after 15 min treatment (asterisk). The inward current persisted for the length of H_2O_2 application (30 min), although it slowly declined. (F) Time course of mIPSC frequency during TTX/APV/CNQX and H_2O_2 application shows biphasic rise with recovery on washout. Arrows and asterisks correspond to record sections indicated in E. (G) Plot of cumulative probability distribution of mIPSC amplitude that was shifted to the right by 1 mM H_2O_2 (dashed line). In TTX/APV/CNQX condition, the cumulative probability plot comprised 154 events, while after H_2O_2 it included 365 events. w.o., washout.

Fig. 18 E, F exemplifies the timecourse of changes in holding current and mIPSP frequency during H_2O_2 application: after the slight outward current and fall in event frequency observed with the administration of TTX, CNQX and APV (filled arrow), superfusion with H_2O_2 (red arrow) elicited a slow increase in holding current (peaking at 15 min, asterisk) together with a large rise in event frequency, thereafter the holding current faded, despite the persistently high event frequency that was attenuated on washout. Fig. 18 G shows that the action of H_2O_2 consisted in broad increase in the probability of event detection without affecting threshold or maximum. These data, thus, suggest that H_2O_2 not only caused an inward (depolarizing) current, but it also facilitated inhibitory transmitter release through apparently distinct mechanisms.

Parallel tests done after block of glycine and GABA receptors with 0.4 μM strychnine and 10 μM bicuculline (Donato & Nistri, 2000) indicated that H_2O_2 significantly increased input resistance (263±40 MΩ *versus* 227±30 MΩ TTX, Student's *t*-test, $t_5 = 2.396$, * $P = 0.043$, $n = 6$; Fig. 19 A). However, as exemplified in Fig. 20, under these conditions, there was no significant change in baseline holding current (-51.7±7.4 pA I_{peak} *versus* -42.5±6.9 pA TTX, Student's *t*-test, $t_5 = -2.015$, $P = 0.100$, $n = 6$; -50.8±6.8 pA I_{res}, Student's *t*-test, $t_5 = -2.076$, $P = 0.093$, $n = 6$; Fig. 19 B). While the frequency of mEPSCs is usually low (Quitadamo *et al*., 2005; Lamanauskas & Nistri, 2008), H_2O_2 evoked a significant event frequency increase that, on average, was 0.93±0.16 Hz (*versus* 0.58±0.08 Hz in control, Student's *t*-test, $t_5 = 3.130$, # $P = 0.014$, $n = 6$; Fig. 19 C) without altering their amplitude (-12.6±0.9 pA *versus* -15.0±1.2 pA TTX, Student's *t*-test, $t_5 = 2.252$, $P = 0.054$, $n = 6$; Fig. 19 D). Fig. 19 E, F shows that H_2O_2 induced a leftward parallel shift in the event probability plot, and that the largest number of events appeared in the amplitude region of -8 to -12 pA (without changes in holding current; Fig. 20).

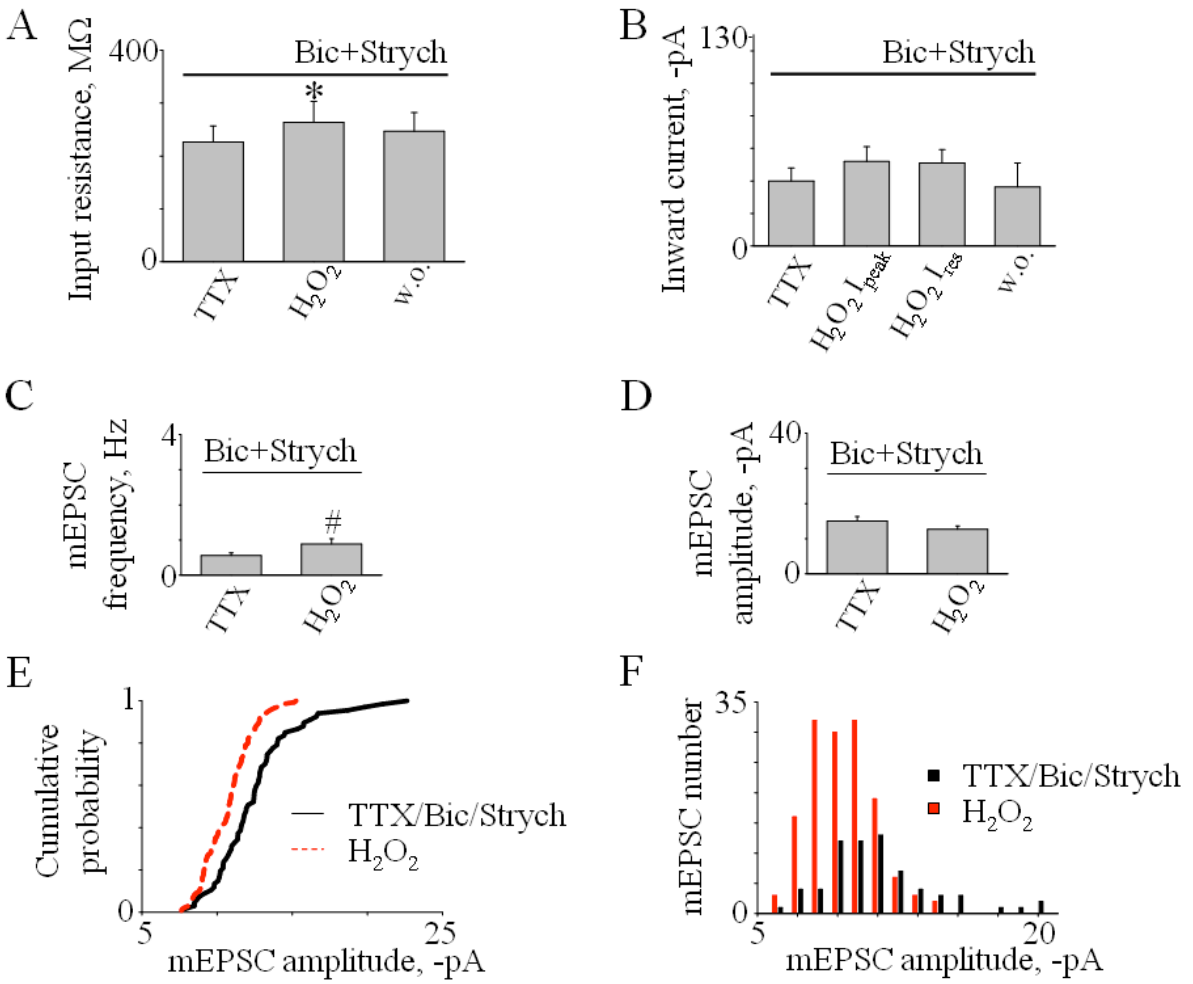

Fig. 19. Contribution of GABAergic and glycinergic transmission to H_2O_2 effects on HM electrophysiological properties. (A) In the presence of bicuculline (10 μM) and strychnine (0.4 μM), H_2O_2 could enhance HM input resistance (Student's *t*-test, $t_5 = 2.396$, * $P = 0.043$, $n = 6$). (B) Blockers of $GABA_A$ and glycine receptors prevented the effect of H_2O_2 on baseline inward current (Student's *t*-test; H_2O_2 I_{peak}, $t_5 = -2.015$, $P = 0.100$; H_2O_2 I_{res}, $t_5 = -2.076$, $P = 0.093$; $n = 6$). (C) In the presence of TTX, H_2O_2 enhanced mEPSC frequency (Student's *t*-test, $t_5 = 3.130$, # $P = 0.014$, $n = 6$) without changing mEPSC amplitude (D; Student's *t*-test, $t_5 = 2.252$, $P = 0.054$, $n = 6$). (E) Plot of cumulative probability distribution of mEPSC amplitude was shifted to the left by H_2O_2 application (dashed line). In TTX/bicuculline/strychnine solution, the cumulative probability plot comprised 67 events, while after H_2O_2 it included 143 events. (F) Histograms showing mEPSC amplitude distribution before and after H_2O_2 treatment; data are from the same cell shown in E.

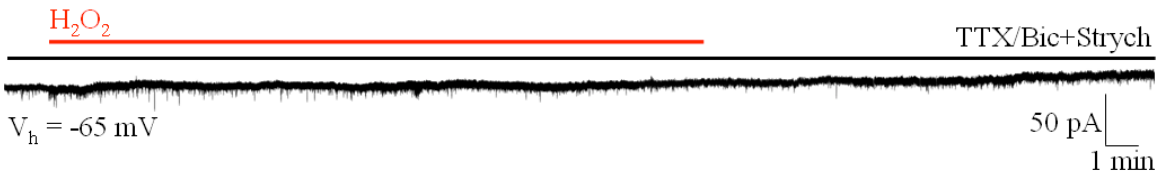

Fig. 20. Example of baseline current recorded (under voltage clamp) from HM in the continuous presence of TTX (1 μM), bicuculline (bic; 10 μM) and strychnine (strych; 0.4

μM) as indicated by the black horizontal bar. Red bar indicates application of H_2O_2 that did not change baseline current. V_h is the holding potential.

These data suggest that miniature excitatory synaptic transmission was also facilitated by H_2O_2 even though the frequency of such events was smaller than the one of inhibitory events. The consistent facilitation of mIPSCs and mEPSCs by H_2O_2 might have been due to a large rise in intracellular free Ca^{2+} to promote transmitter release under resting conditions. Table 2 shows that H_2O_2 significantly enhanced global frequency of miniature events (Student's *t*-test, $t_4 = 3.706$, $P = 0.021$, $n = 5$), an effect mimicked by thapsigargin (1 μM, Student's *t*-test, $t_4 = 2.932$, $P = 0.043$, $n = 5$) that, by blocking Ca^{2+} store pumps, is known to increase intracellular Ca^{2+} (Kirby *et al*., 1992; Reyes & Stanton, 1996; Takahashi *et al*., 2007; Table 2).

Table 2. Similar effects of H_2O_2 and thapsigargin on miniature events frequency

	Miniature frequency, Hz	Student's t_4 value	*P* - value	n
TTX	0.54±0.08	3.706	0.021	5
TTX + H_2O_2	2.33±0.54			
TTX	0.34±0.05	2.932	0.043	5
TTX + thapsigargin	0.99±0.27			

1.3 H_2O_2 treatment modulated persistent Na^+ and Ca^{2+} currents

Our experiments indicated how H_2O_2 affected synaptic transmission and intrinsic properties of HMs, but they did not show if there were also changes in excitability within the membrane potential region of repeated HM firing. Previous studies have shown that persistent inward currents (PICs) expressed by the soma of HMs (Moritz *et al*., 2007) contribute to integration of motoneuron signals for patterned output (Brownstone, 2007), and are mediated by sustained influx of Na^+ and / or Ca^{2+} (Crill, 1996; Russo & Hounsgaard, 1999). Because persistent Na^+ conductance - PIC(Na) - is reported to be increased in motoneurons of the presymptomatic ALS genetic mouse model (Kuo *et al.*, 2005; van Zundert *et al.*, 2008), we explored the possibility that H_2O_2 could affect PICs using a slow ramp protocol (see top schemes in Fig. 21 A, B). In accordance with previous studies (Crill, 1996; Russo & Hounsgaard, 1999; Lamanauskas & Nistri, 2008), we assumed that the Mn^{2+}-sensitive component represented the persistent Ca^{2+} conductance - PIC(Ca) - while the TTX-sensitive

component represented PIC(Na). Fig. 21 A shows an example of global PIC observed in control conditions (Krebs). This response (attenuated by 1 μM TTX to pharmacologically isolate PIC(Ca)) was largely inhibited by H_2O_2 (1 mM; 30 min) as indicated by the superimposed traces of the current responses in the inset to Fig. 21 A. Average data are given in Table 3.

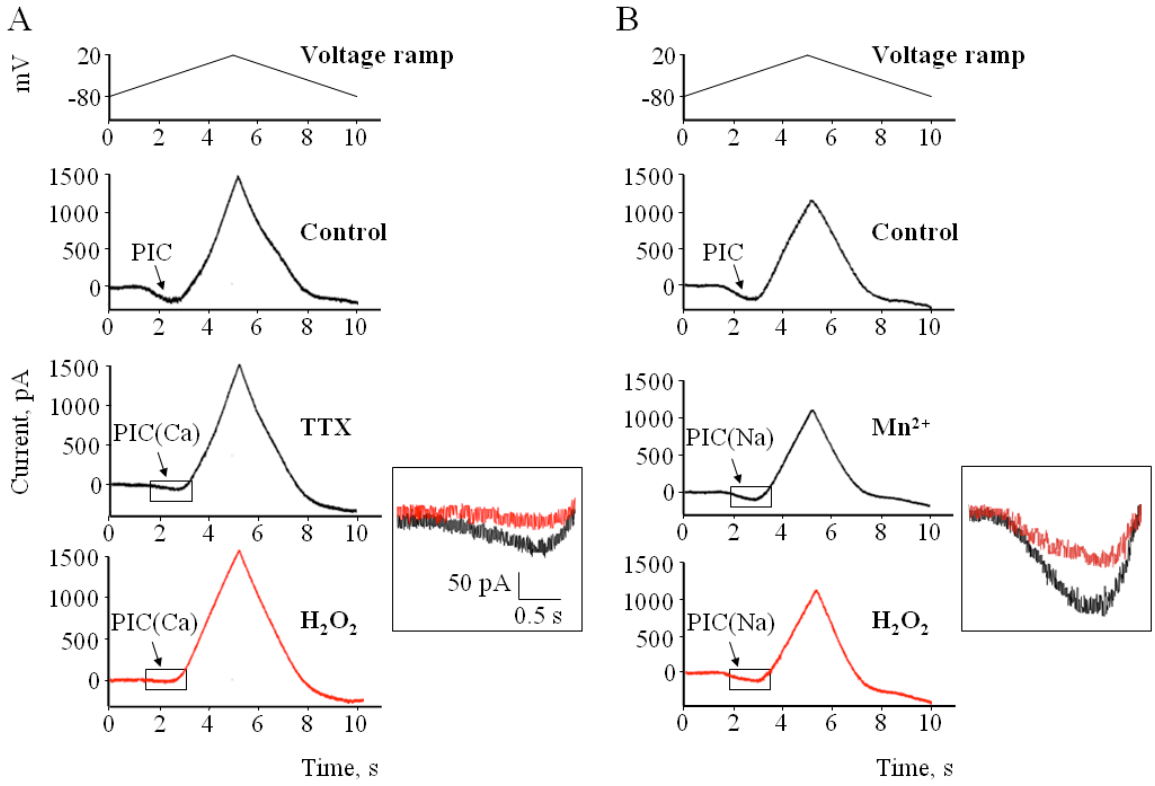

Fig. 21. Voltage-activated PICs were modulated by H_2O_2. (A) On HMs, voltage ramps (from -80 to +20 mV; rate = 21 mV/s; see top scheme) induced PICs (mediated by Na^+ and Ca^{2+}; see arrow) followed by a large outward current in control solution (Krebs). TTX (1 μM) was applied to pharmacologically isolate PIC(Ca) (Crill, 1996; Russo & Hounsgaard, 1999). After H_2O_2 application, PIC(Ca) was depressed as indicated by the superimposed traces of the current responses in the inset. (B) PIC(Na) current, isolated after PIC(Ca) block with 2 mM Mn^{2+}, was also reduced following application of H_2O_2. The superimposed records in the inset depict the reduction (larger current and time bars). Calibrations in inset to A apply also to inset to B.

In a separate set of experiments we applied 2 mM Mn^{2+} to measure PIC(Na) in isolation (Fig. 21 B). Adding Mn^{2+} reduced the amplitude of the global PIC and disclosed PIC(Na) that, following H_2O_2 application, was decreased as depicted by the superimposed records in the inset to Fig. 21 B. Summary data from these tests with Mn^{2+} are shown in Table 3. On average, it appears that H_2O_2 decreased PIC(Ca) amplitude and area by 79 %, while the corresponding falls in PIC(Na) amplitude and area were 38 % and 50 %, respectively,

without any significant variation of activation thresholds. We did not observe recovery in the PIC(Na) or PIC(Ca) amplitude after washout.

Table 3. Persistent inward currents in the presence of H_2O_2

	Amplitude, pA	Area, pA\ms	Threshold, mV
PIC	209 ± 26 *	231 ± 41 □	-60.9 ± 1.2
PIC(Ca)	97 ± 16 #	81 ± 16 ♥	-55.4 ± 3.2
PIC(Ca) after H_2O_2	21 ± 5 □	17 ± 5 ♣	-56.5 ± 2.3

n = 7 for all cases. Amplitude: t_6 = -3.395, P = 0.015 for # *vs*. *; t_6 = -4.860, P = 0.003 for □ *vs*. #; Area: t_6 = -3.106, P = 0.021 for ♥ *vs*. □; t_6 = -3.969, P = 0.007 for ♣ *vs*. ♥; Threshold: t_6 = 1.857, P = 0.122 for PIC(Ca) *vs*. PIC; t_6 = -0.346, P = 0.743 for PIC(Ca) after H_2O_2 *vs*. PIC(Ca).

	Amplitude, pA	Area, pA\ms	Threshold, mV
PIC	127 ± 22 *	133 ± 28 □	-60.4 ± 1.5
PIC(Na)	72 ± 15 #	74 ± 15 ♥	-56.8 ± 2.5
PIC(Na) after H_2O_2	45 ± 15 □	37 ± 12 ♣	-57.4 ± 2.3

n = 5, Amplitude: t_4 = -6.835, P = 0.002 for # *vs*. *; t_4 = -3.056, P = 0.038 for □ *vs*. #; Area: t_4 = -4.164, P = 0.014 for ♥ *vs*. □; t_4 = -5.421, P = 0.006 for ♣ *vs*. ♥; Threshold: t_4 = 2.640, P = 0.058 for PIC(Na) *vs*. PIC; t_4 = -0.535, P = 0.621 for PIC(Na) after H_2O_2 *vs*. PIC(Na). Symbols refer to Student's *t*-test comparison between data pairs.

1.4 Hyperexcitability of HMs treated with H_2O_2

The PIC inhibiting ability of H_2O_2 was surprising in view of the reported hyperexcitability of motoneurons from presymptomatic ALS genetic models (Kuo *et al.*, 2005; van Zundert *et al.*, 2008). Hence, we investigated whether H_2O_2 might influence rat HM firing properties. Fig. 22 A shows an example of HM responses to bath applied H_2O_2 at resting membrane potential (V_m) of -65 mV (on average, initial V_m was -63±1 mV; n = 26). Following application of H_2O_2, there was gradual membrane depolarization (7 mV; on average, V_m after H_2O_2 was -59±1, Student's *t*-test, t_{25} = 5.186, $P \leq 0.001$, n = 26) that persisted during washout. We used rectangular current pulses to induce repeated firing and to detect the sensitivity of spike activity to H_2O_2. Current steps (300 pA for 500 ms) injected into HMs evoked firing as

exemplified in Fig. 22 A, B. In control condition, this motoneuron fired 14 spikes (Fig. 22 B, left trace), while, during H_2O_2 application, the HM (repolarized to the original V_m), responded with 26 spikes superimposed on the larger amplitude of the membrane voltage change (Fig. 22 B, right trace). The example of Fig. 22 C shows a plot of instantaneous firing frequency *versus* time (during the 500 ms pulse) in control (filled circles) or in the presence of H_2O_2 (open circles). There was an upward shift of the graph that was best fitted with double exponential (τ_1 and τ_2) decay (in accordance with the study by Sawczuk *et al*., 1995) with values of 0.01 s τ_1 and 8.33 s τ_2 for control, and 0.02 s τ_1 and 11.11 s τ_2 for H_2O_2 treatment. The adequacy of the fit was confirmed by the correlation values $r = 0.9980$ and 0.9925 for control and H_2O_2, respectively.

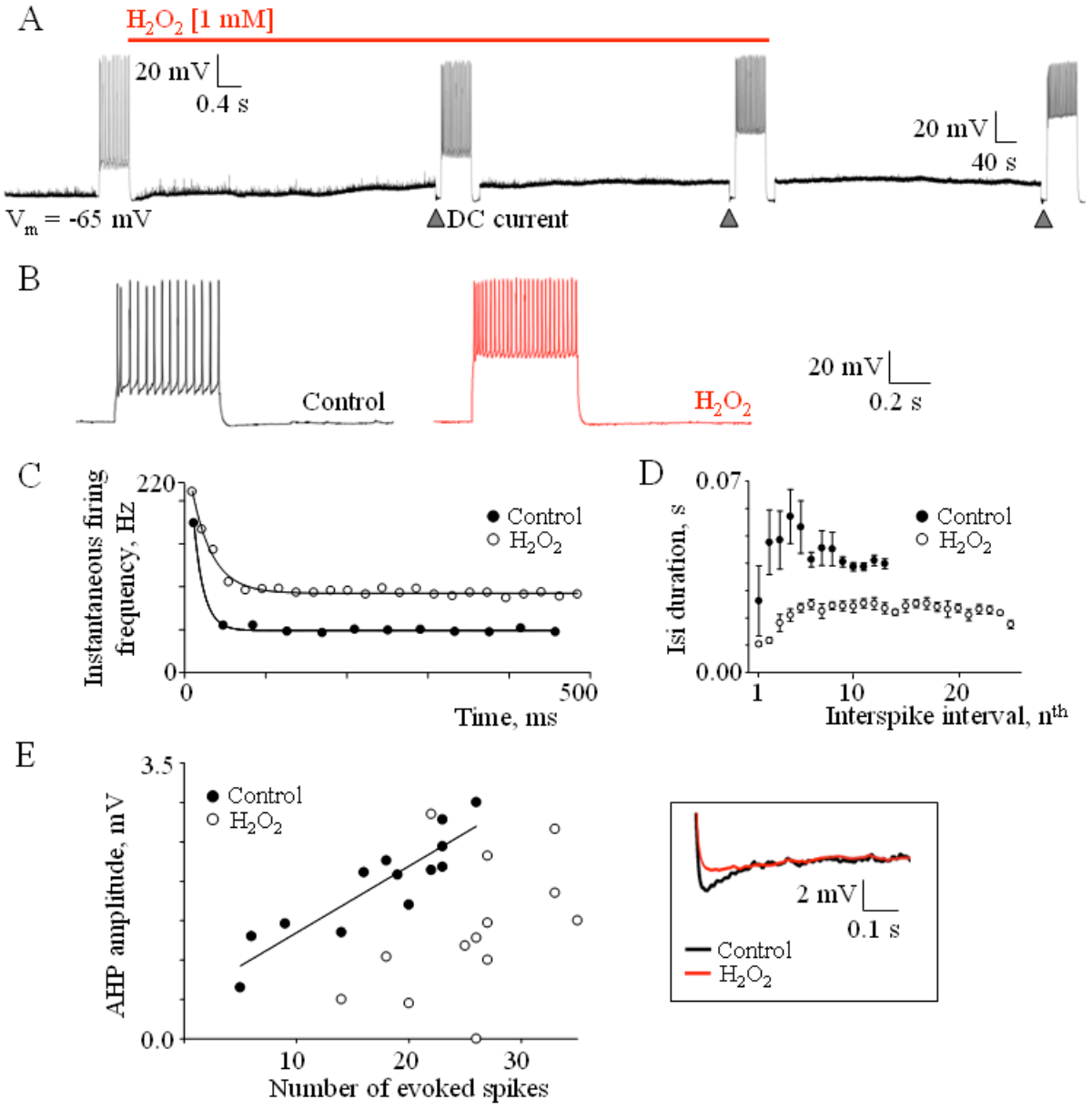

Fig. 22. Changes in HM excitability induced by H_2O_2. (A) Examples of responses of HM to bath applied H_2O_2. Trace is a continuous, slow record of a cell with initial V_m of -65 mV. Segments of this trace are also shown on a faster time base to depict spike firing evoked by intracellular injection of 300 pA (500 ms). Note that, following application of H_2O_2, there is gradual membrane depolarization (7 mV) associated with enhanced spike activity (when the V_m is repolarized back to rest). Prolonged washout was not able to reverse the observed effects. (B) Fast time base example of evoked firing (300 pA; 500 ms) in control and after H_2O_2 application. Note the higher number of spikes and the larger amplitude of the membrane voltage response to the same current injection pulse following H_2O_2. (C) Example of instantaneous firing frequency in control (filled symbols) and following H_2O_2 application (open symbol). Data are fitted with double exponential function in accordance with Sawczuk et al. (1995). (D) Plot of average (n = 6 cells) interspike interval (isi) *versus* spike interval in the 500 ms train. Data were fitted with a cubic polynomial function (see methods) and the curves difference integral for the first 13 spikes calculated. Subtraction of the treated area (open circles) from control (filled circles) gave $\int_1^{13} (y_1 - y_2) = 0.6141$, indicating the change evoked by H_2O_2. Control area was $\int_1^{13} y_1 = 1.1206$. After normalization, the H_2O_2-mediated decrease in area was equal to 0.6141/ 1.1206 * 100 = 55 %. (E) Scatter plot of the AHP amplitude versus the number of evoked spikes in control condition (filled symbols) and following H_2O_2 bath application (open symbols). AHP amplitude was measured at the end of a 300 pA depolarizing current pulse, applied at the same V_m before and after H_2O_2 treatment (n = 13). In control condition, the AHP amplitude increased with the number of evoked spikes (regression equation: y = 0.08 x + 0.50; $r = 0.895$; $P \leq 0.001$). In the presence of H_2O_2 the linear relation was lost ($r = 0.437$; $P = 0.135$) and, despite the larger number of action potentials, the AHP amplitude was decreased (Student's t-test, $t_{12} = 2.335$, $P = 0.038$, n = 13). The inset shows that, at -65 mV, superimposed AHPs (evoked by 20 spikes) were markedly different between control (1.70 mV; black trace) and H_2O_2 solution (0.45 mV; red trace).

Fig. 22 D demonstrates that, on 6 cells held at the same membrane potential (-65 mV), there was a relatively consistent interspike interval value throughout the firing phase when H_2O_2 was applied (open circles; see Lape and Nistri, 2000), unlike the complex changes detected prior to the treatment. Using the function described in the methods for fitting data of Fig. 22 D, we observed a 55 % area difference between controls and H_2O_2-treated responses.

Averaging out data for 26 HMs showed that H_2O_2 significantly enhanced the mean firing frequency (45±2 Hz *versus* 31±2 Hz, Student's t-test, $t_{25} = 9.588$, $P \leq 0.001$, $n = 26$). This phenomenon was accompanied by a significant rise in input resistance (179±15 MΩ *versus* 128±9 MΩ control; Student's t-test, $t_{25} = 4.986$, $P \leq 0.001$, $n = 26$). Table 4 shows that H_2O_2 increased input resistance, spike firing and evoked membrane depolarization even when applied in the presence of APV and CNQX, or bicuculline and strychnine, suggesting that these effects were, at least in part, due to a direct action on HMs.

Table 4. Changes in input resistance, average firing frequency and membrane potential evoked by H_2O_2 in standard solution or in the presence of blockers of glutamatergic

transmission (CNQX and APV) or inhibitory synaptic transmission (bicuculline and strychnine).

	Input resistance MΩ	Firing frequency Hz	Membrane potential mV
Control	117±15	17±4	-63±1
H_2O_2	169±16 *	33±5 *	-56±2 *
Statistics	Student's *t*-test, $t_5 = 5.234$, * $P = 0.003$, $n = 6$	Student's *t*-test, $t_5 = 5.237$, * $P = 0.003$, $n = 6$	Student's *t*-test, $t_5 = 6.740$, * $P = 0.001$, $n = 6$
APV+CNQX	138±17	32±3	-62±1
APV+CNQX+ H_2O_2	203±30 *	46±2 *	-60±2 *
Statistics	Student's *t*-test, $t_9 = 3.627$, * $P = 0.006$, $n = 10$	Student's *t*-test, $t_9 = 5.659$, * $P \leq 0.001$, $n = 10$	Student's *t*-test, $t_9 = 2.473$, * $P = 0.035$, $n = 10$
Bic+Strych	128±7	36±3	-64±1
Bic+Strych+H_2O_2	162±13 *	49±4 *	-61±1 *
Statistics	Student's *t*-test, $t_9 = 2.729$, * $P = 0.020$, $n = 10$	Student's *t*-test, $t_9 = 5.180$, * $P \leq 0.001$, $n = 10$	Student's *t*-test, $t_9 = 5.842$, * $P \leq 0.001$, $n = 10$

Ca^{2+}-activated K^+ conductances responsible for the spike afterhyperpolarization (AHP) are activated by PIC(Ca) in rat motoneurons (Li & Bennett, 2007) and powerfully modulate the cell excitability (Rekling *et al.*, 2000b; Kuo *et al.*, 2005). Since our results demonstrated that H_2O_2 induced a preferential reduction of PIC(Ca) associated with hyperexcitability in rat HMs, we wondered if these effects could be explained by decreased AHP amplitude by H_2O_2. Thus, we measured the amplitude of the slow AHP at the end of the 300 pA depolarizing current pulse (at the same V_m before and during H_2O_2 application) and correlated it to the number of spikes (Fig. 22 E, $n = 13$). In control condition (filled symbols), there was the expected linear relation between the AHP amplitude and the spikes number ($r = 0.895$, $P \leq 0.001$). In the presence of H_2O_2 (Fig. 22 E, open symbols), not only this relation was lost ($r = 0.437$, $P = 0.135$), but the AHP amplitude was reduced in spite of augmented firing (1.39±0.24 mV *versus* 1.96±0.18 mV control, Student's *t*-test, $t_{12} = 2.335$, $P = 0.038$, $n = 13$). The inset to Fig. 22 E shows that, at -65 mV, superimposed AHPs (evoked by 20 spikes) were markedly different in amplitude between control (1.70 mV; black trace) and H_2O_2 solution (0.45 mV; red trace).

1.5 H_2O_2 was effective in inducing oxidative stress damage to HMs

To demonstrate the HM redox stress induced by 1 mM H_2O_2, we used dihydrorhodamine 123, a non-fluorescent and lipophilic molecule that, by oxidation, yields the fluorescent probe rhodamine 123 (Sánchez-Carbente *et al.*, 2005; Jiang *et al.*, 2006). Fig. 23 A compares confocal images of intracellular generation of reactive oxygen species (ROS, red pseudocolour) following incubation (for 30 min) in Krebs solution (top, left) or H_2O_2 (bottom, left). Hoechst 33342 was used as a cell counterstain (blue pseudocolour). Note that, despite the analogous number of Hoechst positive cells in either condition, the number of rhodamine 123 positive cells (with >25 µm soma) was higher following H_2O_2. These observations are quantified in the histograms of Fig. 23 B in which the confocal images throughout the slices were reconstructed in 3D and the rhodamine signal expressed as fraction of the Hoechst 33342 one (0.26±0.04 *versus* 0.13±0.05, Mann-Whitney Rank Sum Test, $T = 489.00$, * $P = 0.002$, $n = 5$ rats).

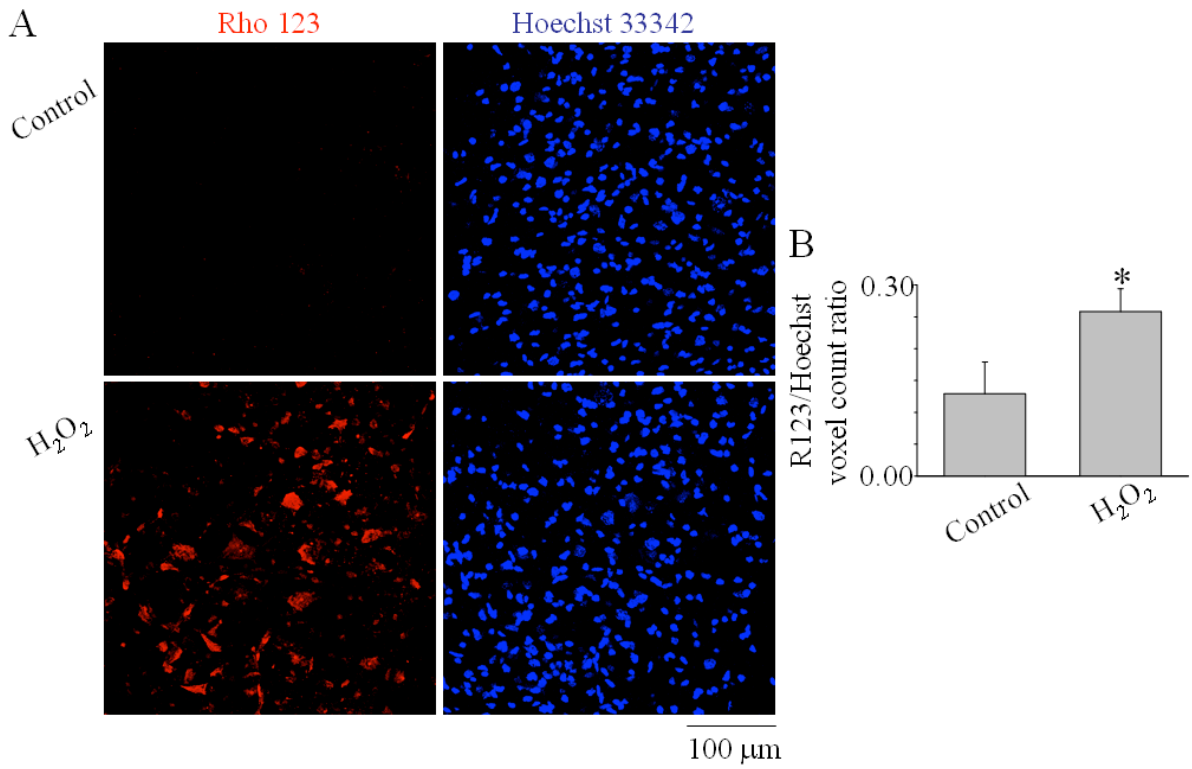

Fig. 23. Oxidative stress of HMs caused by H_2O_2. (A) Histological example of rhodamine 123 staining of cells in hypoglossal slices incubated for 30 min in Krebs solution or in the presence of H_2O_2 (1 mM). After rinsing, cells were stained with dihydrorhodamine 123 (red pseudocolour) to reveal intracellular oxidative processes (Sánchez-Carbente *et al.*, 2005; Jiang *et al.*, 2006) and Hoechst 33342 (blue pseudocolour) to show cell nuclei. Note that, notwithstanding the analogous number of Hoechst positive cells, there was a larger number

of rhodamine 123 positive, large soma cells following H_2O_2. (B) Histograms show the ratio of rhodamine positive cells over Hoechst positive cells, indicating a significant rise after H_2O_2. Data are from 5 animals and were quantified with ImageJ software (Mann-Whitney Rank Sum Test, $T = 489.00$, * $P = 0.002$).

1.6 H_2O_2 did not alter short-term cell survival

Since H_2O_2 application was accompanied by increased intracellular oxidative processes, we next addressed the question whether this phenomenon actually affected HM survival. First, we investigated the consequence of H_2O_2 application on the global hypoglossal nucleus cell population (Kitamura *et al.*, 1983; Boone & Aldes 1984; Viana *et al.*, 1990) in unfixed specimens using the nuclear dye PI, which penetrates into cells only after membrane disruption (Kristensen *et al.*, 2001; Bonde *et al.*, 2003; Babot *et al.*, 2005; Bösel *et al.*, 2005). The total number of cells (intact as well as damaged) within each hypoglossal nucleus section was estimated with Hoechst 33342. Fig. 24 A shows staining with PI and Hoechst 33342 within the nucleus hypoglossus after incubation in Krebs solution (left) or after applying H_2O_2 for 30 min (top right) or 1 h (bottom right). In each example there was presence of co-staining, indicating a degree of cell damage in control or after treatment. Quantification of these observations (Fig. 24 B) demonstrates that after either 30 min or 1 h application of H_2O_2 there was no significant increase in cell death (Mann-Whitney Rank Sum Test, $T = 1283.00$ or 919.00, $P = 0.240$ or 0.202 for 30 min or 1 h, respectively, $n = 8$ rats). Likewise, analysis of HM numbers with the motoneuron marker SMI 32 (Fig. 24 C), a monoclonal antibody against the non-phosphorylated form of neurofilament H (Jacob *et al.*, 2005; Raoul *et al.*, 2005), confirmed similar presence in control (Krebs, left) or after H_2O_2 application (right). The histograms of Fig. 24 D related to the sampled area (see inset to Fig. 24 D) indicate that, on average, H_2O_2 did not change the number of HMs within the nucleus hypoglossus (53±1 *versus* 50±4, Mann-Whitney Rank Sum Test, $T = 25.00$, $P = 0.690$, $n = 5$ rats).

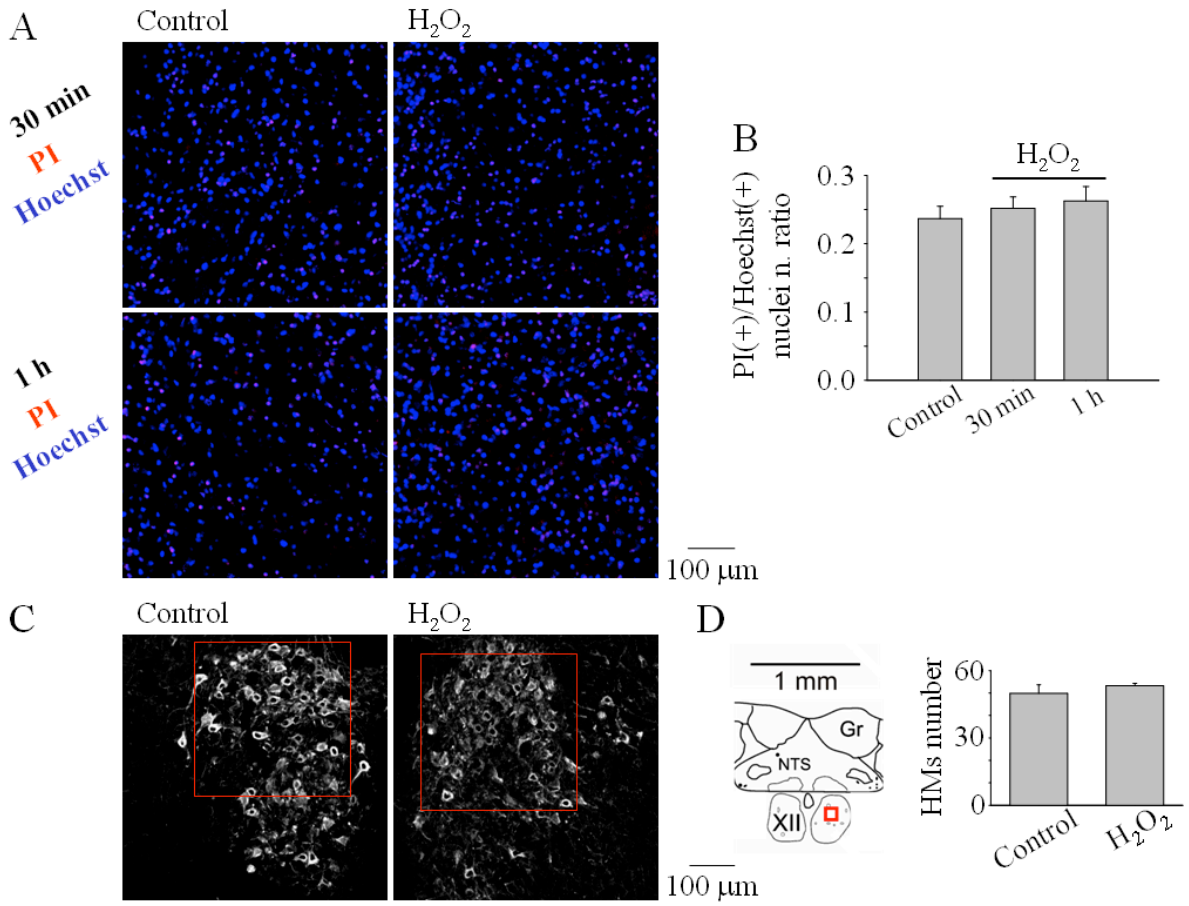

Fig. 24. H_2O_2 did not alter short-term cell survival. (A) Examples of fluorescence cell counts after staining with PI, a DNA dye that labels membrane-damaged cells (red pseudocolour), and Hoechst 33342 (blue pseudocolour) in two experimental protocols: Krebs *versus* either 30 min H_2O_2 (top row) or 1 h H_2O_2 (bottom row). In each panel, PI positive cells are indicative of dead cells. (B) Histograms showing no increase in cell death after exposure to either 30 min H_2O_2 or 1 h H_2O_2 (control value comprises cells damaged by the brain-slicing preparation). Data (collected from 8 rats) were quantified with ImageJ software and expressed as ratio of PI positive cells over Hoechst positive cells. Mann-Whitney Rank Sum Test gave $T = 1283.00$, $P = 0.240$ for the difference between Krebs and 30 min H_2O_2; $T = 919.00$, $P = 0.202$ for the difference between Krebs and 1 h H_2O_2. (C) Example of confocal images of HMs labeled with the motoneuron marker SMI 32 (Jacob *et al.*, 2005; Raoul *et al.*, 2005) in control condition and after 30 min H_2O_2 (the red box is the sample area used to count HMs). (D) Left, scheme of sampled area used for confocal images, shown in red within one nucleus hypoglossus. Right, histograms quantifying the number of HMs (SMI 32 positive) with no significant difference between control and H_2O_2 treatment. Data were quantified with CellCounter (Mann-Whitney Rank Sum Test, $T = 25.00$, $P = 0.690$, $n = 5$ rats).

1.7 ATF-3 expression by HMs treated with H_2O_2

The dissociation between intracellular redox stress and unchanged survival of HMs after H_2O_2 application, led us to look for a biomarker that could signal motoneuron damage. For this purpose, we used ATF-3, a member of the ATF / CREB family of transcription factors,

whose expression has been shown to rise after injurious stimuli (Tsujino *et al.*, 2000; Hai & Hartman, 2001; Vlug *et al.*, 2005). Fig. 25 A shows staining by ATF-3 (bottom) or SMI 32 (top) of hypoglossal nuclei fixed 1 h after washout of 1 mM H_2O_2 (right) or control solution (left). While the total number of HMs (SMI 32 immunopositive cells) was comparable between control (Krebs) and after H_2O_2, HMs expressing ATF-3 were more frequently detected in slices treated with H_2O_2. We next quantified the simultaneous occurrence of SMI 32 and ATF-3 within the same HMs. For this purpose we expressed co-staining for these markers as covariance values (see methods). Fig. 25 B summarises these observations: whereas in Krebs solution the covariance value between ATF-3 and SMI 32 fluorescence was 139±50, this value significantly increased to 434±128 in the presence of H_2O_2 (Mann-Whitney Rank Sum Test, $T = 46.00$, * $P = 0.021$, $n = 8$ rats).

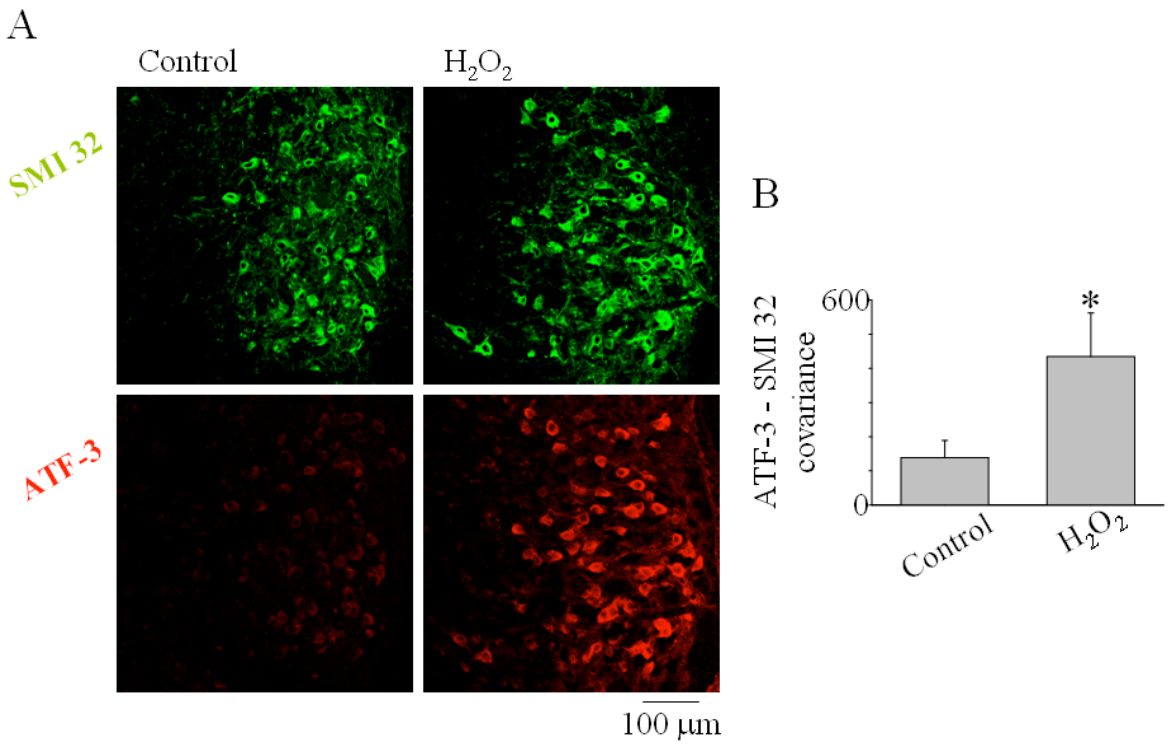

Fig. 25. ATF-3 expression by HMs treated with H_2O_2. (A) Examples of SMI 32 (top) and ATF-3 (bottom) immunoreactivity of nucleus hypoglossus in control (left) and after H_2O_2 (right). Note that, despite a similar number of HMs (SMI 32 positive), ATF-3 staining was highly enhanced following H_2O_2. ATF-3, a member of the ATF / CREB family of transcription factors, is proposed to be a marker of neuronal injury (Tsujino *et al.*, 2000; Hai & Hartman, 2001; Vlug *et al.*, 2005). (B) Histograms show the covariance between ATF-3 staining and SMI 32 staining, indicating a significant rise after H_2O_2. Data are from 8 animals and were quantified with MATLAB 7.1 software (Mann-Whitney Rank Sum Test, $T = 46.00$, * $P = 0.021$).

1.8 H_2O_2 did not alter S100B immunoreactivity of protoplasmic astrocytes

In ALS non-neuronal cells play key roles in disease etiology and loss of motoneurons (Clement *et al*., 2003; Boillée *et al*., 2006). Therefore, our aim was to investigate whether astroglial cells were affected by H_2O_2 application.

The anti-S100 polyclonal antibody targets the S100B calcium binding protein found in the cytoplasm and nucleus of protoplasmic astrocytes (see Material & Methods). Former studies have reported changes in S100B immunoreactivity in association with brain damage and degenerative brain disease including ALS (Migheli *et al.*, 1999; Rothermundt *at al.*; 2003; Blackburn *et al.*, 2009). Fig. 26 A shows that 30 min application of H_2O_2 did not change S100B immunolabeling in the nucleus hypoglossus as compared to control slices. Quantification of S100B immunopositive cells is shown in the histograms of Fig. 26 B (63±3, control; 59±2, H_2O_2; Student's *t*-test, $t_{32} = 0.938$, $P = 0.355$, $n = 3$ rats).

This observation suggests that the oxidative challenge exerted by H_2O_2 did not produce early damage to astroglia in the nucleus hypoglossus.

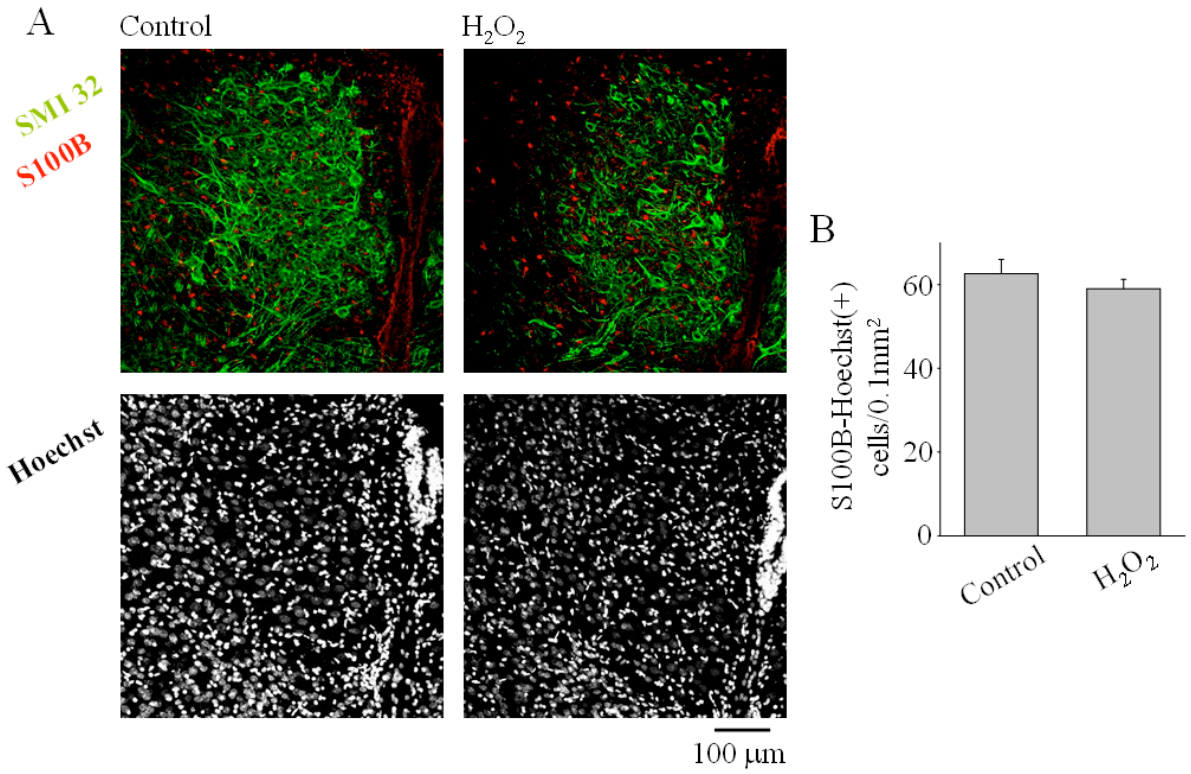

Fig. 26. S100B immunolabeling in the nucleus hypoglossus after H_2O_2 treatment. (A) Examples of confocal microscopy images showing S100B+SMI 32 (top row; red and green pseudocolors, respectively) and Hoechst 33342 (bottom row; gray pseudocolor) immunoreactivity of nucleus hypoglossus after 30 min incubation in control (left), or 1 mM H_2O_2 (right). Note that S100B immunoreactivity was also present in ependymal cells (see

Material & Methods). (B) Histograms quantify the number of cells positive to both S100B and Hoechst 33342 staining (identified as protoplasmic astrocytes, see Material & Methods) in both conditions. Data were quantified with ImageJ software (Student's *t*-test, $t_{32} = 0.938$, $P = 0.355$, $n = 3$ rats).

2. Sodium nitroprusside and nitrosative stress

2.1 HM electrophysiological changes induced by NaNP treatment

Nitric oxide (NO) is a well-known signaling molecule, identified more than two decades ago as an endothelium-derived relaxing factor (Palmer *et al*., 1987; Furchgott, 1999) with potent vasodilator activity. Since then, increasing numbers of biochemical pathways have been shown to be modulated by NO. Imbalance of NO signaling has also been linked to different human diseases. In particular, increasing evidence suggests that S-nitrosylation is involved in the pathogenic process of various neurodegenerative disorders like ALS (Beal *et al*., 1997).

Thus, we decided to investigate the effect of nitrosative stress on HM by bath-applying 500 µM sodium nitroprusside (NaNP), a NO donor (Southam & Garthwaite, 1991; Dawson *et al*., 1993; Liu & Martin, 2001; Hall *et al*., 2009).

Fig. 27 A shows an example of HM response (V_h = -60 mV) to bath applied NaNP (500 µM). Following application of the NO donor, there was the onset of an outward current which stabilized at plateau within ≈ 1 min. This outward current lasted throughout the treatment (usually 30 min), with no recovery on washout. On average, baseline current was -117±18 pA in control, -68±10 pA after both NaNP treatment and washout (Student's *t*-test, $t_9 = -4.396$, * $P = 0.002$ for NaNP *versus* control; $t_9 = -3.741$, # $P = 0.005$ for w.o. *versus* control; $n = 10$; Fig. 27 B). The change in baseline current was accompanied by a rise in input resistance (250±35 MΩ *versus* 206±30 MΩ control, Student's *t*-test, $t_9 = 2.629$, * $P = 0.027$, $n = 10$; Fig. 27 C). Furthermore, 500 µM NaNP induced global depression of spontaneous postsynaptic currents frequency (1.12±0.18 Hz *versus* 2.06±0.46 Hz control, Student's *t*-test, $t_9 = -2.341$, * $P = 0.047$, $n = 10$), with partial recovery on washout (1.57±0.38 Hz, Student's *t*-test, $t_9 = -1.273$, $P = 0.239$, $n = 10$; see histograms in Fig. 27 D). Fig. 27 E shows the distribution of synaptic events peak amplitude in control and following NaNP: the Gaussian distribution characteristic of the control condition was skewed to the left following the treatment as a result of the prevalence of small amplitude events. The cumulative plot in Fig. 27 F demonstrates that the probability of observing slowly decaying events increased after NaNP application. Even though it is necessary to investigate this phenomenon further, the

analysis suggests that synaptic activity depression was mainly concerned with fast, large events.

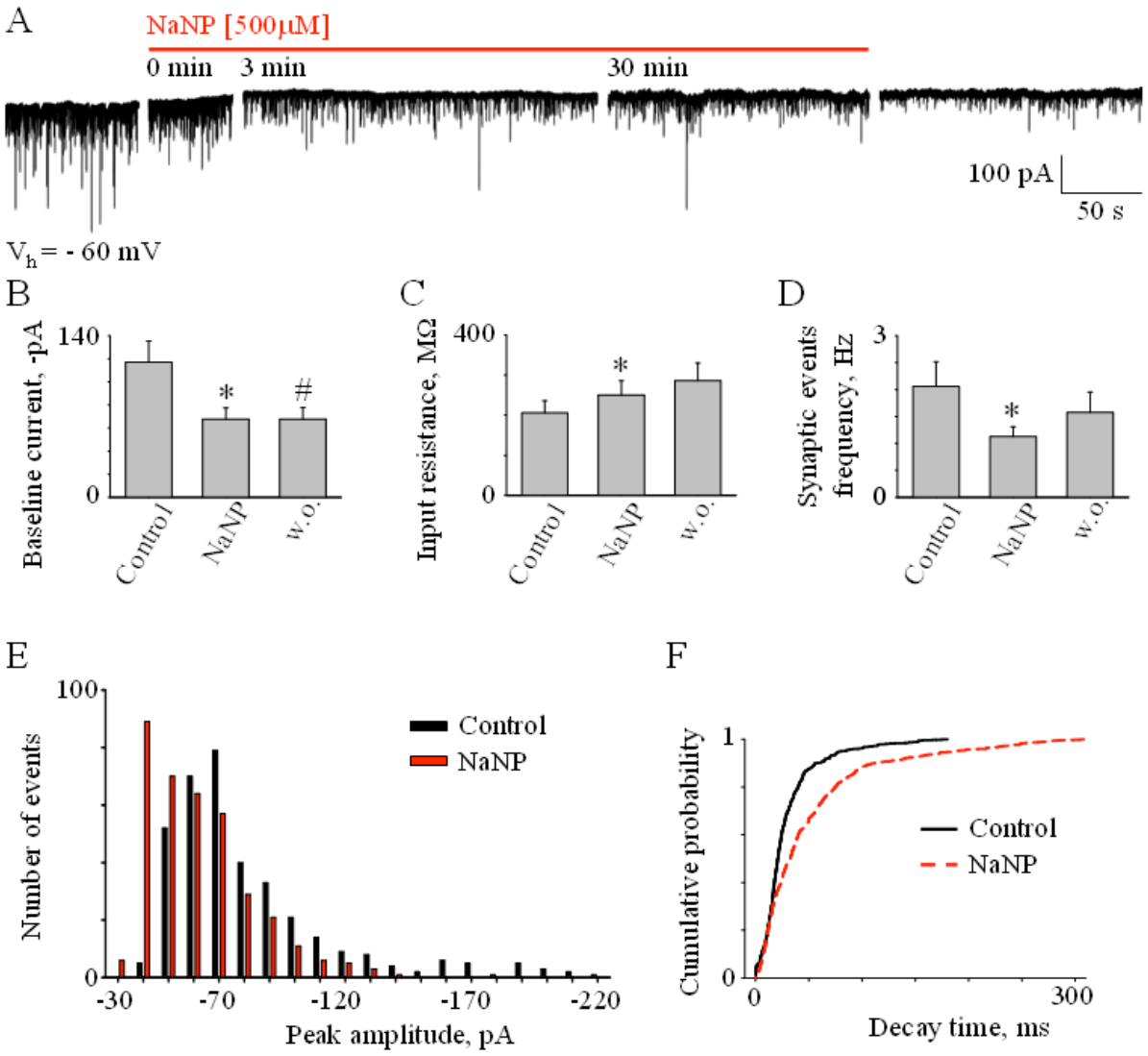

Fig. 27. HM electrophysiological characteristics after application of 500 µM NaNP. (A) Sample record under voltage clamp configuration (V_h = -60 mV) showing the onset of an outward current rapidly stabilizing following the application of NaNP, with no recovery on washout. (B) Histograms quantify the HM baseline current in control, following NaNP, and in washout (Student's *t*-test, t_9 = -4.396, * P = 0.002 for NaNP *versus* control; t_9 = -3.741, # P = 0.005 for w.o. *versus* control; n = 10). (C) Histograms showing an increase in HM input resistance following NaNP application (Student's *t*-test, t_9 = 2.629, * P = 0.027, n = 10). (D) Histograms quantify the global depression of spontaneous postsynaptic currents frequency (Student's *t*-test, t_9 = -2.341, * P = 0.047, n = 10). (E) Histograms showing spontaneous synaptic events amplitude distribution before and after NaNP treatment. The analysis comprised 361 events; different cell from (A). (F) Plot of cumulative probability distribution of spontaneous synaptic events decay time that was shifted to the right by 500 µM NaNP (red dashed line). The analysis comprised 457 events; data are from the same cell shown in E.

2.2 NaNP treatment modulated persistent inward currents (PICs)

We investigated the possibility that NaNP could affect PICs using a slow ramp protocol (see top scheme in Fig. 28). Fig. 28 shows an example of global PIC observed in control conditions (Krebs). This response was inhibited by NaNP (500 µM; 30 min) as indicated by the superimposed traces of the current responses in the inset to Fig. 13 (91±15 pA \ ms *versus* 133±15 pA \ ms control, Student's *t*-test, t_9 = -4.930, * P = 0.003, n = 10). On average, it appears that NaNP decreased PICs area by 32 %; we did not observe recovery in PICs area after washout.

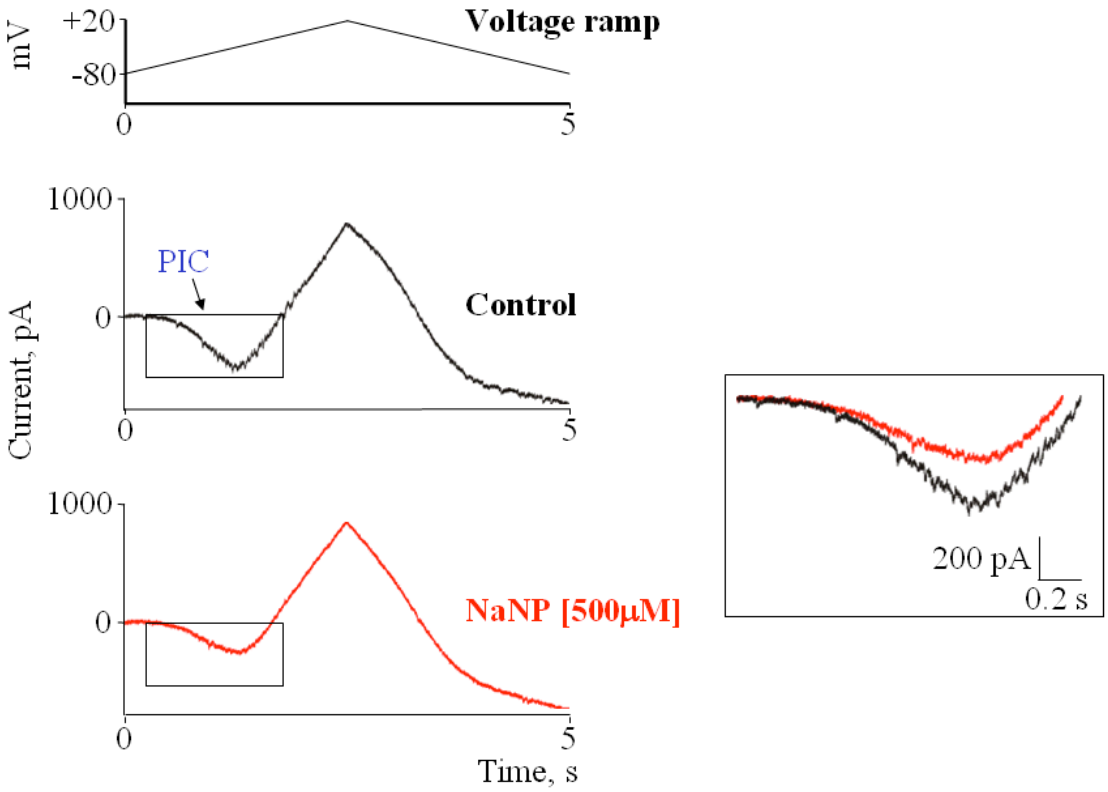

Fig. 28. NaNP treatment modulated persistent inward currents. On HMs, voltage ramps (from -80 to +20 mV; rate = 42 mV / s; see top scheme) induced PICs (see arrow) followed by a large outward current in control solution (Krebs). After NaNP application, PICs were depressed as indicated by the superimposed traces of the current responses in the inset.

2.3 Hyperexcitability of HMs treated with NaNP

We then investigated whether NaNP might influence HM firing properties.

To induce repeated firing and to detect the sensitivity of spike activity to NaNP, we used rectangular current pulses. Current steps (300 pA for 500 ms) injected into HMs evoked firing as exemplified in Fig. 29 A. In control condition, this motoneuron fired 7 spikes (V_m = -65 mV, Fig. 29 A, top trace), while, at the end of NaNP application, the HM (tested at the

same V_m), responded with 19 spikes (Fig. 29 A, bottom trace). Averaging out data for 8 HMs showed that NaNP significantly enhanced the mean firing frequency (36±8 Hz *versus* 24±7 Hz, Wilcoxon Signed Rank Test, W = -36.00, P = 0.008, n = 8, Fig. 29 B), without altering the slow AHP amplitude measured at the end of the 300 pA depolarizing current pulse, and at the same V_m before and after NaNP application (2.64±0.69 mV *versus* 2.85±0.59 mV control, Student's *t*-test, t_7 = -0.602, P = 0.566, n = 8, Fig. 29 C). Moreover, in all tested neurons bath-applied NaNP (500 μM; 30 min) increased input resistance that, on average, rose from 135±19 MΩ to 166±23 MΩ when measured on the same neurons before and after application (Student's *t*-test, t_7 = 2.787, * P = 0.027, n = 8, Fig. 29 D). Fig. 29 E shows, for each cell, the change in V_m due to NaNP treatment. On a total number of 8 cells, NaNP could depolarize 5 of them (black symbols). In the remaining three cells, the NO donor application had the effect of hyperpolarizing them (red symbols).

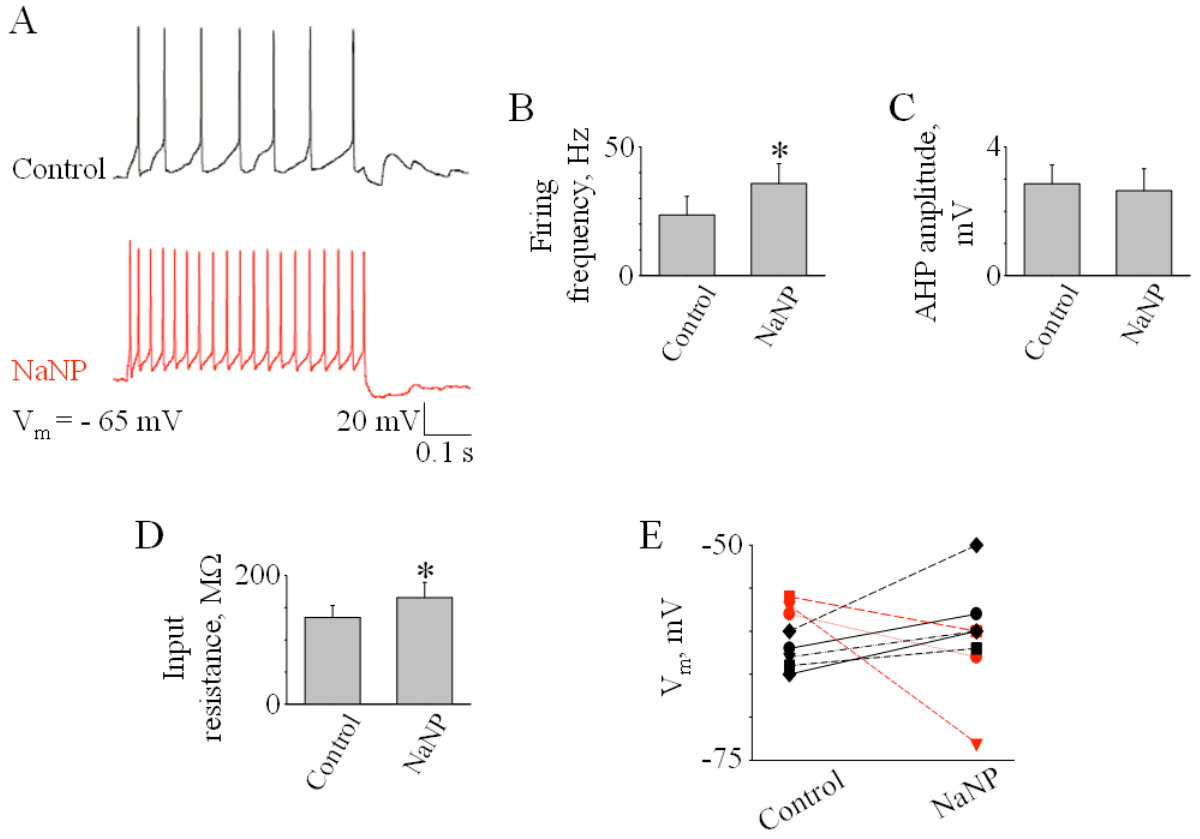

Fig. 29. Changes in HM excitability induced by NaNP. (A) Example of evoked firing (300 pA; 500 ms) in control and after NaNP application. Note the higher number of spikes in response to the same current injection pulse following NaNP. (B) Histograms quantify the HM firing frequency in control and following NaNP application (Wilcoxon Signed Rank Test, W = -36.00, * P = 0.008, n = 8). (C) Histograms showing no change in the AHP amplitude after NaNP treatment (Student's *t*-test, t_7 = -0.602, P = 0.566, n = 8). (D) Histograms quantify the rise in HM input resistance following NaNP application (Student's *t*-

test, t_7 = 2.787, * P = 0.027, n = 8). (E) Scatter plot demonstrating the V_m variation dependent on NaNP application. Each line represents an individual neuron (black and red symbols for depolarizing and hyperpolarizing neurons, respectively).

2.4 Hypoglossal nucleus expression of nNOS and GC

To assess the HM sensitivity to NO, we studied, in the hypoglossal nucleus, the expression of brain NO synthetic enzyme and its main intracellular signal transduction mechanism, namely the neuronal nitric oxide synthase (nNOS) and guanylate cyclase (GC), respectively.

Fig. 30 A, B demonstrates that the expression of nNOS was limited to a subset of cells in the dorsal division of the nucleus, while ventral motoneurons rarely expressed this enzyme. The nNOS immunoreactivity was mainly localized to neuronal perikarya and proximal processes, but not to the nuclear area. Out of 85±1 SMI 32 immunopositive cells counted in the whole hypoglossal nucleus area (mean value: 89060±1928 μm^2, n = 3 rats), 18±1 co-expressed nNOS: 17±2 HMs were located in the dorsal part of the nucleus (identified as the HN dorsal area covering the 50 % of the whole HN area, evaluated, with imageJ software, for each analysed image), while 1±0.5 HM was located in the nucleus ventral division (Fig. 30 C). Since HMs are myotopically organized within the hypoglossal nucleus, the ones expressing nNOS are those known to innervate tongue retractor muscles (McClung & Goldberg, 1999; 2000). Our observation is in agreement with the report of Vazquez *et al*. (1999) who have demonstrated that nNOS expression is limited to a few cells labeled in the dorsal division of the nucleus.

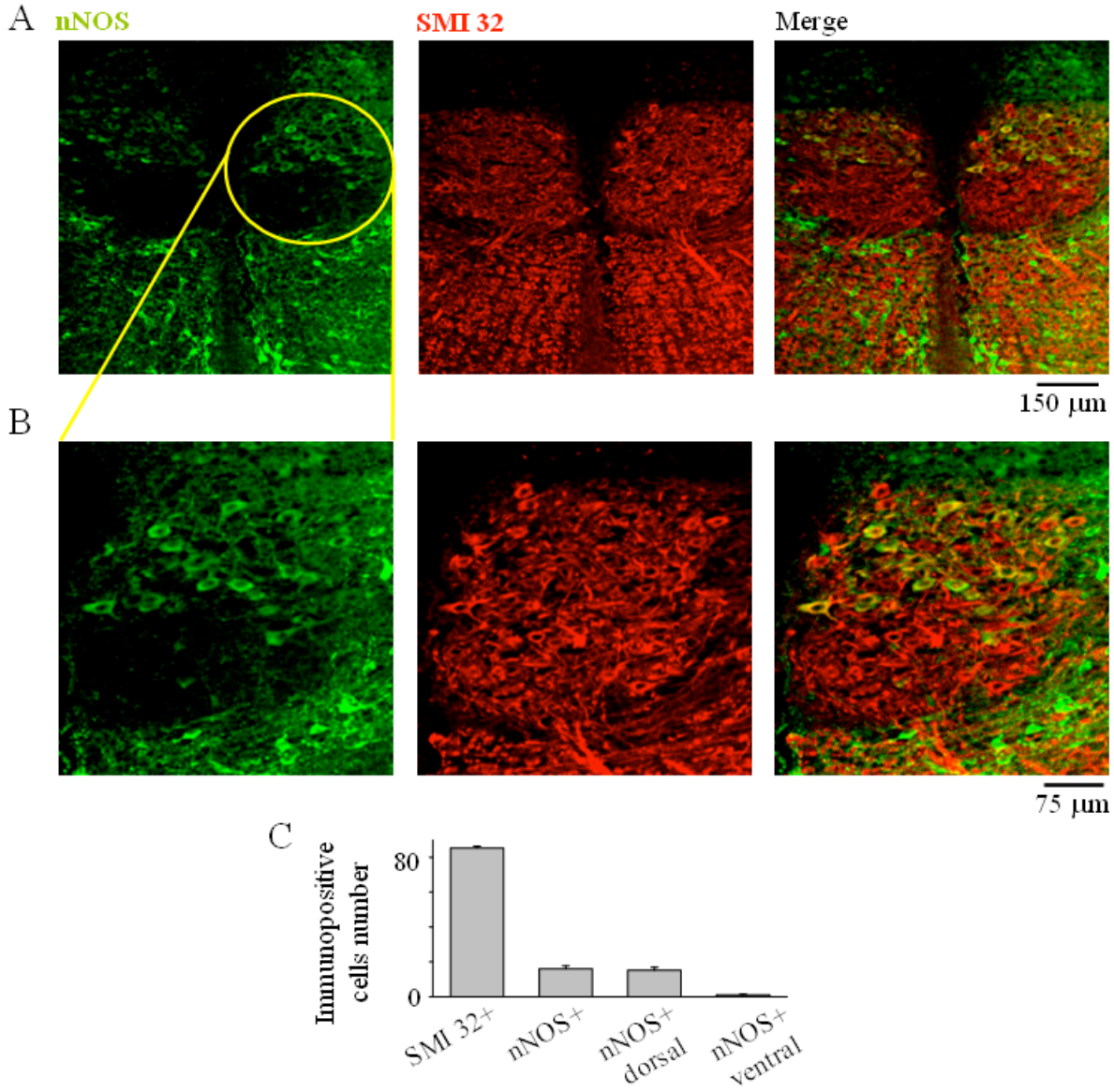

Fig. 30. Hypoglossal nucleus expression of nNOS. (A) Example of confocal images of hypoglossal nuclei stained for the nNOS enzyme (green pseudocolour, left), the motoneuron marker SMI 32 (red pseudocolour, centre), and the merge (right). (B) Magnifications of the previous images to underline the different nNOS expression pattern within the nucleus hypoglossus. (C) Histograms quantifying the number of cells immunopositive to SMI 32 and nNOS in the whole hypoglossal nucleus, nNOS in the nucleus dorsal part, nNOS in the nucleus ventral part, respectively.

The GC antibody recognizes a peptide corresponding to amino acids 189-207 of the β1 subunit of this effector enzyme. The two isoforms of GC show different cellular distribution in the brain (Budworth *et al*., 1999; Gibb & Garthwaite, 2001; Mergia *et al*., 2003; Szabadits *et al*., 2007) and diverse location at subcellular level (Russwurm *et al*., 2001; Zabel *et al*., 2002; Jones *et al*., 2008). Unlike nNOS, the expression of GC was observed in the cytoplasm of all HMs, without any topographical differentiation (Fig. 31 A, B).

This histochemical analysis revealed that, even though only a small proportion of motoneurons in the dorsal hypoglossal nucleus could synthesize NO, the whole nucleus might be able to sense the effects of this diffusing signaling molecule because virtually all cells can express the enzyme GC.

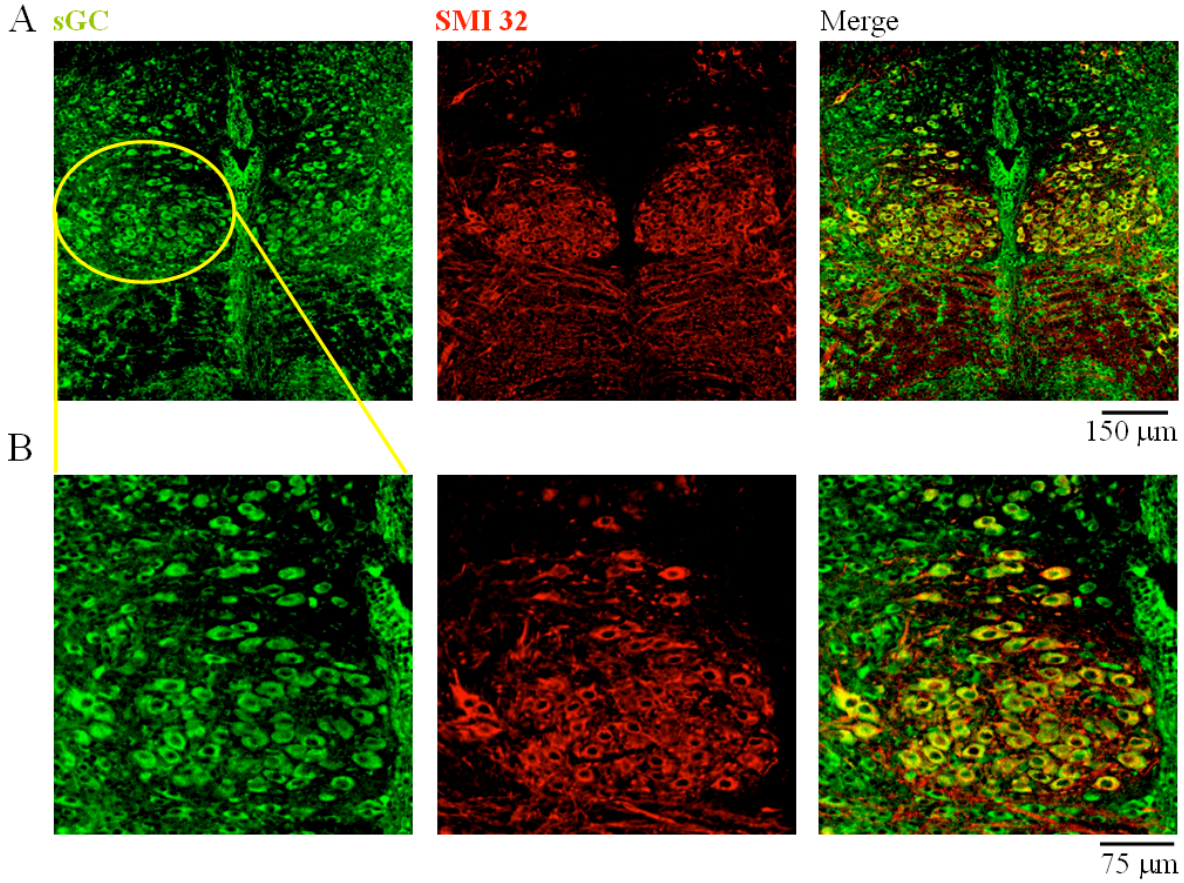

Fig. 31. Hypoglossal nucleus expression of GC. (A) Example of confocal images of hypoglossal nuclei stained for the GC enzyme (β1 subunit, green pseudocolour, left), the motoneuron marker SMI 32 (red pseudocolour, centre), and the merge (right). (B) Magnifications of the previous images to underline the GC expression pattern within the nucleus hypoglossus.

Discussion

The principal finding of the present report is the characterization of the early changes of rat HMs transiently exposed to H_2O_2. This treatment generated a complex chain of events that included reduced network activity and enhanced HM firing. These effects were not accompanied by either early cell death or astroglia injury, but were associated with activation of the motoneuronal stress factor ATF-3. Our data suggest that acute oxidative stress induced a series of functional changes hitherto unreported and potentially relevant to the theory of oxidative damage in ALS (Turner *et al*., 2009; Vucic & Kiernan, 2009). Furthermore, we obtained a few preliminary data concerning the effects of NaNP, a NO donor, on HMs electrophysiological properties.

1. H_2O_2 application as a model to investigate oxidative stress of HMs

Although the neuropathological results obtained from human ALS autopsy cases are valuable and important, almost all such cases represent only the terminal stage of the disease. This makes it difficult to clarify how and why ALS motoneurons are impaired at each clinical stage from disease onset to death, and as a consequence, human autopsy cases alone yield little insight into potential therapies for ALS (Kato, 2008). Clinical electrophysiology data suggest that the ALS disease is widespread at the time of diagnosis, implying that it has been active and disseminated through the motor system for some time prior to presentation with weakness and atrophy (Swash & Ingram, 1988). This realization calls for experimental models that can yield important information for clarifying the early pathogenesis of ALS in humans (Kato, 2008).

Current theories of ALS propose that motoneuron damage may result from oxidative stress as indicated by the host (>140) of SOD-1 mutations implicated in the genetic forms of ALS that, however, are only 10 % of all clinical cases and have generated a large number of mouse genetic models (Vucic & Kiernan, 2009). Such experimental studies have not provided a uniform theory to account for motoneuron damage and have been primarily conducted with mouse motoneurons. Since some experimental manipulations are difficult on mice because of their innate size, rat models of ALS have also been developed. Like its murine counterpart, the rat G93A model reproduces the major phenotype of motoneuron degeneration (Aoki *et al*., 2005), although spinal rather than brainstem motoneurons are primarily affected (Lladó *et al*., 2006).

Since the vast majority of ALS cases are sporadic and presumably imply an environmental toxic agent (Cleveland & Rothstein, 2001), we wished to understand how rat HMs could respond to strong oxidative stress to identify certain mechanisms that might lead to motoneuron degeneration. Of course, the present study suffers from certain intrinsic limitations like the use of neonatal motoneurons and the inability to follow up the long term evolution of damage because brain slices have restricted survival *in vitro*. Nevertheless, the present results offer a novel insight into the early events of oxidative stress and could contribute to identify certain mechanisms that might lead to motoneuron degeneration.

2. Early consequences of H_2O_2 application on synaptic transmission and HM excitability

H_2O_2 evoked a slowly developing inward current (depolarization) with input resistance rise and relatively poor recovery on washout. Regardless of the application of receptor or channel blockers, and of voltage or current clamp recording, we consistently found a significant rise in input resistance evoked by H_2O_2. This observation implied depression of a leak background current that was not inhibited by intracellular Cs^+ contained in the patch pipette. Previous studies indicated that rat motoneurons possess a background K^+ current rather resistant to Cs^+ (Fisher & Nistri, 1993) subsequently identified as a member of the TASK family of K^+ channels, whose main constituent, namely TASK-1, is expressed chiefly by motoneurons (Talley *et al*., 2000; Bayliss *et al*., 2001). In accordance with this notion, in the presence of hydrogen peroxide, the current response had a very negative extrapolated reversal potential with linear I/V plot, consistent with the properties of TASK-1. It is likely that the larger input resistance of motoneurons contributed to their higher excitability.

This phenomenon, accompanied by a significant reduction in the frequency of sPSCs, suggested a complex scenario that might have comprised changes in the release of various transmitters. To examine this issue more directly, we used TTX to investigate how miniature synaptic events responded to H_2O_2. Blocking fast glutamatergic transmission with APV and CNQX did not prevent the effects by H_2O_2 on baseline current or input resistance, and revealed a paradoxical rise in the frequency of inhibitory synaptic events that are known to be mediated by glycine and GABA (Donato & Nistri, 2000) whose reversal potential, in our recording conditions, was ≈ 0 mV (see also Donato & Nistri, 2000).

Since H_2O_2 is known to raise intracellular free Ca^{2+} (Zheng & Shen, 2005; Takahashi *et al*., 2007; Gerich *et al*., 2009) and its action was mimicked by thapsigargin, our data accord with

the potentiation by H_2O_2 of GABAergic miniature event frequency via increased intracellular free Ca^{2+} (Takahashi *et al*., 2007). Furthermore, Hahm *et al*. (2010) have found that H_2O_2 increases GABAergic mIPSC frequency through the cAMP protein kinase A (PKA)-dependent pathway in isolated cerebral cortical neurons of the rat. Neurochemical experiments on rat hippocampal slices also demonstrate that H_2O_2 markedly potentiates GABA release (Saransaari & Oja, 2008). Blocking inhibitory synaptic transmission with strychnine and bicuculline eliminated the effects by H_2O_2 on motoneuron baseline current, yet enabled us to observe a significant increase in glutamatergic miniature events as well as in input resistance. Thus, H_2O_2 seemingly facilitated release of glutamate, GABA and glycine, indicating a presynaptic origin for this process at the level of network-independent release.

While our data indicate enhancement of miniature event frequency, they contrast with the observed fall in network-mediated synaptic events. The latter finding has been reported for hippocampal pyramidal neurons on which H_2O_2 depresses electrically-evoked excitatory and inhibitory synaptic potentials (Pellmar, 1987). This discrepancy led us to investigate changes in voltage dependent currents that may be responsible for changes in neuronal excitability.

3. Raised HM firing despite PIC suppression by H_2O_2

Previous studies have shown that mammalian spinal neuron excitability is largely mediated by PICs that comprised PIC(Na) (Darbon *et al*., 2004; Harvey *et al*., 2006; Zhong *et al*., 2007) and PIC(Ca) (Li & Bennett, 2007). These currents are also expressed by neonatal rat HMs (Lamanauskas & Nistri, 2008) and are found to be potentiated in the mouse $SOD1^{G93A}$ model (van Zundert *et al*., 2008), in analogy with $SOD1^{G93A}$ spinal motoneurons in culture (Kuo *et al*., 2005). It is, however, interesting that spinal motoneurons of the $SOD1^{G85R}$ model display less excitability than wildtype cells (Bories *et al*., 2007), even if their repeated firing is proposed to be regulated by PIC(Na) (Amendola *et al*., 2007). The same group (Pambo-Pambo *et al.*, 2009) has demonstrated that $SOD1^{G93A}$ low expressor mutant is hyperexcitable to current pulses, whereas $SOD1^{G93A}$ low expressor and $SOD1^{G85R}$ models have a lower gain with current ramps stimulation. Changes in the threshold and intensities of Na^+ and Ca^{2+} persistent inward currents have been also observed. $SOD1^{G93A}$ low expressor mutants show reduced total persistent inward currents compared with control motoneurons.

In the present study we observed that H_2O_2 induced a larger reduction of PIC(Ca) (79 %) than of PIC(Na) (38 %) without threshold alteration. Notwithstanding the impaired amplitude

of PICs by H_2O_2, we detected accelerated firing rates of HMs with strong inhibition of the AHP. Since H_2O_2 only partly depressed PIC(Na), this effect would not be sufficient to change excitability because nearly complete block of PIC(Na) is necessary for strong depression of HM firing (Lamanauskas & Nistri, 2008).

Blocking Ca^{2+} channels often prolongs the action potential and raises neuronal excitability, an effect opposite to the one expected from blocking the entry of positively charged ions (Bean, 2007). This reflects powerful and rapid coupling of Ca^{2+} entry to the activation of Ca^{2+}-activated K^+ channels, so that the net effect of blocking Ca^{2+} influx is to inhibit a net outward current and, therefore, to increase excitability (Bean, 2007). In accordance with this notion, we suggest that H_2O_2 enhanced firing because it largely depressed Ca^{2+} influx, as shown by the decreased in PIC(Ca), important for the activation of the Ca^{2+} dependent K^+ conductances underlying the AHP (Umemiya & Berger, 1994; Lape & Nistri, 1999; Li & Bennett, 2007). These effects were apparently distinct from the facilitation by H_2O_2 of Ca^{2+} release from presynaptic intracellular stores (as discussed above), a phenomenon that developed in the absence of firing following TTX application.

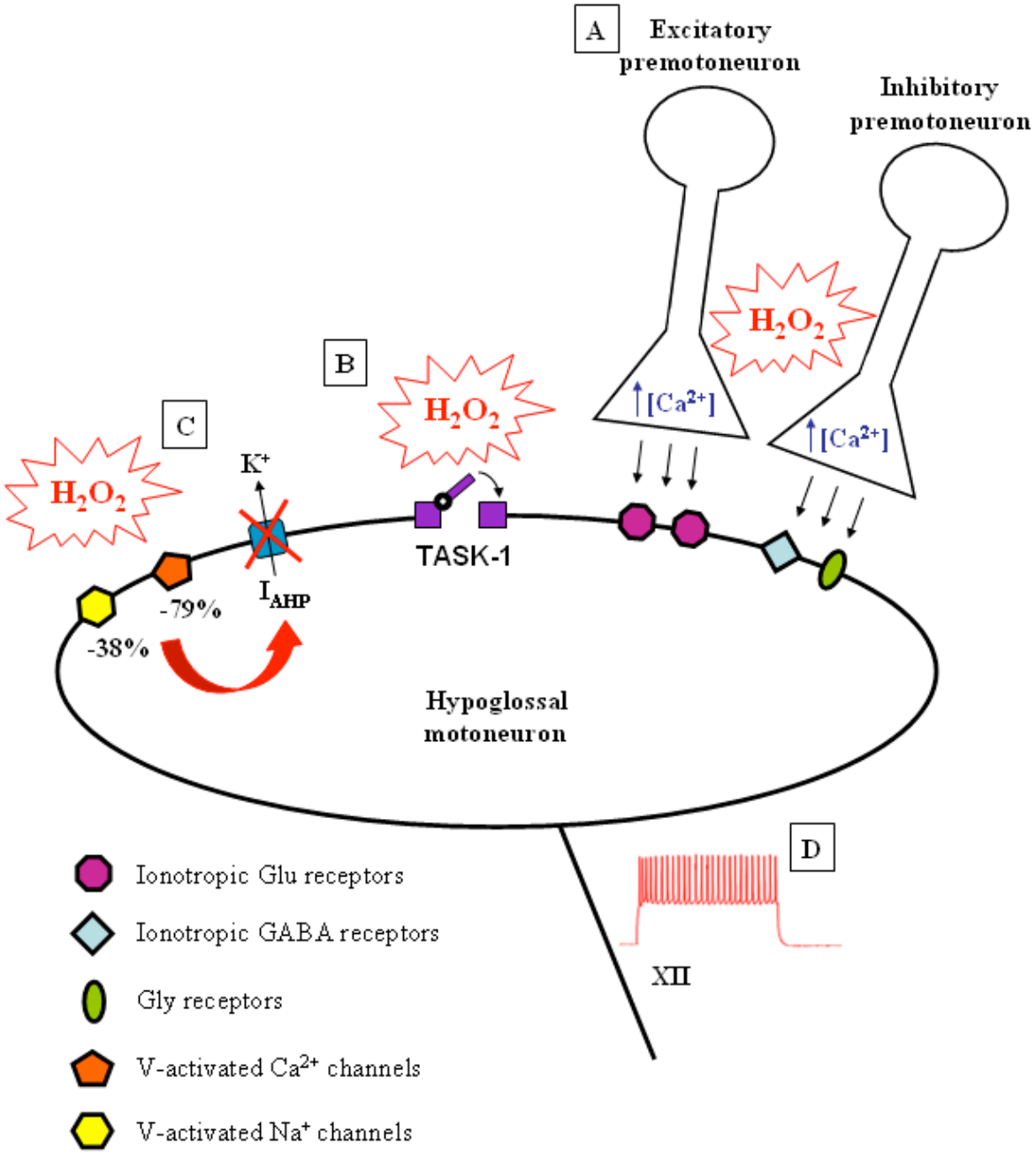

Fig. 32. Scheme summarizing H_2O_2 effects on hypoglossal motoneuron (HM) electrophysiological properties. (A) H_2O_2 enhanced the frequency of both excitatory and inhibitory miniature events presumably via increased intracellular free Ca^{2+} in premotoneuron synaptic terminals. (B) H_2O_2 augmented HM input resistance possibly by depressing the leak background current mediated by TASK-1, a member of the TASK family of K^+ channels, chiefly expressed by motoneurons. (C) H_2O_2 induced a larger reduction of PIC(Ca) (79 %, mediated by V-activated Ca^{2+} channels) than of PIC(Na) (38 %, mediated by V-activated Na^+ channels). Thus, the lessened Ca^{2+} influx had a negative effect on the activation of Ca^{2+} dependent K^+ conductances underlying the AHP. Inhibition of such a net outward current, together with the HM larger input resistance (see B), is likely to contribute to HM higher excitability (D).

4. Early motoneuron damage by H_2O_2

We next explored whether, as a result of exposure to H_2O_2, HMs were damaged. We first ascertained that this treatment was actually accompanied by a significant rise in intracellular oxidative processes. It is interesting that advanced oxidation protein products are higher in the CSF of ALS patients, with concurrent decrease in antioxidant capacity, compared with controls with other neurological diseases (Siciliano *et al*., 2007). Furthermore, we counted the number of PI positive cells or SMI 32 positive HMs to find out if there had been a rapid and extensive cell death. Our results indicated that there was no change in the number of motoneurons in the slices, suggesting that oxidative stress, albeit of strong intensity, did not produce early motoneuronal death. It was, however, apparent that the H_2O_2 application had evoked an important reaction in HMs because of the large increase in their immunocytochemical expression of ATF-3.

ATF-3 is a transcription factor induced by harmful extracellular stimuli that trigger intracellular kinase activity responsible for neosynthesis of ATF-3 and its translocation to the cell nucleus where it can be observed after neuronal lesion (Tsujino *et al*., 2000; Nakagomi *et al*., 2003; Lindwall *et al*., 2004). ATF-3 has a Janus-like function subserving either damage repair or degeneration depending on the nature of the insult (Tsujino *et al*., 2000; Nakagomi *et al*., 2003; Vlug *et al*., 2005). In SOD^{G93A} mouse motoneurons ATF-3 is strongly expressed prior to neurodegeneration (Vlug *et al*., 2005). We suggest that the ATF-3 signal observed in the present study was an index of initial distress of motoneuron subsequent to H_2O_2 treatment. Its cytoplasmic location was probably due to the fact that the DNA transcriptional effects of ATF-3 require its de novo protein synthesis in the cytosol (Lindwall *et al*., 2004).

In conclusion, most research into neurophysiological biomarkers of ALS has focussed on the development of surrogate markers of motor unit loss (Turner *et al*., 2009). Electrophysiological studies of early stage ALS have shown increased motoneuron excitability attributed to dysfunction of motor cortex (Turner *et al*., 2009). However, lower motoneuron hyperexcitability is also an important feature of the disease presentation. If we assume that oxidative stress may be a significant contributor to ALS pathology (Turner *et al*., 2009; Vucic & Kiernan, 2009), our current results suggest that an oxidative stress, even when transient, can render brainstem motoneuron hyperexcitable through a combination of enhanced input resistance and firing rate, a condition accompanied by ATF-3 activation.

5. H_2O_2 effects on astroglia

Although progressive paralysis in ALS arises from degeneration and death of motoneurons, evidence from several directions has converged to demonstrate that toxicity is non-cell-autonomous, but it derives from damage also developed within cell types other than motoneurons (Clement *et al*., 2003; Boillée *et al*., 2006). In the postnatal rat central nervous system the main astrocyte type is the protoplasmic one (Miller & Raff, 1984) which is readily labeled by immunostaining its Ca^{2+}-binding protein S100B (Cocchia, 1981; Didier *et al.*, 1986). S100B is involved in a variety of intracellular and extracellular activities (Donato, 2001), and, in particular, it can exert beneficial (neurotrophic) or detrimental (neurotoxic) effects on surrounding glia and neurons depending on its concentration (Rothermundt *et al.*, 2003). Changes in S100B immunoreactivity have, in fact, been associated with brain damage and degenerative brain diseases (Rothermundt *et al.*, 2003; Blackburn *et al.*, 2009) including ALS: indeed, it is interesting that S100B immunoreactivity has been found to be upregulated in astrocytes in the spinal cord of ALS patients (Migheli *et al.*, 1999). The present study observed that 30 min application of H_2O_2 did not change S100B immunoreactivity in the nucleus hypoglossus; it is likely that the exposure time of brainstem slices to the oxidative challenge was not prolonged enough to produce damage to astroglia in this nucleus. In keeping with this view, Zagami *et al*. (2009), using primary cultures of neurons and astrocytes treated with 300 μM H_2O_2, have demonstrated that reducing cell viability by 50 % (considering 100 % as the maximal effect obtained) requires 47 min of incubation. More recently, our lab has reported that, in spinal cord preparations subjected for 1 h to a "pathological medium" (PM, i.e. hypoxic / aglycemic solution containing toxic radicals), active caspase-3 positive cells are identified almost exclusively in the ventrolateral white matter 2 h after washout of PM and are found to overlap with those positive for GFAP or O4, suggesting late-onset of apoptotic cell death of white matter fibrous astrocytes and oligodendrocytes. Furthermore, in PM treated spinal cords, pyknosis starts to occur in the white matter 2 h after treatment (Kuzhandaivel *et al*., 2010). Thus, following hypoxic-dysmetabolic perturbations, white matter glial cells, especially fibrous astrocytes (GFAP+) and oligodendrocytes (O4+), are more vulnerable than neurons and astroglial cells (S100B+) of the gray matter, and signs of cell-death commitment begin to appear 2 h after PM application (Kuzhandaivel *et al*., 2010).

6. NaNP influenced HM synaptic transmission and excitability: preliminary considerations

Our immunohistochemical analysis of the nucleus hypoglossus revealed that the expression of nNOS is limited to a subset of cells in the dorsal division of the nucleus, while ventral motoneurons rarely expresse this enzyme, as previously reported by Vazquez *et al*. (1999). Nonetheless, the whole nucleus motoneuronal population expressed the enzyme GC, thus rendering HMs able to sense the effects of NO.

In order to generate NO, we exposed brainstem slices to 500 μM NaNP; this dose, accordingly to Southam and Garthwaite (1991), should correspond to a concentration in the recording chamber of 0.05 μM, large enough to evoke toxic effects typically observed with near-micromolar concentrations (Dawson *et al*., 1993; Liu & Martin, 2001; Hall *et al*., 2009). The application of the NO donor NaNP caused the onset of an outward current accompanied by an increase in input resistance. This result suggested the depression of a sustained inward conductance active at resting V_m. Previous studies have indicated that NO decreases $GABA_AR$ function (Robello *et al*., 1996; Wexler *et al*., 1998; Wall, 2003). Robello *et al*. (1996) have demonstrated, both in adult rat cerebral cortex and in neonatal rat cerebellar granule cells, a reduction in GABA-stimulated Cl^- influx by treatment with NO chemical donors. Wexler *et al*. (1998) have reported that NO analogs decrease GABA-gated currents in cultured retinal amacrine cells via coactivation of cGMP-dependent kinase and phosphodiesterase. Finally, following a reduction in the concentration of endogenous NO in adult rat cerebellum, Wall (2003) has observed effects consistent with enhanced granule cell $GABA_AR$ activation.

In the present study, spontaneous synaptic events occurred at lower rate in the presence of NaNP, a phenomenon most likely due to the decreased activity of premotoneurons. Sunico *et al*. (2010) have recently demonstrated that gain in neuronal NO signaling (obtained through either nNOS retrograde transfection or 6 h exposure to a long half-life NO donor) is sufficient to induce excitatory and inhibitory synapse withdrawal and to reduce evoked EPSPs in neonatal HMs via paracrine action on presynaptic structure. Thus, the result obtained might be the first step of a complex chain of events leading to synapse detachment. Further studies will be required to clarify the mode of action of NO on HMs baseline current and network premotoneurons.

We were also interested in clarifying NO effects on voltage-activated conductances. It has been previously reported that NO could modulate persistent Na^+ conductances. Sawada *et al*.

(1995) have studied the effects of micropressure-ejected NO generators on the membrane of identified neurons in the *Aplysia kurodai* abdominal ganglion; they have demonstrated the induction of a slow inward current associated with an increase in Na^+ conductance mediated by a rise in the intracellular level of cGMP. The effects of NO donors on persistent Na^+ current have been examined also in rat hippocampal neurons (Hammarström & Gage, 1999); in particular, these authors have reported an increase (by 60-80 %) within a few minutes of exposure to either NaNP or S-nitroso-N-acetyl-DL-penicillamine (SNAP). The amplitude of the transient Na^+ current is not changed significantly by NO donors, indicating a selective effect on the persistent component. Our experimental data revealed that NaNP decreased total PICs area, mediated by both Na^+ and Ca^{2+} (Crill, 1996; Russo & Hounsgaard, 1999), by 32 %. Further investigations are needed to elucidate the specific contribution of the Mn^{2+}-sensitive component – PIC(Ca) – and the TTX-sensitive component – PIC(Na) – to the observed reduction.

In current clamp experiments, we consistently found a significant rise in input resistance evoked by NaNP, together with enhanced spike firing and unchanged AHP amplitude. Previous studies have showed a positive regulation of the firing rate exerted by NO donors, both in locus coeruleus neurons (Xu *et al*., 1998) and in the vagal dorsal motor nucleus (Travagli & Gillis, 1994). Despite the impairing action of NaNP on PICs, known to be involved in mammalian neuron excitability (Darbon *et al*., 2004; Harvey *et al*., 2006; Zhong *et al*., 2007), it is likely that the larger input resistance of motoneurons contributed to their higher excitability and compensated for the PICs area decrease. Furthermore, on a total number of 8 cells recorded under current clamp configuration, 5 HMs (V_m < -60 mV) depolarized following NaNP application, while the remaining 3 cells (V_m > -60 mV) hyperpolarized, indicating that motoneurons are not a homogeneous population with regard to their V_m response to NO. The most parsimonious interpretation is that the leak conductance modulated by NaNP might have a reversal potential in the range of the recorded cells V_m. NO donors are known to depolarize different neuronal preparation: adult mouse locus coeruleus neurons (Pineda *et al*., 1996), adult rat type II paraventricular nucleus neurons (Bains & Ferguson, 1997), adult guinea pig trigeminal motoneurons (Abudara *et al*., 2002), juvenile rat and mouse optic nerve (Garthwaite *et al.*, 2006), rat P6-P9 hypoglossal motoneurons (González-Forero *et al.*, 2007; Montero *et al.*, 2008). This action is proposed to be exerted through an NO action on different conductances, namely the hyperpolarization-activated cationic current (I_h), hyperpolarization-activated cyclic nucleotide-gated channels

(HCN), and TASK-like K^+ conductances (Abudara *et al*., 2002; Garthwaite *et al.*, 2006; González-Forero *et al.*, 2007; Montero *et al.*, 2008). Unlike the previous observations, Xu *et al*. (1998) have reported that NO donors caused both hyperpolarization and depolarization in locus coeruleus neurons.

Our data concerning the effects of NO on HMs are preliminary; from an electrophysiological point of view, they will need experiments performed in the presence of synaptic transmission blockers, and of selective blockers of PIC(Na) and PIC(Ca). Moreover, immunohistochemical analysis will be required to investigate the potential toxic effect of 500 μM NaNP on HMs and astroglia. The present results revealed, however, that the NO effect on HMs was different from the one exerted by hydrogen peroxide, suggesting that oxidative and nitrosative damage might occur through distinct mechanisms of action, even if HMs ultimately show enhanced firing in either case. Future studies will be necessary to find out if motoneuron injury induced by these two processes might evolve with different time course and outcome.

Our report left, thus, (1) to be clarified what conductance/s is/are involved in the reported effect of NO on HM baseline current/membrane potential; (2) to be evaluated the mechanism through which NaNP modify motoneuronal excitability; and (3) to be investigated the nitrosative stress consequences on hypoglossal nucleus cell populations, in terms of damage and survival.

References

Abe, K., Pan, L.H., Watanabe, M., Kato, T. & Itoyama, Y. (1995) Induction of nitrotyrosine-like immunoreactivity in the lower motor neuron of amyotrophic lateral sclerosis. Neurosci Lett., 199, 152-154.

Abe, K., Pan, L.H., Watanabe, M., Konno, H., Kato, T. & Itoyama, Y. (1997) Upregulation of protein-tyrosine nitration in the anterior horn cells of amyotrophic lateral sclerosis. Neurol Res., 19, 124-128.

Abudara, V., Alvarez, A.F., Chase, M.H. & Morales, F.R. (2002) Nitric oxide as an anterograde neurotransmitter in the trigeminal motor pool. J Neurophysiol., 88, 497-506.

Afifi, A., Aleu, F., Goodgold, J. & MacKay, B. (1966) Ultrastructure of atrophic muscle in amyotrophic lateral sclerosis. Neurology, 16, 475-481.

Ahern, G.P., Klyachko, V.A. & Jackson, M.B. (2002) cGMP and S-nitrosylation: two routes for modulation of neuronal excitability by NO. Trends Neurosci., 25, 510-517.

Alderton, W.K., Cooper, C.E. & Knowles, R.G. (2001) Nitric oxide synthases: structure, function and inhibition. Biochem J., 357, 593-615.

Aldes, L.D. (1995) Subcompartmental organization of the ventral (protrusor) compartment in the hypoglossal nucleus of the rat. J Comp Neurol., 353, 89-108.

Amendola, J., Verrier, B., Roubertoux, P. & Durand, J. (2004) Altered sensorimotor development in a transgenic mouse model of amyotrophic lateral sclerosis. Eur J Neurosci., 20, 2822-6.

Amendola, J., Gueritaud, J.P., d'Incamps, B.L., Bories, C., Liabeuf, S., Allene, C., Pambo-Pambo, A. & Durand, J. (2007) Postnatal electrical and morphological abnormalities in lumbar motoneurons from transgenic mouse models of amyotrophic lateral sclerosis. Arch Ital Biol., 145, 311-23.

Amendola, J. & Durand, J. (2008) Morphological differences between wild-type and transgenic superoxide dismutase 1 lumbar motoneurons in postnatal mice. J Comp Neurol., 511, 329-41.

Ames, B.N. & Shigenaga, M.K. (1992) Oxidants are a major contributor to aging. Ann N Y Acad Sci., 663, 85-96.

Andrus, P.K., Fleck, T.J., Gurney, M.E. & Hall, E.D. (1998) Protein oxidative damage in a transgenic mouse model of familial amyotrophic lateral sclerosis. J Neurochem., 71, 2041-2048.

Aoki, M., Kato, S., Nagai, M. & Itoyama, Y. (2005) Development of a rat model of amyotrophic lateral sclerosis expressing a human SOD1 transgene. Neuropathology, 25, 365-70.

Aracri, P., Colombo, E., Mantegazza, M., Scalmani, P., Curia, G., Avanzini, G. & Franceschetti, S. (2006) Layer-specific properties of the persistent sodium current in sensorimotor cortex. J Neurophysiol., 95, 3460-3468.

Arai, T., Hasegawa, M., Akiyama, H., Ikeda, K., Nonaka, T., Mori, H., Mann, D., Tsuchiya, K., Yoshida, M., Hashizume, Y. & Oda, T. (2006) TDP-43 is a component of ubiquitin-positive tau-negative inclusions in frontotemporal lobar degeneration and amyotrophic lateral sclerosis. Biochem Biophys Res Commun., 351, 602-611.

Arrigo, A.P. (1999) Gene expression and the thiol redox state. Free Radic Biol Med., 27, 936-944.

Atsumi, T. (1981) The ultrastructure of intramuscular nerves in amyotrophic lateral sclerosis. Acta Neuropath., 55, 193-198.

Babot, Z., Cristofol, R. & Sunol, C. (2005) Excitotoxic death induced by released glutamate in depolarized primary cultures of mouse cerebellar granule cells is dependent on GABAA receptors and niflumic acid-sensitive chloride channels. Eur J Neurosci., 21, 103-112.

Bains, J.S. & Ferguson, A.V. (1997) Nitric oxide depolarizes type II paraventricular nucleus neurons in vitro. Neuroscience, 79, 149-59.

Banati, R.B., Gehrmann, J., Schubert, P. & Kreutzberg, G.W. (1993) Cytotoxicity of microglia. Glia, 7, 111-118.

Banci, L., Bertini, I., Boca, M., Girotto, S., Martinelli, M., Valentine, J.S. & Vieru, M. (2008) SOD1 and amyotrophic lateral sclerosis: mutations and oligomerization. PLoS One, 3, e1677.

Barber, S.C., Mead R.J. & Shaw, P.J. (2006) Oxidative stress in ALS: A mechanism of neurodegeneration and a therapeutic target. Biochim Biophys Acta, 1762, 1051-1067.

Barber, S.C., Higginbottom, A., Mead, R., Barber, S. & Shaw, P.J. (2009) An in vitro screening cascade for anti-oxidant drugs in motor neuron disease models. Free Radic Biol Med., 46, 1127-1138.

Barber, S.C. & Shaw, P.J. (2010) Oxidative stress in ALS: Key role in motor neuron injury and therapeutic target. Free Radic Biol Med., 48, 629-641.

Barnard, E.A., Sutherland, M., Zaman, S., Matsumoto, M., Nayeem, N., Green, T., Darlison, M.G. & Bateson, A.N. (1993) Multiplicity, structure, and function in GABAA receptors. Ann N Y Acad Sci., 707, 116-125.

Bartoszewski, R., Rab, A., Jurkuvenaite, A., Mazur, M., Wakefield, J., Collawn, J.F. & Bebok, Z. (2008) Activation of the unfolded protein response by F508 CFTR. Am J Respir Cell Mol Biol., 39, 448-457.

Bayliss, D.A., Talley, E.M., Sirois, J.E. & Lei, Q. (2001) TASK-1 is a highly modulated pH-sensitive 'leak' K+ channel expressed in brainstem respiratory neurons. Respir Physiol., 129, 159-74.

Beal, M.F., Ferrante, R.J., Browne, S.E., Matthews, R.T., Kowall, N.W. & Brown, R.H. Jr. (1997) Increased 3-nitrotyrosine in both sporadic and familial amyotrophic lateral sclerosis. Ann Neurol., 42, 644-654.

Beal, M.F. (2002) Oxidatively modified proteins in aging and disease. Free Radic Biol Med., 32, 797-803.

Bean, B.P. (2007) The action potential in mammalian central neurons. Nat Rev Neurosci., 8, 451-65.

Beckman, J.S., Beckman, T.W., Chen, J., Marshall, P.A. & Freeman, B.A. (1990) Apparent hydroxyl radical production by peroxynitrite: implications for endothelial injury from nitric oxide and superoxide. Proc Natl Acad Sci USA., 87, 1620-1624.

Beckman, J.S., Carson, M., Smith, C.D. & Koppenol, W.H. (1993) ALS, SOD and peroxynitrite. Nature, 364, 584.

Beckman, J.S. & Koppenol, W.H. (1996) Nitric oxide, superoxide, and peroxynitrite: the good, the bad, and ugly. Am J Physiol., 271, C1424-1437.

Bedard, K. & Krause, K.H. (2007) The NOX family of ROS-generating NADPH oxidases: physiology and pathophysiology. Physiol Rev., 87, 245-313.

Beers, D.R., Henkel, J.S., Xiao, Q., Zhao, W., Wang, J., Yen, A.A., Siklos, L., McKercher, S.R. & Appel, S.H. (2006) Wild-type microglia extend survival in PU.1 knockout mice with familial amyotrophic lateral sclerosis. Proc Natl Acad Sci USA., 103,16021-16026.

Bendotti, C., Calvaresi, N., Chiveri, L., Prelle, A., Moggio, M., Braga, M., Silani, V. & De Biasi, S. (2001) Early vacuolization and mitochondrial damage in motor neurons of FALS mice are not associated with apoptosis or with changes in cytochrome oxidase histochemical reactivity. J Neurol Sci., 191, 25-33.

Bergemalm, D., Jonsson, P.A., Graffmo, K.S., Andersen, P.M., Brännström, T., Rehnmark, A. & Marklund, SL. (2006) Overloading of stable and exclusion of unstable human superoxide dismutase-1 variants in mitochondria of murine amyotrophic lateral sclerosis models. J Neurosci., 26, 4147-4154.

Bergeron, C., Beric-Maskarel, K., Muntasser, S., Weyer, L., Somerville, M.J. & Percy, M.E. (1994) Neurofilament light and polyadenylated mRNA levels are decreased in amyotrophic lateral sclerosis motor neurons. J Neuropathol Exp Neurol., 53, 221-230.

Blackburn, D., Sargsyan, S., Monk, P.N. & Shaw, P.J. (2009) Astrocyte function and role in motor neuron disease: a future therapeutic target? Glia, 57, 1251-1264.

Bogdan, C. (2001). Nitric oxide and the immune response. Nat Immunol., 2, 907-916.

Bogdanov, M., Brown, R.H., Matson, W., Smart, R., Hayden, D., O'Donnell, H., Flint Beal, M. & Cudkowicz, M. (2000) Increased oxidative damage to DNA in ALS patients. Free Radical Biol Med., 29, 652-658.

Boillée, S., Yamanaka, K., Lobsiger, C.S., Copeland, N.G., Jenkins, N.A., Kassiotis, G., Kollias, G. & Cleveland, D.W. (2006) Onset and progression in inherited ALS determined by motor neurons and microglia. Science, 312, 1389-1392.

Boillée, S. & Cleveland, D.W. (2008) Revisiting oxidative damage in ALS: microglia, Nox, and mutant SOD1. J Clin Invest., 118, 474-478.

Bon, C.L. & Garthwaite, J. (2003) On the role of nitric oxide in hippocampal long-term potentiation. J Neurosci., 23, 1941-1948.

Bonde, C., Sarup, A., Schousboe, A., Gegelashvili, G., Zimmer, J. & Noraberg, J. (2003) Neurotoxic and neuroprotective effects of the glutamate transporter inhibitor dl-threo-betabenzyloxyaspartate (DL-TBOA) during physiological and ischemia-like conditions. Neurochem Int., 43, 371-380.

Boone, T.B. & Aldes, L.D. (1984) The ultrastructure of two distinct neuron populations in the hypoglossal nucleus of the rat. Exp Brain Res., 54, 321-326.

Borchelt, D.R., Lee, M.K., Slunt, H.S., Guarnieri, M., Xu, Z.S., Wong, P.C., Brown Jr., R.H., Price, D.L., Sisodia, S.S. & Cleveland, D.W. (1994) Superoxide dismutase 1 with mutations linked to familial amyotrophic lateral sclerosis possesses significant activity. Proc Natl Acad Sci USA., 91, 8292-8296.

Bories, C., Amendola, J., Lamotte d'Incamps, B. & Durand, J. (2007) Early electrophysiological abnormalities in lumbar motoneurons in a transgenic mouse model of amyotrophic lateral sclerosis. Eur J Neurosci., 25, 451-9.

Borke, R.C., Nau, M.E. & Ringler, R.L. (1983) Brain stem afferents of hypoglossal neurons in the rat. Brain Res., 269, 47-55.

Bösel, J., Gandor, F., Harms, C., Synowitz, M., Harms, U., Djoufack, P.C., Megow, D., Dirnagl, U., Hörtnagl, H., Fink, K.B. & Endres, M. (2005) Neuroprotective effects of atorvastatin against glutamate-induced excitotoxicity in primary cortical neurones. J Neurochem., 92, 1386-98.

Bostock, H. (1983) The strength-duration relationship for excitation of myelinated nerve: computed dependence on membrane parameters. J Physiol., 341, 59-74.

Bostock, H. & Rothwell, J.C. (1997) Latent addition in motor and sensory fibres of human peripheral nerve. J Physiol., 498, 277-94.

Bredt, D.S., Hwang, P.M. & Snyder, S.H. (1990) Localization of nitric oxide synthase indicating a neural role for nitric oxide. Nature, 347, 768-770.

Bredt, D.S., Glatt, C.E., Hwang, P.M., Fotuhi, M., Dawson, T.M. & Snyder, S.H. (1991) Nitric oxide synthase protein and mRNA are discretely localized in neuronal populations of the mammalian CNS together with NADPH diaphorase. Neuron, 7, 615-624.

Brenman, J.E., Chao, D.S., Gee, S.H., McGee, A.W., Craven, S.E., Santillano, D.R., Wu, Z., Huang, F., Xia, H., Peters, M.F., Froehner, S.C. & Bredt, D.S. (1996) Interaction of nitric oxide synthase with the postsynaptic density protein PSD-95 and alpha1-syntrophin mediated by PDZ domains. Cell, 84, 757-767.

Brooks, B.R., Shodis, K.A., Lewis, D.H., Rawling, J.D., Sanjak, M., Belden, D.S., Hakim, H., DeTan, Y. & Gaffney, J.M. (1995) Natural history of amyotrophic lateral sclerosis: quantification of symptoms, signs, strength, and function. Adv Neurol., 68:163-184.

Brownstone, R.M. (2007) Take your PIC: motoneuronal persistent inward currents may be somatic as well as dendritic. J Neurophysiol., 98, 579-580.

Bruijn, L.I., Becher, M.W., Lee, M.K., Anderson, K.L., Jenkins, N.A., Copeland, N.G., Sisodia, S.S., Rothstein, J.D., Borchelt, D.R., Price, D.L. & Cleveland, D.W. (1997) ALS-linked SOD1 mutant G85R mediates damage to astrocytes and promotes rapidly progressive disease with SOD1-containing inclusions. Neuron, 18, 327-338.

Bruijn, L.I., Houseweart, M.K., Kato, S., Anderson, K.L., Anderson, S.D., Ohama, E., Reaume, A.G., Scott, R.W. & Cleveland, D.W. (1998) Aggregation and motor neuron toxicity of an ALS-linked SOD1 mutant independent from wild-type SOD1. Science, 281, 1851-1854.

Bruijn, L.I., Miller, T.M. & Cleveland, D.W. (2004) Unraveling the mechanisms involved in motor neuron degeneration in ALS. Annu Rev Neurosci., 27, 723-749.

Budworth, J., Meillerais, S., Charles, I. & Powell, K. (1999) Tissue distribution of the human soluble guanylate cyclases. Biochem Biophys Res Commun., 263, 696-701.

Carriedo, S.G., Sensi, S.L., Yin, H.Z. & Weiss, J.H. (2000) AMPA exposures induce mitochondrial Ca(2+) overload and ROS generation in spinal motor neurons in vitro. J Neurosci., 20, 240-250.

de Carvalho, M. & Swash, M. (2000) Nerve conduction studies in amyotrophic lateral sclerosis. Muscle Nerve, 23, 344-52.

Casoni, F., Basso, M., Massignan, T., Gianazza, E., Cheroni, C., Salmona, M., Bendotti, C. & Bonetto, V. (2005) Protein nitration in a mouse model of familial amyotrophic lateral sclerosis: possible multifunctional role in the pathogenesis. J Biol Chem., 280, 16295-16304.

Caughey, B. & Lansbury, P.T. (2003) Protofibrils, pores, fibrils, and neurodegeneration: separating the responsible protein aggregates from the innocent bystanders. Annu Rev Neurosci., 26, 267-298.

Chandra, J., Samali, A. & Orrenius, S. (2000) Triggering and modulation of apoptosis by oxidative stress. Free Radic Biol Med., 29, 323-333.

Chang, Y., Kong, Q., Shan, X., Tian, G., Ilieva, H., Cleveland, D.W., Rothstein, J.D., Borchelt, D.R., Wong, P.C. & Lin, C.L. (2008) Messenger RNA oxidation occurs early in disease pathogenesis and promotes motor neuron degeneration in ALS. PLoS One, 3, e2849.

Chiò, A., Benzi, G., Dossena, M., Mutani, R. & Mora, G. (2005) Severely increased risk of amyotrophic lateral sclerosis among Italian professional football players. Brain, 128, 472-476.

Chou, S.M., Wang, H.S. & Komai, K. (1996) Colocalization of NOS and SOD1 in neurofilament accumulation within motor neurons of amyotrophic lateral sclerosis: an immunohistochemical study. J Chem Neuroanat., 10, 249-258.

Clement, A.M., Nguyen, M.D., Roberts, E.A., Garcia, M.L., Boillée, S., Rule, M., McMahon, A.P., Doucette, W., Siwek, D., Ferrante, R.J., Brown, R.H. Jr., Julien, J.P., Goldstein, L.S. & Cleveland, D.W. (2003) Wild-type nonneuronal cells extend survival of SOD1 mutant motor neurons in ALS mice. Science, 302, 113-117.

Cleveland, D.W. & Rothstein, J.D. (2001) From Charcot to Lou Gehrig: deciphering selective motor neuron death in ALS. Nat Rev Neurosci., 2, 806-819.

Cocchia, D. (1981) Immunocytochemical localization of S-100 protein in the brain of adult rat. An ultrastructural study. Cell Tissue Res., 214, 529-540.

Cookson, M.R., Menzies, F.M., Manning, P., Eggett, C.J., Figlewicz, D.A., McNeil, C.J. & Shaw, P.J. (2002) Cu/Zn superoxide dismutase (SOD1) mutations associated with familial amyotrophic lateral sclerosis (ALS) affect cellular free radical release in the presence of oxidative stress. Amyotroph Lateral Scler Other Motor Neuron Disord., 3, 75-85.

Cox, P.A., Banack, S.A. & Murch, S.J. (2003) Biomagnification of cyanobacterial neurotoxins and neurodegenerative disease among the Chamorro people of Guam. Proc Natl Acad Sci USA., 100, 13380-13383.

Coyle, J.T. & Puttfarcken, P. (1993) Oxidative stress, glutamate, and neurodegenerative disorders. Science, 262, 689-695.

Cramer, N.P., Li, Y. & Keller, A. (2007) The whisking rhythm generator: a novel mammalian network for the generation of movement. J Neurophysiol., 97, 2148-2158.

Crill, W.E. (1996) Persistent sodium current in mammalian central neurons. Annu Rev Physiol., 58, 349-362.

Crow, J.P., Sampson, J.B., Zhuang, Y., Thompson, J.A. & Beckman, J.S. (1997) Decreased zinc affinity of amyotrophic lateral sclerosis-associated superoxide dismutase mutants leads to enhanced catalysis of tyrosine nitration by peroxynitrite. J Neurochem., 69, 1936-1944.

Crow, J.P., Ye, Y.Z., Strong, M., Kirk, M., Barnes, S. & Beckman, J.S. (1997b) Superoxide dismutase catalyzes nitration of tyrosines by peroxynitrite in the rod and head domains of neurofilament-L. J Neurochem., 69, 1945-1953.

Cunningham, E.T. & Jr. Sawchenko, P.E. (2000) Dorsal medullary pathways subserving oromotor reflexes in the rat: implications for the central neural control of swallowing. J Comp Neurol., 417, 448-466.

Cuozzo, J.W. & Kaiser, C.A. (1999) Competition between glutathione and protein thiols for disulphide-bond formation. Nat Cell Biol., 1, 130-135.

Dal Canto, M.C. & Gurney, M.E. (1997) A low expressor line of transgenic mice carrying a mutant human Cu,Zn superoxide dismutase (SOD1) gene develops pathological changes that most closely resemble those in human amyotrophic lateral sclerosis. Acta Neuropathol., 93, 537-550.

Damiano, M., Starkov, A.A., Petri, S., Kipiani, K., Kiaei, M., Mattiazzi, M., Flint Beal, M. & Manfredi, G. (2006) Neural mitochondrial Ca2+ capacity impairment precedes the onset of motor symptoms in G93A Cu/Zn-superoxide dismutase mutant mice. J Neurochem., 96, 1349-1361.

Darbon, P., Yvon, C., Legrand, J.C. & Streit, J. (2004) INaP underlies intrinsic spiking and rhythm generation in networks of cultured rat spinal cord neurons. Eur J Neurosci., 20, 976-988.

Dawson, V.L., Dawson, T.M., Bartley, D.A., Uhl, G.R. & Snyder, S.H. (1993) Mechanisms of nitric oxide-mediated toxicity in primary brain cultures. J Neurosci., 13, 2651-2661.

Del Cano, G.G., Millan, L.M., Gerrikagoitia, I., Sarasa, M. & Matute, C. (1999) Ionotropic glutamate receptor subunit distribution on hypoglossal motoneuronal pools in the rat. J Neurocytol., 28, 455-468.

Deng, H.X., Hentati, A., Tainer, J.A., Iqbal, Z., Cayabyab, A., Hung, W.Y., Getzoff, E.D., Hu, P., Herzfeldt, B., Roos, R.P., Warner, C., Deng, G., Soriano, E., Smyth, C., Parge, H.E., Ahmed, A., Roses, A.D., Hallewell, R.A., Pericak-Vance, M.A. & Siddique, T. (1993) Amyotrophic lateral sclerosis and structural defects in Cu,Zn superoxide dismutase. Science, 261, 1047-1051.

Denninger, J.W. & Marletta, M.A. (1999) Guanylate cyclase and the NO/cGMP signaling pathway. Biochim Biophys Acta, 1411, 334-350.

Denu, J.M. & Tanner, K.G. (1998) Specific and reversible inactivation of protein tyrosine phosphatases by hydrogen peroxide: evidence for a sulfenic acid intermediate and implications for redox regulation. Biochemistry, 37, 5633-5642.

DePaul, R., Abbs, J.H., Caligiuri, M., Gracco, V.L. & Brooks, B.R. (1988) Hypoglossal, trigeminal, and facial motoneuron involvement in amyotrophic lateral sclerosis. Neurology, 38, 281-283.

Didier, M., Harandi, M., Aguera, M., Bancel, B., Tardy, M., Fages, C., Calas, A., Stagaard, M., Møllgård, K. & Belin, M.F. (1986) Differential immunocytochemical staining for glial fibrillary acidic (GFA) protein, S-100 protein and glutamine synthetase in the rat subcommissural organ, nonspecialized ventricular ependyma and adjacent neuropil. Cell Tissue Res., 245, 343-351.

Dobbins, E.G. & Feldman, J.L. (1995) Differential innervation of protruder and retractor muscles of the tongue in rat. J Comp Neurol., 357, 376-394.

Donato, R. (2001) S100: a multigenic family of calcium-modulated proteins of the EF-hand type with intracellular and extracellular functional roles. Int J Biochem Cell Biol., 33, 637-668.

Donato, R. (2003) Intracellular and extracellular roles of S100 proteins. Microsc Res Tech., 60, 540-551.

Donato, R. & Nistri, A. (2000) Relative contribution by GABA or glycine to Cl-mediated synaptic transmission on rat hypoglossal motoneurons in vitro. J Neurophysiol., 84, 2715-2724.

Dreher, D. & Junod, A.F. (1995) Differential effects of superoxide, hydrogen peroxide, and hydroxyl radical on intracellular calcium in human endothelial cells. J Cell Physiol., 162,147-153.

Droge, W. (2003) Oxidative stress and aging. Adv Exp Med Biol., 543, 191-200.

Durand, J., Amendola, J., Bories, C. & Lamotte d'Incamps, B. (2006) Early abnormalities in transgenic mouse models of amyotrophic lateral sclerosis. J Physiol Paris, 99, 211-20.

Durham, H.D., Roy, J., Dong, L. & Figlewicz, D.A. (1997) Aggregation of mutant Cu/Zn superoxide dismutase proteins in a culture model of ALS. J Neuropathol Exp Neurol., 56, 523-530.

Eisen, A., Kim, S. & Pant, B. (1992) Amyotrophic lateral sclerosis (ALS): a phylogenetic disease of the corticomotoneuron? Muscle Nerve, 15, 219-24.

Ellgaard, L., Molinari, M. & Helenius, A. (1999) Setting the standards: quality control in the secretory pathway. Science, 286, 1882-1888.

Eng, L.F. (1985) Glial fibrillary acidic protein (GFAP): the major protein of glial intermediate filaments in differentiated astrocytes. J Neuroimmunol., 8, 203-214.

Enomoto, A., Han, J.M., Hsiao, C.F., Wu, N. & Chandler, S.H. (2006) Participation of sodium currents in burst generation and control of membrane excitability in mesencephalic trigeminal neurons. J Neurosci., 26, 3412-3422.

Ermilova, I.P., Ermilov, V.B., Levy, M., Ho, E., Pereira, C. & Beckman, J.S. (2005) Protection by dietary zinc in ALS mutant G93A SOD transgenic mice. Neurosci Lett., 379, 42-46.

van Es, M.A., Van Vught, P.W., Blauw, H.M., Franke, L., Saris, C.G., Andersen, P.M., Van Den Bosch, L., de Jong, S.W., van 't Slot, R., Birve, A., Lemmens, R., de Jong, V., Baas, F., Schelhaas, H.J., Sleegers, K., Van Broeckhoven, C., Wokke, J.H., Wijmenga, C., Robberecht, W., Veldink, J.H., Ophoff, R.A. & van den Berg, L.H. (2007) ITPR2 as a susceptibility gene in sporadic amyotrophic lateral sclerosis: a genome-wide association study. Lancet Neurol., 6, 869-877.

Essin, K., Nistri, A. & Magazanik, L. (2002) Evaluation of GluR2 subunit involvement in AMPA receptor function of neonatal rat hypoglossal motoneurons. Eur J Neurosci., 15, 1899-1906.

Estevez, A.G., Crow, J.P., Sampson, J.B., Reiter, C., Zhuang, Y., Richardson, G.J., Tarpey, M.M., Barbeito, L. & Beckman, J.S. (1999) Induction of nitric oxide-dependent apoptosis in motor neurons by zinc-deficient superoxide dismutase. Science, 286, 2498-2500.

Facchinetti, F., Sasaki, M., Cutting, F.B., Zhai, P., MacDonald, J.E., Reif, D., Beal, M.F., Huang, P.L., Dawson, T.M., Gurney, M.E. & Dawson, V.L. (1999) Lack of involvement of neuronal nitric oxide synthase in the pathogenesis of a transgenic mouse model of familial amyotrophic lateral sclerosis. Neuroscience, 90, 1483-1492.

Fay, R.A. & Norgren, R. (1997) Identification of rat brainstem multisynaptic connections to the oral motor nuclei using pseudorabies virus. III. Lingual muscle motor systems. Brain Res Brain Res Rev., 25, 291-311.

Feldman, D.E., Chauhan, V. & Koong, A.C. (2005) The unfolded protein response: a novel component of the hypoxic stress response in tumors. Mol Cancer Res., 3, 597-605.

Ferrante, R.J., Browne, S.E., Shinobu, L.A., Bowling, A.C., Baik, M.J., MacGarvey, U., Kowall, N.W., Brown Jr., R.H. & Beal, M.F. (1997) Evidence of increased oxidative damage in both sporadic and familial amyotrophic lateral sclerosis. J Neurochem., 69, 2064-2074.

Ferrante, R.J., Shinobu, L.A., Schulz, J.B., Matthews, R.T., Thomas, C.E., Kowall, N.W., Gurney, M.E. & Beal, M.F. (1997b) Increased 3-nitrotyrosine and oxidative damage in mice with a human copper/zinc superoxide dismutase mutation. Ann Neurol., 42, 326-334.

Fisher, N.D. & Nistri, A. (1993) A study of the barium-sensitive and insensitive components of the action of thyrotropin-releasing hormone on lumbar motoneurons of the rat isolated spinal cord. Eur J Neurosci., 5, 1360-9.

Fitzmaurice, P.S., Shaw, I.C., Kleiner, H.E., Miller, R.T., Monks, T.J., Lau, S.S., Mitchell, J.D. & Lynch, P.G. (1996) Evidence for DNA damage in amyotrophic lateral sclerosis. Muscle Nerve, 19, 797-798.

Forman, H.J., Torres, M. & Fukuto, J. (2002) Redox signaling. Mol Cell Biochem., 234-235, 49-62.

Furchgott, R.F. (1999) Endothelium-derived relaxing factor: discovery, early studies, and identification as nitric oxide. Biosci Rep., 19, 235-251.

Garthwaite, G., Bartus, K., Malcolm, D., Goodwin, D., Kollb-Sielecka, M., Dooldeniya, C. & Garthwaite, J. (2006) Signaling from blood vessels to CNS axons through nitric oxide. J Neurosci., 26, 7730-40.

Garthwaite, J. (2008) Concepts of neural nitric oxide-mediated transmission. Eur J Neurosci., 27, 2783-2802.

Gass, J.N., Gifford, N.M. & Brewer, J.W. (2002) Activation of an unfolded protein response during differentiation of antibody-secreting B cells. J Biol Chem., 277, 49047-49054.

Ge, W.W., Wen, W., Strong, W.L., Leystra-Lantz, C. & Strong, M.J. (2005) Mutant copper/ zinc superoxide dismutase binds to and destabilizes human low molecular weight neurofilament mRNA. J Biol Chem., 280, 118-124.

Genova, M.L., Pich, M.M., Bernacchia, A., Bianchi, C., Biondi, A., Bovina, C., Falasca, A.I., Formiggini, G., Castelli, G.P. & Lenaz, G. (2004) The mitochondrial production of reactive oxygen species in relation to aging and pathology. Ann N Y Acad Sci., 1011, 86-100.

Gerich, F.J., Funke, F., Hildebrandt, B., Fasshauer, M. & Müller, M. (2009) H2O2-mediated modulation of cytosolic signaling and organelle function in rat hippocampus. Pflugers Arch., 458, 937-52.

Gibb, B.J. & Garthwaite, J. (2001) Subunits of the nitric oxide receptor, soluble guanylyl cyclase, expressed in rat brain. Eur J Neurosci., 13, 539-544.

Gibb, S.L., Boston-Howes, W., Lavina, Z.S., Gustincich, S., Brown, R.H. Jr., Pasinelli, P. & Trotti, D. (2007) A caspase-3-cleaved fragment of the glial glutamate transporter EAAT2 is sumoylated and targeted to promyelocytic leukemia nuclear bodies in mutant SOD1-linked amyotrophic lateral sclerosis. J Biol Chem., 282, 32480-32490.

Giulian, D. (1993) Reactive glia as rivals in regulating neuronal survival. Glia, 7, 102-110.

Golino, P., Ragni, M., Cirillo, P., Avvedimento, V.E., Feliciello, A., Esposito, N., Scognamiglio, A., Trimarco, B., Iaccarino, G., Condorelli, M., Chiariello, M. & Ambrosio, G. (1996) Effects of tissue factor induced by oxygen free radicals on coronary flow during reperfusion. Nat Med., 2, 35-40.

Gong, Y.H., Parsadanian, A.S., Andreeva, A., Snider, W.D. & Elliott, J.L. (2000) Restricted expression of G86R Cu/Zn superoxide dismutase in astrocytes results in astrocytosis but does not cause motoneuron degeneration. J Neurosci., 20, 660-665.

González-Forero, D., Portillo, F., Gómez, L., Montero, F., Kasparov, S. & Moreno-López, B. (2007) Inhibition of resting potassium conductances by long-term activation of the NO/cGMP/protein kinase G pathway: a new mechanism regulating neuronal excitability. J Neurosci., 27, 6302-12.

Greenway, M.J., Andersen, P.M., Russ, C., Ennis, S., Cashman, S., Donaghy, C., Patterson, V., Swingler, R., Kieran, D., Prehn, J., Morrison, K.E., Green, A., Acharya, K.R., Brown, R. H. & Hardiman, O. (2006) ANG mutations segregate with familial and 'sporadic' amyotrophic lateral sclerosis. Nat Genet., 38, 411-413.

Guo, H., Lai, L., Butchbach, M.E., Stockinger, M.P., Shan, X., Bishop, G.A. & Lin, C.L. (2003) Increased expression of the glial glutamate transporter EAAT2 modulates excitotoxicity and delays the onset but not the outcome of ALS in mice. Hum Mol Genet., 12, 2519-2532.

Gurney, M.E., Pu, H., Chiu, A.Y., Dal Canto, M.C., Polchow, C.Y., Alexander, D.D., Caliendo, J., Hentati, A., Kwon, Y.W., Deng, H.X., Chen, W.J., Zhai, P., Sufit, R.L. & Siddique, T. (1994) Motor neuron degeneration in mice that express a human Cu,Zn superoxide dismutase mutation. Science, 264, 1772-1775.

Gurney, M.E., Tomasselli, A.G. & Heinrikson, R.L. (2000) Stay the executioner's hand. Science, 288, 283-284.

Gutierrez, J., Ballinger, S.W., Darley-Usmar, V.M. & Landar, A. (2006) Free radicals, mitochondria, and oxidized lipids: the emerging role in signal transduction in vascular cells. Circ Res., 99, 924-932.

Haenggeli, C. & Kato, A.C. (2002) Differential vulnerability of cranial motoneurons in mouse models with motor neuron degeneration. Neurosci Lett., 335, 39-43.

Hahm, E.T., Seo, J.W., Hur, J. & Cho, Y.W. (2010) Modulation of Presynaptic GABA Release by Oxidative Stress in Mechanically-isolated Rat Cerebral Cortical Neurons. Korean J Physiol Pharmacol., 14,127-32.

Hai, T. & Hartman, M.G. (2001) The molecular biology and nomenclature of the activating transcription factor ⁄ cAMP responsive element binding family of transcription factors: activating transcription factor proteins and homeostasis. Gene, 273, 1-11.

Hall, C.N., Keynes, R.G. & Garthwaite, J. (2009) Cytochrome P450 oxidoreductase participates in nitric oxide consumption by rat brain. Biochem J., 419, 411-418.

Halliwell, B. & Gutteridge, J.M.C. (1999) Free Radicals in Biology and Medicine, 3rd ed. Oxford Univ. Press, Oxford.

Hammarström, A.K. & Gage, P.W. (1999) Nitric oxide increases persistent sodium current in rat hippocampal neurons. J Physiol., 520, 451-61.

Harraz, M.M., Marden, J.J., Zhou, W., Zhang, Y., Williams, A., Sharov, V.S., Nelson, K., Luo, M., Paulson, H., Schoneich, C. & Engelhardt, J.F. (2008) SOD1 mutations disrupt redox-sensitive Rac regulation of NADPH oxidase in a familial ALS model. J Clin Invest., 118, 659-670.

Harvey, P.J., Li, Y., Li, X. & Bennett, D.J. (2006) Persistent sodium currents and repetitive firing in motoneurons of the sacrocaudal spinal cord of adult rats. J Neurophysiol., 96, 1141-57.

Haynes, C.M., Titus, E.A. & Cooper, A.A. (2004) Degradation of misfolded proteins prevents ER-derived oxidative stress and cell death. Mol Cell, 15, 767-776.

Heath, P.R. & Shaw, P.J. (2002) Update on the glutamatergic neurotransmitter system and the role of excitotoxicity in amyotrophic lateral sclerosis. Muscle Nerve, 26, 438-458.

Hidalgo, C. (2005) Cross talk between Ca2+ and redox signalling cascades in muscle and neurons through the combined activation of ryanodine receptors/Ca2+ release channels. Philos Trans R Soc Lond B Biol Sci., 360, 2237-2246.

Higgins, C.M., Jung, C., Ding, H. & Xu, Z. (2002) Mutant Cu,Zn superoxide dismutase that causes motoneuron degeneration is present in mitochondria in the CNS. J Neurosci., 22, RC215.

Higgins, C.M., Jung, C. & Xu, Z. (2003) ALS-associated mutant SOD1G93A causes mitochondrial vacuolation by expansion of the intermembrane space and by involvement of SOD1 aggregation and peroxisomes. BMC Neurosci., 4, 16.

Hirano, A., Nakano, I., Kurland, L.T., Mulder, D.W., Holley, P.W. & Saccomanno, G. (1984) Fine structural study of neurofibrillary changes in a family with amyotrophic lateral sclerosis. J Neuropathol Exp Neurol., 43, 471-480.

Hirano, A., Donnenfeld, H., Sasaki, S. & Nakano, I. (1984b) Fine structural observations of neurofilamentous changes in amyotrophic lateral sclerosis. J Neuropathol Exp Neurol., 43, 461-470.

Hodgson, E.K. & Fridovich, I. (1975) The interaction of bovine erythrocyte superoxide dismutase with hydrogen peroxide: inactivation of the enzyme. Biochemistry, 14, 5294-5299.

Hollmann, M., Hartley, M. & Heinemann, S. (1991) Ca^{2+} permeability of KA-AMPA-gated glutamate receptor channels depends on subunit composition. Science, 252, 851-853.

Hopper, R.A. & Garthwaite, J. (2006) Tonic and phasic nitric oxide signals in hippocampal long-term potentiation. J Neurosci., 26, 11513-11521.

Horner, R.D., Kamins, K.G., Feussner, J.R., Grambow, S.C., Hoff-Lindquist, J., Harati, Y., Mitsumoto, H., Pascuzzi, R., Spencer, P.S., Tim, R., Howard, D., Smith, T.C., Ryan, M.A., Coffman, C.J. & Kasarskis, E.J. (2003) Occurrence of amyotrophic lateral sclerosis among Gulf War veterans. Neurology, 61, 742-749.

Howland, D.S., Liu, J., She, Y., Goad, B. & Maragakis, N.J. (2002) Focal loss of the glutamate transporter EAAT2 in a transgenic rat model of SOD1 mutant-mediated amyotrophic lateral sclerosis (ALS). Proc Natl Acad Sci USA., 99, 1604-1609.

Hurt, K.J., Sezen, S.F., Champion, H.C., Crone, J.K., Palese, M.A., Huang, P.L., Sawa, A., Luo, X., Musicki, B., Snyder, S.H. & Burnett, A.L. (2006) Alternatively spliced neuronal nitric oxide synthase mediates penile erection. Proc Natl Acad Sci USA., 103, 3440-3443.

Ignarro, L.J., Buga, G.M., Wood, K.S., Byrns, R.E. & Chaudhuri, G. (1987) Endothelium-derived relaxing factor produced and released from artery and vein is nitric oxide. Proc Natl Acad Sci USA., 84, 9265-9269.

Ihara, Y., Nobukuni, K., Takata, H. & Hayabara, T. (2005) Oxidative stress and metal content in blood and cerebrospinal fluid of amyotrophic lateral sclerosis patients with and without a Cu,Zn-superoxide dismutase mutation. Neurol Res., 27, 105-108.

Ince, P.G., Shaw, P.J., Slade, J.Y., Jones, C. & Hudgson, P. (1996) Familial amyotrophic lateral sclerosis with a mutation in exon 4 of the Cu/Zn superoxide dismutase gene: pathological and immunocytochemical changes. Acta Neuropathol., 92, 395-403.

Isler, J.A., Skalet, A.H. & Alwine, J.C. (2005) Human cytomegalovirus infection activates and regulates the unfolded protein response. J Virol., 79, 6890- 6899.

Ito, D. & Suzuki, N. (2009) Seipinopathy: a novel endoplasmic reticulum stress-associated disease. Brain, 132, 8-15.

Jacob, D.A., Bengston, C.L. & Forger, N.G. (2005) Effects of Bax gene deletion on muscle and motoneuron degeneration in a sexually dimorphic neuromuscular system. J Neurosci., 25, 5638-5644.

Jacoby, S., Sims, R.E. & Hartell, N.A. (2001) Nitric oxide is required for the induction and heterosynaptic spread of long-term potentiation in rat cerebellar slices. J Physiol., 535, 825-839.

Jaiswal, M.K. & Keller, B.U. (2009) Cu/Zn superoxide dismutase typical for familial amyotrophic lateral sclerosis increases the vulnerability of mitochondria and perturbs Ca2+ homeostasis in SOD1G93A mice. Mol Pharmacol., 75, 478-89.

Janssen-Heininger, Y.M., Mossman, B.T., Heintz, N.H., Forman, H.J., Kalyanaraman, B., Finkel, T., Stamler, J.S., Rhee, S.G. & van der Vliet, A. (2008) Redox-based regulation of signal transduction: principles, pitfalls, and promises. Free Radic Biol Med., 45, 1-17.

Jiang, Z.G., Lu, X.C., Nelson, V., Yang, X., Pan, W., Chen, R.W., Lebowitz, M.S., Almassian, B., Tortella, F.C., Brady, R.O. & Ghanbari, H.A. (2006) A multifunctional cytoprotective agent that reduces neurodegeneration after ischemia. Proc Nat Acad Sci USA., 103, 1581-1586.

Johnston, J.A., Dalton, M.J., Gurney, M.E. & Kopito, R.R. (2000) Formation of high molecular weight complexes of mutant Cu,Zn-superoxide dismutase in a mouse model for familial amyotrophic lateral sclerosis. Proc Natl Acad Sci USA., 97, 12571-12576.

Jones, D.P. (2002) Redox potential of GSH/GSSG couple: assay and biological significance. Methods Enzymol., 348, 93-112.

Jones, J.D., Carney, S.T., Vrana, K.E., Norford, D.C. & Howlett, A.C. (2008) Cannabinoid receptor-mediated translocation of NO-sensitive guanylyl cyclase and production of cyclic GMP in neuronal cells. Neuropharmacology, 54, 23-30.

Jones, K.H. & Senft, J.A. (1985) An improved method to determine cell viability by simultaneous staining with fluorescein diacetate-propidium iodide. J Histochem Cytochem., 33, 77-9.

Jonsson, P.A., Ernhill, K., Andersen, P.M., Bergemalm, D., Brännström, T., Gredal, O., Nilsson, P. & Marklund, S.L. (2004) Minute quantities of misfolded mutant superoxide dismutase-1 cause amyotrophic lateral sclerosis. Brain, 127, 73-88.

Joseph, J.A., Erat, S., Denisova, N. & Villalobos-Molina, R. (1998) Receptor and age-selective effects of dopamine oxidation on receptor-G protein interactions in the striatum. Free Radic Biol Med., 24, 827-834.

Jung, C., Higgins, C.M. & Xu, Z. (2002) Mitochondrial electron transport chain complex dysfunction in a transgenic mouse model for amyotrophic lateral sclerosis. J Neurochem., 83, 535-545.

Kabashi, E., Valdmanis, P.N., Dion, P., Spiegelman, D., McConkey, B.J., Vande Velde, C., Bouchard, J.P., Lacomblez, L., Pochigaeva, K., Salachas, F., Pradat, P.F., Camu, W., Meininger, V., Dupre, N. & Rouleau, G.A. (2008) TARDBP mutations in individuals with sporadic and familial amyotrophic lateral sclerosis. Nat Genet., 40, 572-574.

Kamsler, A. & Segal, M. (2004) Hydrogen peroxide as a diffusible signal molecule in synaptic plasticity. Mol Neurobiol., 29, 167-178.

Kanai, K., Kuwabara, S., Arai, K., Sung, J.Y., Ogawara, K. & Hattori, T. (2003) Muscle cramp in Machado-Joseph disease: altered motor axonal excitability properties and mexiletine treatment. Brain, 126, 965-73.

Kasarskis, E.J., Lindquist, J.H., Coffman, C.J., Grambow, S.C., Feussner, J.R., Allen, K.D., Oddone, E.Z., Kamins, K.A. & Horner, R.D. (2009) Clinical aspects of ALS in Gulf War veterans. Amyotroph Lateral Scler., 10, 35-41.

Kato, S. (2008) Amyotrophic lateral sclerosis models and human neuropathology: similarities and differences. Acta Neuropathol., 115, 97-114.

Kiernan, M.C., Burke, D., Andersen, K.V. & Bostock, H. (2000) Multiple measures of axonal excitability: a new approach in clinical testing. Muscle Nerve, 23, 399-409.

Kiernan, M. & Burke, D. (2004) Threshold electrotonus and the assessment of nerve excitability in amyotrophic lateral sclerosis. Eisen A, ed. Clinical neurophysiology of motor neuron diseases. Amsterdam, Elsevier, 359-66.

Kikuchi, H., Almer, G., Yamashita, S., Guegan, C., Nagai, M., Xu, Z., Sosunov, A.A., McKhann 2nd, G.M. & Przedborski, S. (2006) Spinal cord endoplasmic reticulum stress associated with a microsomal accumulation of mutant superoxide dismutase-1 in an ALS model. Proc Natl Acad Sci USA., 103, 6025-6030.

Kim, N.H., Jeong, M.S., Choi, S.Y. & Hoon Kang, J. (2004) Oxidative modification of neurofilament-L by the Cu,Zn-superoxide dismutase and hydrogen peroxide system. Biochimie, 86, 553-559.

Kirby, J., Halligan, E., Baptista, M.J., Allen, S., Heath, P.R., Holden, H., Barber, S.C., Loynes, C.A., Wood-Allum, C.A., Lunec, J. & Shaw, P.J. (2005) Mutant SOD1 alters the motor neuronal transcriptome: implications for familial ALS. Brain, 128, 1686-1706.

Kirby, M.S., Sagara, Y., Gaa, S., Inesi, G., Lederer, W.J. & Rogers, T.B. (1992) Thapsigargin inhibits contraction and Ca2+ transient in cardiac cells by specific inhibition of the sarcoplasmic reticulum Ca2+ pump. J Biol Chem., 267, 12545-12551.

Kishida, K.T. & Klann, E. (2007) Sources and targets of reactive oxygen species in synaptic plasticity and memory. Antioxid Redox Signal., 9, 233-244.

Kitamura, S., Nishiguchi, T. & Sakai, A. (1983) Location of cell somata and the peripheral course of axons of the geniohyoid and thyrohyoid motoneurons: a horseradish peroxidase study in the rat. Exp Neurol., 79, 87-96.

Klann, E., Roberson, E.D., Knapp, L.T. & Sweatt, J.D. (1998) A role for superoxide in protein kinase C activation and induction of long-term potentiation. J Biol Chem., 273, 4516-4522.

Klivenyi, P., Ferrante, R.J., Matthews, R.T., Bogdanov, M.B., Klein, A.M., Andreassen, O.A., Mueller, G., Wermer, M., Kaddurah-Daouk, R. & Beal, M.F. (1999) Neuroprotective effects of creatine in a transgenic animal model of amyotrophic lateral sclerosis. Nature Med., 5, 347-350.

Koesling, D., Russwurm, M., Mergia, E., Mullershausen, F. & Friebe, A. (2004) Nitric oxide-sensitive guanylyl cyclase: structure and regulation. Neurochem Int., 45, 813-819.

Kohr, G., Eckardt, S., Luddens, H., Monyer, H. & Seeburg, P.H. (1994) NMDA receptor channels: subunit-specific potentiation by reducing agents. Neuron, 12, 1031-1040.

Kong, J. & Xu, Z. (1998) Massive mitochondrial degeneration in motor neurons triggers the onset of amyotrophic lateral sclerosis in mice expressing a mutant SOD1. J Neurosci., 18, 3241-3250.

Koutsilieri, E., Scheller, C., Tribl, F. & Riederer, P. (2002) Degeneration of neuronal cells due to oxidative stress-microglial contribution. Parkinsonism Relat Disord., 8, 401-406.

Krieger, C., Jones, K., Kim, S.U. & Eisen, A.A. (1994) The role of intracellular free calcium in motor neuron disease. J Neurol Sci., 124, 27-32.

Kristensen, B.W., Noraberg, J. & Zimmer, J. (2001) Comparison of excitotoxic profiles of ATPA, AMPA, KA and NMDA in organotypic hippocampal slice cultures. Brain Res., 917, 21-44.

Kühnlein, P., Gdynia, H.J., Sperfeld, A.D., Lindner-Pfleghar, B., Ludolph, A.C., Prosiegel, M. & Riecker, A. (2008) Diagnosis and treatment of bulbar symptoms in amyotrophic lateral sclerosis. Nat Clin Pract Neurol., 4, 366-74.

Kuhse, J., Betz, H. & Kirsch, J. (1995) The inhibitory glycine receptor: architecture, synaptic localization and molecular pathology of a postsynaptic ion-channel complex. Curr Opin Neurobiol., 5, 318-323.

Kuo, J.J., Siddique, T., Fu, R. & Heckman, C.J. (2005) Increased persistent Na+ current and its effect on excitability in motoneurones cultured from mutant SOD1 mice. J Physiol., 563, 843-854.

Kurtzke, J.F. (1982) Epidemiology of amyotrophic lateral sclerosis. Adv Neurol., 36, 281-302.

Kuzhandaivel, A., Margaryan, G., Nistri, A. & Mladinic, M. (2010) Extensive glial apoptosis develops early after hypoxic-dysmetabolic insult to the neonatal rat spinal cord in vitro. Neuroscience, 169, 325-338.

Kvaltinova, Z., Lukovic, L. & Stolc, S. (1993) Effect of incomplete ischemia and reperfusion of the rat brain on the density and affinity of alpha-adrenergic binding sites in the cerebral cortex. Prevention of changes by stobadine and vitamin E. Neuropharmacology, 32, 785-791.

Kwak, M.K., Itoh, K., Yamamoto, M. & Kensler, T.W. (2002) Enhanced expression of the transcription factor Nrf2 by cancer chemopreventive agents: role of antioxidant response element-like sequences in the nrf2 promoter. Mol Cell Biol., 22, 2883-2892.

Kwiatkowski Jr., T.J., Bosco, D.A., Leclerc, A.L., Tamrazian, E., Vanderburg, C.R., Russ, C., Davis, A., Gilchrist, J., Kasarskis, E.J., Munsat, T., Valdmanis, P., Rouleau, G.A., Hosler, B.A., Cortelli, P., de Jong, P.J., Yoshinaga, Y., Haines, J.L., Pericak-Vance, M.A., Yan, J., Ticozzi, N., Siddique, T., McKenna-Yasek, D., Sapp, P.C., Horvitz, H.R., Landers, J.E. & Brown Jr., R.H. (2009) Mutations in the FUS/TLS gene on chromosome 16 cause familial amyotrophic lateral sclerosis. Science, 323, 1205-1208.

Ladewig, T., Kloppenburg, P., Lalley, P.M., Zipfel, W.R., Webb, W.W. & Keller, B.U. (2003) Spatial profiles of store-dependent calcium release in motoneurones of the nucleus hypoglossus from newborn mouse. J Physiol., 547, 775-787.

Lagier-Tourenne, C. & Cleveland, D.W. (2009) Rethinking ALS: the FUS about TDP-43. Cell, 136, 1001-1004.

Lamanauskas, N. & Nistri, A. (2006) Persistent rhythmic oscillations induced by nicotine on neonatal rat hypoglossal motoneurons in vitro. Eur J Neurosci., 24, 2543-2556.

Lamanauskas, N. & Nistri, A. (2008) Riluzole blocks persistent Na+ and Ca2+ currents and modulates release of glutamate via presynaptic NMDA receptors on neonatal rat hypoglossal motoneurons in vitro. Eur J Neurosci., 27, 2501-2514.

Lape, R. & Nistri, A. (1999) Voltage-activated K+ currents of hypoglossal motoneurons in a brain stem slice preparation from the neonatal rat. J Neurophysiol., 81, 140-8.

Lape, R. & Nistri, A. (2000) Current and voltage clamp studies of the spike medium afterhyperpolarization of hypoglossal motoneurons in a rat brain stem slice preparation. J Neurophysiol., 83, 2987-95.

Laslo, P., Lipski, J., Nicholson, L.F., Miles, G.B. & Funk, G.D. (2000) Calcium binding proteins in motoneurons at low and high risk for degeneration in ALS. Neuroreport, 11, 3305-8.

Laslo, P., Lipski, J. & Funk, G.D. (2001) Differential expression of Group I metabotropic glutamate receptors in motoneurons at low and high risk for degeneration in ALS. Neuroreport, 12, 1903-8.

Laslo, P., Lipski, J., Nicholson, L.F., Miles, G.B. & Funk, G.D. (2001b) GluR2 AMPA receptor subunit expression in motoneurons at low and high risk for degeneration in amyotrophic lateral sclerosis. Exp Neurol., 169, 461-71.

Launey, T., Ivanov, A., Kapus, G., Ferrand, N., Tarnawa, I. & Gueritaud, J.P. (1999) Excitatory amino acids and synaptic transmission in embryonic rat brainstem motoneurons in organotypic culture. Eur J Neurosci., 11, 1324-1334.

Lee, A.S. (1992) Mammalian stress response: induction of the glucose-regulated protein family. Curr Opin Cell Biol., 4, 267-273.

Lee, J.P., Gerin, C., Bindokas, V.P., Miller, R., Ghadge, G. & Roos, R.P. (2002) No correlation between aggregates of Cu/Zn superoxide dismutase and cell death in familial amyotrophic lateral sclerosis. J Neurochem., 82, 1229-1238.

Leigh, P.N., Anderton, B.H., Dodson, A., Gallo, J.M., Swash, M. & Power, D.M. (1988) Ubiquitin deposits in anterior horn cells in motor neurone disease. Neurosci Lett., 93, 197-203.

Leigh, P.N. (2007) Amyotrophic lateral sclerosis. Eisen, A.A. & Shaw, P.J. (Eds.), Motor Neuron Disorders and Related Diseases, Elsevier, Edinburgh, 249-278.

Lenaz, G. (1998) Role of mitochondria in oxidative stress and ageing. Biochim Biophys Acta, 1366, 53-67.

Lenaz, G., Bovina, C., D'Aurelio, M., Fato, R., Formiggini, G., Genova, M.L., Giuliano, G., Merlo Pich, M., Paolucci, U., Parenti Castelli, G. & Ventura, B. (2002) Role of mitochondria in oxidative stress and ageing. Ann N Y Acad Sci., 959, 199-213.

Lewén, A., Matz, P. & Chan, P.H. (2000) Free radical pathways in CNS injury. J Neurotrauma, 17, 871-890.

von Lewinski, F., Fuchs, J., Vanselow, B.K. & Keller, B.U. (2008) Low Ca2+ buffering in hypoglossal motoneurons of mutant SOD1 (G93A) mice. Neurosci Lett., 445, 224-8.

Li, M., Ona, V.O., Chen, M., Kaul, M., Tenneti, L., Zhang, X., Stieg, P.E., Lipton, S.A. & Friedlander, R.M. (2000) Functional role of caspase-1 and caspase-3 in an ALS transgenic mouse model. Science, 288, 335-339.

Li, X. & Bennett, D.J. (2007) Apamin-sensitive calcium-activated potassium currents (SK) are activated by persistent calcium currents in rat motoneurons. J Neurophysiol., 97, 3314-30.

Lindwall, C., Dahlin, L., Lundborg, G. & Kanje, M. (2004) Inhibition of c-Jun phosphorylation reduces axonal outgrowth of adult rat nodose ganglia and dorsal root ganglia sensory neurons. Mol Cell Neurosci., 27, 267-79.

Lips, M.B. & Keller, B.U. (1999) Activity-related calcium dynamics in motoneurons of the nucleus hypoglossus from mouse. J Neurophysiol., 82, 2936-2946.

Lipson, K.L., Fonseca, S.G., Ishigaki, S., Nguyen, L.X., Foss, E., Bortell, R., Rossini, A.A. & Urano, F. (2006) Regulation of insulin biosynthesis in pancreatic beta cells by an endoplasmic reticulum-resident protein kinase IRE1. Cell Metab., 4, 245-254.

Lipton, S.A., Choi, Y.B., Takahashi, H., Zhang, D., Li, W., Godzik, A. & Bankston, L.A. (2002) Cysteine regulation of protein function--as exemplified by NMDA-receptor modulation. Trends Neurosci., 25, 474-480.

Liu, D., Wen, J., Liu, J. & Li, L. (1999) The roles of free radicals in amyotrophic lateral sclerosis: reactive oxygen species and elevated oxidation of protein, DNA, and membrane phospholipids. FASEB J., 13, 2318-2328.

Liu, J., Lillo, C., Jonsson, P.A., Vande Velde, C., Ward, C.M., Miller, T.M., Subramaniam, J.R., Rothstein, J.D., Marklund, S., Andersen, P.M., Brännström, T., Gredal, O., Wong, P.C., Williams, D.S. & Cleveland, D.W. (2004) Toxicity of familial ALS-linked SOD1 mutants from selective recruitment to spinal mitochondria. Neuron, 43, 5-17.

Liu, R., Althaus, J.S., Ellerbrock, B.R., Becker, D.A. & Gurney, M.E. (1998) Enhanced oxygen radical production in a transgenic mouse model of familial amyotrophic lateral sclerosis. Ann Neurol., 44, 763-770.

Liu, Z. & Martin, L.J. (2001) Motor neurons rapidly accumulate DNA single-strand breaks after in vitro exposure to nitric oxide and peroxynitrite and in vivo axotomy. J Comp Neurol., 432, 35-60.

Lladó, J., Haenggeli, C., Pardo, A., Wong, V., Benson, L., Coccia, C., Rothstein, J.D., Shefner, J.M. & Maragakis, N.J. (2006) Degeneration of respiratory motor neurons in the SOD1 G93A transgenic rat model of ALS. Neurobiol Dis., 21, 110-8.

Lowe, A.A. (1980) The neural regulation of tongue movements. Prog Neurobiol., 15, 295-344.

Lyons, T.J., Liu, H., Goto, J.J., Nersissian, A., Roe, J.A., Graden, J.A., Cafe, C., Ellerby, L.M., Bredesen, D.E., Gralla, E.B. & Valentine, J.S. (1996) Mutations in copper-zinc superoxide dismutase that cause amyotrophic lateral sclerosis alter the zinc binding site and the redox behavior of the protein. Proc Natl Acad Sci USA., 93, 12240-12244.

Magistretti, J., Castelli, L., Forti, L. & D'Angelo, E. (2006) Kinetic and functional analysis of transient, persistent and resurgent sodium currents in rat cerebellar granule cells in situ: an electrophysiological and modeling study. J Physiol., 573, 83-106.

Marden, J.J., Harraz, M.M., Williams, A.J., Nelson, K., Luo, M., Paulson, H. & Engelhardt, J.F. (2007) Redox modifier genes in amyotrophic lateral sclerosis in mice. J Clin Invest., 117, 2913-2919.

Mattiazzi, M., D'Aurelio, M., Gajewski, C.D., Martushova, K., Kiaei, M., Beal, M.F. & Manfredi, G. (2002) Mutated human SOD1 causes dysfunction of oxidative phosphorylation in mitochondria of transgenic mice. J Biol Chem., 277, 29626-29633.

Mazzone, G.L., Margaryan, G., Kuzhandaivel, A., Nasrabady, S.E., Mladinic, M. & Nistri, A. (2010) Kainate-induced delayed onset of excitotoxicity with functional loss unrelated to the extent of neuronal damage in the in vitro spinal cord. Neuroscience, 168, 451-462.

McClung, J.R. & Goldberg, S.J. (1999) Organization of motoneurons in the dorsal hypoglossal nucleus that innervate the retrusor muscles of the tongue in the rat. Anat Rec., 254, 222-230.

McClung, J.R. & Goldberg, S.J. (2000) Functional anatomy of the hypoglossal innervated muscles of the rat tongue: a model for elongation and protrusion of the mammalian tongue. Anat Rec., 260, 378-386.

Medina, L., Figueredo, C.G., Rothstein, J.D. & Reiner, A. (1996) Differential abundance of glutamate transporter subtypes in amyotrophic lateral scleroses (ALS)-vulnerable versus ALS-resistant brain stem motor cell groups. Exp Neurol., 142, 287-295.

Menzies, F.M., Cookson, M.R., Taylor, R.W., Turnbull, D.M., Chrzanowska-Lightowlers, Z.M., Dong, L., Figlewicz, D.A. & Shaw, P.J. (2002) Mitochondrial dysfunction in a cell culture model of familial amyotrophic lateral sclerosis. Brain, 125, 1522-1533.

Menzies, F.M., Grierson, A.J., Cookson, M.R., Heath, P.R., Tomkins, J., Figlewicz, D.A., Ince, P.G. & Shaw, P.J. (2002b) Selective loss of neurofilament expression in Cu/Zn superoxide dismutase (SOD1) linked amyotrophic lateral sclerosis. J Neurochem., 82, 1118-1128.

Mergia, E., Russwurm, M., Zoidl, G. & Koesling, D. (2003) Major occurrence of the new alpha(2)beta(1) isoform of NO-sensitive guanylyl cyclase in brain. Cell Signal., 15, 189-195.

Migheli, A., Cordera, S., Bendotti, C., Atzori, C., Piva, R. & Schiffer, D. (1999) S-100beta protein is upregulated in astrocytes and motor neurons in the spinal cord of patients with amyotrophic lateral sclerosis. Neurosci Lett., 261, 25-28.

Miles, G.B., Lipski, J., Lorier, A.R., Laslo, P. & Funk, G.D. (2004) Differential expression of voltage-activated calcium channels in III and XII motoneurones during development in the rat. Eur J Neurosci., 20, 903-13.

Miller, R.H. & Raff, M.C. (1984) Fibrous and protoplasmic astrocytes are biochemically and developmentally distinct. J Neurosci., 4, 585-592.

Miller, T.M. & Layzer, R.B. (2005) Muscle cramps. Muscle Nerve, 32, 431-42.

Mogyoros, I., Kiernan, M.C. & Burke, D. (1996) Strength-duration properties of human peripheral nerve. Brain, 119, 439-47.

Montero, F., Portillo, F., González-Forero, D. & Moreno-López, B. (2008) The nitric oxide/cyclic guanosine monophosphate pathway modulates the inspiratory-related activity of hypoglossal motoneurons in the adult rat. Eur J Neurosci., 28, 107-16.

Moritz, A.T., Newkirk, G., Powers, R.K. & Binder, M.D. (2007) Facilitation of somatic calcium channels can evoke prolonged tail currents in rat hypoglossal motoneurons. J Neurophysiol., 98, 1042-1047.

Morrison, B.M., Gordon, J.W., Ripps, M.E. & Morrison, J.H. (1996) Quantitative immunocytochemical analysis of the spinal cord in G86R superoxide dismutase transgenic mice: neurochemical correlates of selective vulnerability. J Comp Neurol., 373, 619-631.

Muakkassah-Kelly, S.F., Andresen, J.W., Shih, J.C. & Hochstein, P. (1982) Decreased [3H]serotonin and [3H]spiperone binding consequent to lipid peroxidation in rat cortical membranes. Biochem Biophys Res Commun., 104, 1003-1010.

Nagai, M., Aoki, M., Miyoshi, I., Kato, M., Pasinelli, P., Kasai, N., Brown, R.H. Jr. & Itoyama, Y. (2001) Rats Expressing Human Cytosolic Copper-Zinc Superoxide Dismutase Transgenes with Amyotrophic Lateral Sclerosis: Associated Mutations Develop Motor Neuron Disease. J Neurosci., 21, 9246-9254.

Nagata, T., Ilieva, H., Murakami, T., Shiote, M., Narai, H., Ohta, Y., Hayashi, T., Shoji, M. & Abe, K. (2007) Increased ER stress during motor neuron degeneration in a transgenic mouse model of amyotrophic lateral sclerosis. Neurol Res., 29, 767-71.

Nakagomi, S., Suzuki, Y., Namikawa, K., Kiryu-Seo, S. & Kiyama, H. (2003) Expression of the activating transcription factor 3 prevents c-Jun N-terminal kinase-induced neuronal death by promoting heat shock protein 27 expression and Akt activation. J Neurosci., 23, 5187-96.

Nakamura, K., Hori, T., Sato, N., Sugie, K., Kawakami, T. & Yodoi, J. (1993) Redox regulation of a src family protein tyrosine kinase p56lck in T cells. Oncogene, 8, 3133-3139.

Neumann, M., Sampathu, D.M., Kwong, L.K., Truax, A.C., Micsenyi, M.C., Chou, T.T., Bruce, J., Schuck, T., Grossman, M., Clark, C.M., McCluskey, L.F., Miller, B.L., Masliah, E., Mackenzie, I.R., Feldman, H., Feiden, W., Kretzschmar, H.A., Trojanowski, J.Q. & Lee, V.M. (2006) Ubiquitinated TDP-43 in frontotemporal lobar degeneration and amyotrophic lateral sclerosis. Science, 314, 130-133.

Nguyen, T., Nioi, P. & Pickett, C.B. (2009) The nrf2-antioxidant response element signaling pathway and its activation by oxidative stress. J Biol Chem., 284, 13291-13295.

Nishimura, A.L., Mitne-Neto, M., Silva, H.C., Richieri-Costa, A., Middleton, S., Cascio, D., Kok, F., Oliveira, J.R., Gillingwater, T., Webb, J., Skehel, P. & Zatz, M. (2004) A mutation in the vesicle-trafficking protein VAPB causes late-onset spinal muscular atrophy and amyotrophic lateral sclerosis. Am J Hum Genet., 75, 822-831.

Nishitoh, H., Kadowaki, H., Nagai, A., Maruyama, T., Yokota, T., Fukutomi, H., Noguchi, T., Matsuzawa, A., Takeda, K. & Ichijo, H. (2008) ALS-linked mutant SOD1 induces ER stress- and ASK1-dependent motor neuron death by targeting Derlin-1. Genes Dev., 22, 1451-1464.

O'Brien, J.A., Isaacson, J.S. & Berger, A.J. (1997) NMDA and non-NMDA receptors are co-localized at excitatory synapses of rat hypoglossal motoneurons. Neurosci Lett., 227, 5-8.

O'Brien, J.A. & Berger, A.J. (1999) Cotransmission of GABA and glycine to brain stem motoneurons. J Neurophysiol., 82, 1638-1641.

Okado-Matsumoto, A. & Fridovich, I. (2002) Amyotrophic lateral sclerosis: a proposed mechanism. Proc Natl Acad Sci USA., 99, 9010-9014.

Orrell, R.W. (2000) Amyotrophic lateral sclerosis: copper/zinc superoxide dismutase (SOD1) gene mutations. Neuromuscul Disord., 10, 63-68.

Ouardouz, M. & Durand, J. (1994) Involvement of AMPA receptors in trigeminal post-synaptic potentials recorded in rat abducens motoneurons in vivo. Eur J Neurosci., 6, 1662-1668.

Pagnotta, S.E., Lape, R., Quitadamo, C. & Nistri, A. (2005) Pre- and postsynaptic modulation of glycinergic and GABAergic transmission by muscarinic receptors on rat hypoglossal motoneurons in vitro. Neuroscience, 130, 783-795.

Palmer, R.M., Ferrige, A.G. & Moncada, S. (1987) Nitric oxide release accounts for the biological activity of endothelium-derived relaxing factor. Nature, 327, 524-526.

Pambo-Pambo, A., Durand, J. & Gueritaud, J.P. (2009) Early excitability changes in lumbar motoneurons of transgenic SOD1G85R and SOD1G(93A-Low) mice. J Neurophysiol., 102, 3627-42.

Parkinson, N., Ince, P.G., Smith, M.O., Highley, R., Skibinski, G., Andersen, P.M., Morrison, K.E., Pall, H.S., Hardiman, O., Collinge, J., Shaw, P.J. & Fisher, E.M. (2006) ALS phenotypes with mutations in CHMP2B (charged multivesicular body protein 2B). Neurology, 67, 1074-1077.

Pasinelli, P., Belford, M.E., Lennon, N., Bacskai, B.J., Hyman, B.T., Trotti, D. & Brown, R.H. Jr. (2004) Amyotrophic lateral sclerosis-associated SOD1 mutant proteins bind and aggregate with Bcl-2 in spinal cord mitochondria. Neuron, 43, 19-30.

Pasinelli, P. & Brown, R.H. (2006) Molecular biology of amyotrophic lateral sclerosis: insights from genetics. Nat Rev Neurosci., 7, 710-723.

Pellmar, T.C. (1987) Peroxide alters neuronal excitability in the CA1 region of guinea-pig hippocampus in vitro. Neuroscience, 23, 447-56.

Pieri, M., Carunchio, I., Curcio, L., Mercuri, N.B. & Zona, C. (2009) Increased persistent sodium current determines cortical hyperexcitability in a genetic model of amyotrophic lateral sclerosis. Exp Neurol., 215, 368-79.

Pineda, J., Kogan, J.H. & Aghajanian, G.K. (1996) Nitric oxide and carbon monoxide activate locus coeruleus neurons through a cGMP-dependent protein kinase: involvement of a nonselective cationic channel. J Neurosci., 16, 1389-99.

Piotukh, K., Kosslick, D., Zimmermann, J., Krause, E. & Freund, C. (2007) Reversible disulfide bond formation of intracellular proteins probed by NMR spectroscopy. Free Radic Biol Med., 43, 1263-1270.

Poon, H.F., Hensley, K., Thongboonkerd, V., Merchant, M.L., Lynn, B.C., Pierce, W.M., Klein, J.B., Calabrese, V. & Butterfield, D.A. (2005) Redox proteomics analysis of oxidatively modified proteins in G93A-SOD1 transgenic mice-a model of familial amyotrophic lateral sclerosis. Free Radic Biol Med., 39, 453-462.

Pramatarova, A., Laganiere, J., Roussel, J., Brisebois, K. & Rouleau, G.A. (2001) Neuron specific expression of mutant superoxide dismutase 1 in transgenic mice does not lead to motor neuron impairment. J Neurosci., 21, 3369-3374.

Prudencio, M., Hart, P.J., Borchelt, D.R. & Andersen, P.M. (2009) Variation in aggregation propensities among ALS-associated variants of SOD1: correlation to human disease. Hum Mol Genet., 18, 3217-3226.

Pryor, W.A. & Squadrito, G.L. (1995) The chemistry of peroxynitrite: a product from the reaction of nitric oxide with superoxide. Am J Physiol., 268, L699-722.

Ptak, K., Zummo, G.G., Alheid, G.F., Tkatch, T., Surmeier, D.J. & McCrimmon, D.R. (2005) Sodium currents in medullary neurons isolated from the pre-Botzinger complex region. J Neurosci., 25, 5159-5170.

Quitadamo, C., Fabbretti, E., Lamanauskas, N. & Nistri, A. (2005) Activation and desensitization of neuronal nicotinic receptors modulate glutamatergic transmission on neonatal rat hypoglossal motoneurons. Eur J Neurosci., 22, 2723-2734.

Rakhit, R., Cunningham, P., Furtos-Matei, A., Dahan, S., Qi, X.F., Crow, J.P., Cashman, N.R., Kondejewski, L.H. & Chakrabartty, A. (2002) Oxidation-induced misfolding and aggregation of superoxide dismutase and its implications for amyotrophic lateral sclerosis. J Biol Chem., 277, 47551-47556.

Rakhit, R., Crow, J.P., Lepock, J.R., Kondejewski, L.H., Cashman, N.R. & Chakrabartty, A. (2004) Monomeric Cu,Zn-superoxide dismutase is a common misfolding intermediate in the oxidation models of sporadic and familial amyotrophic lateral sclerosis. J Biol Chem., 279, 15499-15504.

Rao, S.D., Yin, H.Z. & Weiss, J.H. (2003) Disruption of glial glutamate transport by reactive oxygen species produced in motor neurons. J. Neurosci., 23, 2627-2633.

Rao, S.D. & Weiss, J.H. (2004) Excitotoxic and oxidative cross-talk between motor neurons and glia in ALS pathogenesis. Trends Neurosci., 27, 17-23.

Raoul, C., Abbas-Terki, T., Bensadoun, J.C., Guillot, S., Haase, G., Szulc, J., Henderson, C.E. & Aebischer, P. (2005) Lentiviral-mediated silencing of SOD1 through RNA interference retards disease onset and progression in a mouse model of ALS. Nat Med., 11, 423-428.

Reaume, A.G., Elliott, J.L., Hoffman, E.K., Kowall, N.W., Ferrante, R.J., Siwek, D.F., Wilcox, H.M., Flood, D.G., Beal, M.F., Brown Jr., R.H., Scott, R.W. & Snider, W.D. (1996) Motor neurons in Cu/Zn superoxide dismutase-deficient mice develop normally but exhibit enhanced cell death after axonal injury. Nat Genet., 13, 43-47.

Rego, A.C., Santos, M.S. & Oliveira, C.R. (1996) Oxidative stress, hypoxia, and ischemia-like conditions increase the release of endogenous amino acids by distinct mechanisms in cultured retinal cells. J Neurochem., 66, 2506-2516.

Rekling, J.C., Shao, X.M. & Feldman, J.L. (2000) Electrical coupling and excitatory synaptic transmission between rhythmogenic respiratory neurons in the preBotzinger complex. J Neurosci., 20, RC113.

Rekling, J.C., Funk, G.D., Bayliss, D.A., Dong, X.W. & Feldman, J.L. (2000b) Synaptic control of motoneuronal excitability. Physiol Rev., 80, 767-852.

Reyes, M. & Stanton, P.K. (1996) Induction of hippocampal long-term depression requires release of Ca2+ from separate presynaptic and postsynaptic intracellular stores. J Neurosci., 16, 5951-5960.

Reynolds, M.F. & Burstyn, J.N. (2000) Mechanism of activation of soluble guanylyl cyclase by NO. Ignarro, L. (ed): Nitric Oxide Biology and Pathobiology. San Diego, Academic Press, 57-82.

Ripps, M.E., Huntley, G.W., Hof, P.R., Morrison, J.H. & Gordon, J.W. (1995) Transgenic mice expressing an altered murine superoxide dismutase gene provide an animal model of amyotrophic lateral sclerosis. Proc Natl Acad Sci USA., 92, 689-93.

Rizzardini, M., Lupi, M., Mangolini, A., Babetto, E., Ubezio, P. & Cantoni, L. (2006) Neurodegeneration induced by complex I inhibition in a cellular model of familial amyotrophic lateral sclerosis. Brain Res Bull., 69, 465-474.

Robello, M., Amico, C., Bucossi, G., Cupello, A., Rapallino, M.V. & Thellung, S. (1996) Nitric oxide and GABAA receptor function in the rat cerebral cortex and cerebellar granule cells. Neuroscience, 74, 99-105.

Roberts, B.R., Tainer, J.A., Getzoff, E.D., Malencik, D.A., Anderson, S.R., Bomben, V.C., Meyers, K.R., Karplus, P.A. & Beckman, J.S. (2007) Structural characterization of zinc-deficient human superoxide dismutase and implications for ALS. J Mol Biol., 373, 877-890.

Rodriguez, J.A., Valentine, J.S., Eggers, D.K., Roe, J.A., Tiwari, A., Brown Jr., R.H. & Hayward, L.J. (2002) Familial amyotrophic lateral sclerosis-associated mutations decrease the thermal stability of distinctly metallated species of human copper/zinc superoxide dismutase. J Biol Chem., 277, 15932-15937.

Roe, J.A., Wiedau-Pazos, M., Moy, V.N., Goto, J.J., Gralla, E.B. & Valentine, J.S. (2002) In vivo peroxidative activity of FALS-mutant human CuZnSODs expressed in yeast. Free Radic Biol Med., 32, 169-174.

Rosen, D.R., Siddique, T., Patterson, D., Figlewicz, D.A., Sapp, P., Hentati, A., Donaldson, D., Goto, J., O'Regan, J.P., Deng, H.X., Rahmani, Z., Krizus, A., McKenna-Yasek, D., Cayabyab, A., Gaston, S.M., Berger, R., Tanzi, R.E., Halperin, J.J., Herzfeldt, B., Van den Bergh, R., Hung, W., Bird, T., Deng, G., Mulder, D.W., Smyth, C., Laing, N.G., Soriano, E., Pericak-Vance, M.A., Haines, J., Rouleau, G.A., Gusella, J.S., Horvitz, H.R. & Brown Jr.,

R.H. (1993) Mutations in Cu/Zn superoxide dismutase gene are associated with familial amyotrophic lateral sclerosis. Nature, 362, 59-62.

Ross, C.A. & Poirier, M.A. (2004) Protein aggregation and neurodegenerative disease. Nat Med., 10, (Suppl. 1), S10-S17.

Ross, C.A. & Poirier, M.A. (2005) Opinion: what is the role of protein aggregation in neurodegeneration? Nat Rev Mol Cell Biol., 6, 891-898.

Roth, G. (1984) Fasciculations and their F-response. Localisation of their axonal origin. J Neurol Sci., 63, 299-306.

Rothermundt, M., Peters, M., Prehn, J.H.M. & Arolt, V. (2003) S100B in brain damage and neurodegeneration. Microsc Res Tech., 60, 614-632.

Rothstein, J.D., Van Kammen, M., Levey, A.I., Martin, L.J. & Kuncl, R.W. (1995) Selective loss of glial glutamate transporter GLT-1 in amyotrophic lateral sclerosis. Ann Neurol., 38, 73-84.

Russo, R.E. & Hounsgaard, J. (1999) Dynamics of intrinsic electrophysiological properties in spinal cord neurones. Prog Biophys Mol Biol., 72, 329-365.

Russwurm, M., Wittau, N. & Koesling, D. (2001) Guanylyl cyclase / PSD-95 interaction: targeting of the NO-sensitive alpha2beta1 guanylyl cyclase to synaptic membranes. J Biol Chem., 276, 44647-44652.

Ryberg, H., Soderling, A.S., Davidsson, P., Blennow, K., Caidahl, K. & Persson, L.I. (2004) Cerebrospinal fluid levels of free 3-nitrotyrosine are not elevated in the majority of patients with amyotrophic lateral sclerosis or Alzheimer's disease. Neurochem Int., 45, 57-62.

Sah, R. & Schwartz-Bloom, R.D. (1999) Optical imaging reveals elevated intracellular chloride in hippocampal pyramidal neurons after oxidative stress. J Neurosci., 19, 9209-9217.

Sánchez-Carbente, M.R., Castro-Obregón, S., Covarrubias, L. & Narváez, V. (2005) Motoneuronal death during spinal cord development is mediated by oxidative stress. Cell Death and Differentiation, 12, 279-291.

Saransaari, P. & Oja, S.S. (1998) Release of endogenous glutamate, aspartate, GABA, and taurine from hippocampal slices from adult and developing mice under cell-damaging conditions. Neurochem Res., 23, 563-570.

Saransaari, P. & Oja, S.S. (2008) Characteristics of GABA release induced by free radicals in mouse hippocampal slices. Neurochem Res., 33, 384-93.

Sarlette, A., Krampfl, K., Grothe, C., Neuhoff, N., Dengler, R. & Petri, S. (2008) Nuclear erythroid 2-related factor 2-antioxidative response element signaling pathway in motor cortex and spinal cord in amyotrophic lateral sclerosis. J Neuropathol Exp Neurol., 67, 1055-1062.

Sasaki, S., Warita, H., Murakami, T., Abe, K. & Iwata, M. (2004) Ultrastructural study of mitochondria in the spinal cord of transgenic mice with a G93A mutant SOD1 gene. Acta Neuropathol., 107, 461-474.

Sathasivam, S., Ince, P.G. & Shaw, P.J. (2001) Apoptosis in amyotrophic lateral sclerosis: a review of the evidence. Neuropathol Appl Neurobiol., 27, 257-274.

Sawada, M., Ichinose, M. & Hara, N. (1995) Nitric oxide induces an increased Na+ conductance in identified neurons of Aplysia. Brain Res., 670, 248-56.

Sawczuk, A., Powers, R.K. & Binder, M.D. (1995) Spike frequency adaptation studied in hypoglossal motoneurons of the rat. J Neurophysiol., 73, 1799-810.

Saxena, S., Cabuy, E. & Caroni, P. (2009) A role for motoneuron subtype-selective ER stress in disease manifestations of FALS mice. Nat Neurosci., 12, 627-636.

Schafer, F.Q. & Buettner, G.R. (2001) Redox environment of the cell as viewed through the redox state of the glutathione disulfide/glutathione couple. Free Radic Biol Med., 30, 1191-1212.

Schonhoff, C.M., Matsuoka, M., Tummala, H., Johnson, M.A., Estevez, A.G., Wu, R., Kamaid, A., Ricart, K.C., Hashimoto, Y., Gaston, B., Macdonald, T.L., Xu, Z. & Mannick, J.B. (2006) S-nitrosothiol depletion in amyotrophic lateral sclerosis. Proc Natl Acad Sci USA., 103, 2404-2409.

Schubert, U., Antón, L.C., Gibbs, J., Norbury, C.C., Yewdell, J.W. & Bennink, J.R. (2000) Rapid degradation of a large fraction of newly synthesized proteins by proteasomes. Nature, 404, 770-774.

Schwartz, R.D. (1988) The GABAA receptor-gated ion channel: biochemical and pharmacological studies of structure and function. Biochem Pharmacol., 37, 3369-3375.

Schwindt, P.C. & Crill, W.E. (1980) Properties of a persistent inward current in normal and TEA-injected motoneurons. J Neurophysiol., 43, 1700-24.

Serrano, F. & Klann, E. (2004) Reactive oxygen species and synaptic plasticity in the aging hippocampus. Ageing Res Rev., 3, 431-443.

Sharifullina, E. & Nistri, A. (2006) Glutamate uptake block triggers deadly rhythmic bursting of neonatal rat hypoglossal motoneurons. J Physiol., 572, 407-423.

Shaw, P.J., Ince, P.G., Falkous, G. & Mantle, D. (1995) Oxidative damage to protein in sporadic motor neuron disease spinal cord. Ann Neurol., 38, 691-695.

Shaw, P.J. & Ince, P.G. (1997) Glutamate, excitotoxicity and amyotrophic lateral sclerosis. J Neurol., 244, 3-14.

Shibata, N., Asayama, K., Hirano, A. & Kobayashi, M. (1996) Immunohistochemical study on superoxide dismutases in spinal cords from autopsied patients with amyotrophic lateral sclerosis. Dev Neurosci., 18, 492-498.

Shibata, N., Hirano, A., Kobayashi, M., Siddique, T., Deng, H.X., Hung, W.Y., Kato, T. & Asayama, K. (1996b) Intense superoxide dismutase-1 immunoreactivity in intracytoplasmic hyaline inclusions of familial amyotrophic lateral sclerosis with posterior column involvement. J Neuropathol Exp Neurol., 55, 481-490.

Shibata, N., Nagai, R., Uchida, K., Horiuchi, S., Yamada, S., Hirano, A., Kawaguchi, M., Yamamoto, T., Sasaki, S. & Kobayashi, M. (2001) Morphological evidence for lipid peroxidation and protein glycoxidation in spinal cords from sporadic amyotrophic lateral sclerosis patients. Brain Res., 917, 97-104.

Siciliano, G., Piazza, S., Carlesi, C., Del Corona, A., Franzini, M., Pompella, A., Malvaldi, G., Mancuso, M., Paolicchi, A. & Murri, L. (2007) Antioxidant capacity and protein oxidation in cerebrospinal fluid of amyotrophic lateral sclerosis. J Neurol., 254, 575-80.

Siklós, L., Engelhardt, J., Harati, Y., Smith, R.G., Joó, F. & Appel, S.H. (1996) Ultrastructural evidence for altered calcium in motor nerve terminals in amyotrophic lateral sclerosis. Ann Neurol., 39, 203-216.

Simpson, E.P., Henry, Y.K., Henkel, J.S., Smith, R.G. & Appel, S.H. (2004) Increased lipid peroxidation in sera of ALS patients: a potential biomarker of disease burden. Neurology, 62, 1758-1765.

Singh, R.J., Karoui, H., Gunther, M.R., Beckman, J.S., Mason, R.P. & Kalyanaraman, B. (1998) Reexamination of the mechanism of hydroxyl radical adducts formed from the reaction between familial amyotrophic lateral sclerosis-associated Cu,Zn superoxide dismutase mutants and H_2O_2. Proc Natl Acad Sci USA., 95, 6675-6680.

Smith, A.P. & Lee, N.M. (2007) Role of zinc in ALS. Amyotroph Lateral Scler., 8, 131-143.

Smith, R.G., Henry, Y.K., Mattson, M.P. & Appel, S.H. (1998) Presence of 4-hydroxynonenal in cerebrospinal fluid of patients with sporadic amyotrophic lateral sclerosis. Ann Neurol., 44, 696-699.

Sokoloff, A.J. (2000) Localization and contractile properties of intrinsic longitudinal motor units of the rat tongue. J Neurophysiol., 84, 827-835.

Son, H., Hawkins, R.D., Martin, K., Kiebler, M., Huang, P.L., Fishman, M.C. & Kandel, E.R. (1996) Long-term potentiation is reduced in mice that are doubly mutant in endothelial and neuronal nitric oxide synthase. Cell, 87, 1015-1023.

Son, M., Fathallah-Shaykh, H.M. & Elliott, J.L. (2001) Survival in a transgenic model of FALS is independent of iNOS expression. Ann Neurol., 50, 273.

Southam, E. & Garthwaite, J. (1991) Comparative effects of some nitric oxide donors on cyclic GMP levels in rat cerebellar slices. Neurosci Lett., 130, 107-111.

Southam, E. & Garthwaite, J. (1993) The nitric oxide-cyclic GMP signaling pathway in rat brain. Neuropharmacology, 32, 1267-1277.

Sreedharan, J., Blair, I.P., Tripathi, V.B., Hu, X., Vance, C., Rogelj, B., Ackerley, S., Durnall, J.C., Williams, K.L., Buratti, E., Baralle, F., de Belleroche, J., Mitchell, J.D., Leigh, P.N., Al-Chalabi, A., Miller, C.C., Nicholson, G. & Shaw, C.E. (2008) TDP-43 mutations in familial and sporadic amyotrophic lateral sclerosis. Science, 319, 1668-1672.

Stamler, J.S., Toone, E.J., Lipton, S.A. & Sucher, N.J. (1997) (S)NO signals: translocation, regulation, and a consensus motif. Neuron, 18, 691-6.

Stamler, J.S., Lamas, S. & Fang, F.C. (2001) Nitrosylation: the prototypic redox-based signaling mechanism. Cell, 106, 675-683.

Stuehr, D.J., Santolini, J., Wang, Z.Q., Wei, C.C. & Adak, S. (2004) Update on mechanism and catalytic regulation in the NO synthases. J Biol Chem., 279, 36167-36170.

Subramaniam, J.R., Lyons, W.E., Liu, J., Bartnikas, T.B., Rothstein, J., Price, D.L., Cleveland, D.W., Gitlin, J.D. & Wong, P.C. (2002) Mutant SOD1 causes motor neuron disease independent of copper chaperone-mediated copper loading. Nat Neurosci., 5, 301-307.

Suh, J.H., Shenvi, S.V., Dixon, B.M., Liu, H., Jaiswal, A.K., Liu, R.M. & Hagen, T.M. (2004) Decline in transcriptional activity of Nrf2 causes age-related loss of glutathione synthesis, which is reversible with lipoic acid. Proc Natl Acad Sci USA., 101, 3381-3386.

Sunico, C.R., González-Forero, D., Domínguez, G., García-Verdugo, J.M. & Moreno-López, B. (2010) Nitric oxide induces pathological synapse loss by a protein kinase G-, Rho kinase-dependent mechanism preceded by myosin light chain phosphorylation. J Neurosci., 30, 973-84.

Suzuki, Y.J., Forman, H.J. & Sevanian, A. (1997) Oxidants as stimulators of signal transduction. Free Radic Biol Med., 22, 269-285.

Swash, M. & Ingram, D. (1988) Preclinical and subclinical events in motor neuron disease. J Neurol Neurosurg Psychiatry, 51, 165-8.

Szabadits, E., Cserep, C., Ludanyi, A., Katona, I., Gracia-Llanes, J., Freund, T.F. & Nyiri, G. (2007) Hippocampal GABAergic synapses possess the molecular machinery for retrograde nitric oxide signaling. J Neurosci., 27, 8101-8111.

Taccola, G., Margaryan, G., Mladinic, M. & Nistri, A. (2008) Kainate and metabolic perturbation mimicking spinal injury differentially contribute to early damage of locomotor networks in the in vitro neonatal rat spinal cord. Neuroscience, 155, 538-55.

Takahashi, A., Mikami, M. & Yang, J. (2007) Hydrogen peroxide increases GABAergic mIPSC through presynaptic release of calcium from IP3 receptor-sensitive stores in spinal cord substantia gelatinosa neurons. Eur J Neurosci., 25, 705-716.

Takeuchi, H., Ishigaki, Y., Doyu, S.M. & Sobue, G. (2002) Mitochondrial localization of mutant superoxide dismutase 1 triggers caspase-dependent cell death in a cellular model of familial amyotrophic lateral sclerosis. J Biol Chem., 277, 50966-50972.

Talley, E.M., Lei, Q., Sirois, J.E. & Bayliss, D.A. (2000) TASK-1, a two-pore domain K+ channel, is modulated by multiple neurotransmitters in motoneurons. Neuron, 25, 399-410.

Tamura, N., Kuwabara, S., Misawa, S., Kanai, K., Nakata, M., Sawai, S. & Hattori, T. (2006) Increased nodal persistent Na+ currents in human neuropathy and motor neuron disease estimated by latent addition. Clin Neurophysiol., 117, 2451-8.

Theiss, R.D., Kuo, J.J. & Heckman, C.J. (2007) Persistent inward currents in rat ventral horn neurones. J Physiol., 580, 507-522.

Tohgi, H., Abe, T., Yamazaki, K., Murata, T., Ishizaki, E. & Isobe, C. (1999) Remarkable increase in cerebrospinal fluid 3-nitrotyrosine in patients with sporadic amyotrophic lateral sclerosis. Ann Neurol., 46, 129-131.

Travagli, R.A. & Gillis, R.A. (1994) Nitric oxide-mediated excitatory effect on neurons of dorsal motor nucleus of vagus. Am J Physiol., 266, G154-60.

Travers, J.B. & Norgren, R. (1983) Afferent projections to the oral motor nuclei in the rat. J Comp Neurol., 220, 280-298.

Trotti, D., Rossi, D., Gjesdal, O., Levy, L.M., Racagni, G., Danbolt, N.C. & Volterra, A. (1996) Peroxynitrite inhibits glutamate transporter subtypes. J Biol Chem., 271, 5976-5979.

Trotti, D., Danbolt, N.C. & Volterra, A. (1998) Glutamate transporters are oxidant vulnerable: a molecular link between oxidative and excitotoxic neurodegeneration? Trends Pharmacol Sci., 19, 328-334.

Tsujino, H., Kondo, E., Fukuoka, T., Dai, Y., Tokunaga, A., Miki, K., Yonenobu, K., Ochi, T. & Noguchi, K. (2000) Activating transcription factor 3 (ATF3) induction by axotomy in sensory and motoneurons: a novel neuronal marker of nerve injury. Mol Cell Neurosci., 15, 170-182.

Tu, B.P. & Weissman, J.S. (2004) Oxidative protein folding in eukaryotes: mechanisms and consequences. J Cell Biol., 164, 341-346.

Tu, P.H., Raju, P., Robinson, K.A., Gurney, M.E., Trojanowski, J.Q. & Lee, V.M. (1996) Transgenic mice carrying a human mutant superoxide dismutase transgene develop neuronal cytoskeletal pathology resembling human amyotrophic lateral sclerosis lesions. Proc Natl Acad Sci USA., 93, 3155-3160.

Turner, M.R., Kiernan, M.C., Leigh, P.N. & Talbot, K. (2009) Biomarkers in amyotrophic lateral sclerosis. Lancet Neurol., 8, 94-109.

Umemiya, M. & Berger, A.J. (1994) Properties and function of low- and high-voltage activated Ca2+ channels in hypoglossal motoneurons. J Neurosci., 14, 5652-60.

Valdmanis, P.N. & Rouleau, G.A. (2008) Genetics of familial amyotrophic lateral sclerosis. Neurology, 70, 144-152.

Valentine, J.S. & Hart, P.J. (2003) Misfolded CuZnSOD and amyotrophic lateral sclerosis. Proc Natl Acad Sci USA., 100, 3617-3622.

Vance, C., Rogelj, B., Hortobagyi, T., De Vos, K.J., Nishimura, A.L., Sreedharan, J., Hu, X., Smith, B., Ruddy, D., Wright, P., Ganesalingam, J., Williams, K.L., Tripathi, V., Al-Saraj, S., Al-Chalabi, A., Leigh, P.N., Blair, I.P., Nicholson, G., de Belleroche, J., Gallo, J.M., Miller, C.C. & Shaw, C.E. (2009) Mutations in FUS, an RNA processing protein, cause familial amyotrophic lateral sclerosis type 6. Science, 323, 1208-1211.

Van Damme, P., Van Den Bosch, L., Van Houtte, E., Callewaert, G. & Robberecht, W. (2002) GluR2-dependent properties of AMPA receptors determine the selective vulnerability of motor neurons to excitotoxicity. J Neurophysiol., 88, 1279-1287.

Vazquez, C., Anesetti, G. & Martinez Palma, L. (1999) Transient expression of nitric oxide synthase in the hypoglossal nucleus of the rat during early postnatal development. Neurosci Lett., 5, 5-8.

Viana, F., Gibbs, L. & Berger, A.J. (1990) Double- and triple-labeling of functionally characterized central neurons projecting to peripheral targets studied in vitro. Neuroscience, 38, 829-841.

Vincent, S.R. & Kimura, H. (1992) Histochemical mapping of nitric oxide synthase in the rat brain. Neuroscience, 46, 755-784.

Volterra, A., Trotti, D., Tromba, C., Floridi, S. & Racagni, G. (1994) Glutamate uptake inhibition by oxygen free radicals in rat cortical astrocytes. J Neurosci., 14, 2924-2932.

Vlug, A.S., Teuling, E., Haasdijk, E.D., French, P., Hoogenraad, C.C. & Jaarsma, D. (2005) ATF3 expression precedes death of spinal motoneurons in amyotrophic lateral sclerosis-SOD1 transgenic mice and correlates with c-Jun phosphorylation, CHOP expression, somato dendritic ubiquitination and Golgi fragmentation. Eur J Neurosci., 22, 1881-94.

Vucic, S. & Kiernan, M.C. (2006) Axonal excitability properties in amyotrophic lateral sclerosis. Clin Neurophysiol., 117, 1458-66.

Vucic, S. & Kiernan, M.C. (2006b) Novel threshold tracking techniques suggest that cortical hyperexcitability is an early feature of motor neuron disease. Brain, 129, 2436-46.

Vucic, S., Nicholson, G.A. & Kiernan, M.C. (2008) Cortical hyperexcitability may precede the onset of familial amyotrophic lateral sclerosis. Brain, 131, 1540-50.

Vucic, S. & Kiernan, M.C. (2009) Pathophysiology of neurodegeneration in familial amyotrophic lateral sclerosis. Curr Mol Med., 9, 255-72.

Vucic, S. & Kiernan, M.C. (2010) Upregulation of persistent sodium conductances in familial ALS. J Neurol Neurosurg Psychiatry, 81, 222-7.

Wall, M.J. (2003) Endogenous nitric oxide modulates GABAergic transmission to granule cells in adult rat cerebellum. Eur J Neurosci., 18, 869-78.

Wang, J., Slunt, H., Gonzales, V., Fromholt, D., Coonfield, M., Copeland, N.G., Jenkins, N.A. & Borchelt, D.R. (2003) Copper-binding-site-null SOD1 causes ALS in transgenic mice: aggregates of non-native SOD1 delineate a common feature. Hum Mol Genet., 12, 2753-2764.

Wang, J., Xu, G., Slunt, H.H., Gonzales, V., Coonfield, M., Fromholt, D., Copeland, N.G., Jenkins, N.A. & Borchelt, D.R. (2005) Coincident thresholds of mutant protein for paralytic disease and protein aggregation caused by restrictively expressed superoxide dismutase cDNA. Neurobiol Dis., 20, 943-952.

van der Want, J.J., Nunes Cardozo, J.J. & van der Togt, C. (1992) GABAergic neurons and circuits in the pretectal nuclei and the accessory optic system of mammals. Prog Brain Res., 90, 283-305.

Watanabe, M., Dykes-Hoberg, M., Culotta, V.C., Price, D.L., Wong, P.C. & Rothstein, J.D. (2001) Histological evidence of protein aggregation in mutant SOD1 transgenic mice and in amyotrophic lateral sclerosis neural tissues. Neurobiol Dis., 8, 933-941.

Wexler, E.M., Stanton, P.K. & Nawy, S. (1998) Nitric oxide depresses GABAA receptor function via coactivation of cGMP-dependent kinase and phosphodiesterase. J Neurosci., 18, 2342-9.

Whisler, R.L., Goyette, M.A., Grants, I.S. & Newhouse, Y.G. (1995) Sublethal levels of oxidant stress stimulate multiple serine/threonine kinases and suppress protein phosphatases in Jurkat T cells. Arch Biochem Biophys., 319, 23-35.

Wiedau-Pazos, M., Goto, J.J., Rabizadeh, S., Gralla, E.B., Roe, J.A., Lee, M.K., Valentine, J.S. & Bredesen, D.E. (1996) Altered reactivity of superoxide dismutase in familial amyotrophic lateral sclerosis. Science, 271, 515-518.

Wiedemann, F.R., Winkler, K., Kuznetsov, A.V., Bartels, C., Vielhaber, S., Feistner, H. & Kunz, W.S. (1998) Impairment of mitochondrial function in skeletal muscle of patients with amyotrophic lateral sclerosis. J Neurol Sci., 156, 65-72.

Williams, T.L., Day, N.C., Ince, P.G., Kamboj, R.K. & Shaw, P.J. (1997) Calcium-permeable alpha-amino-3-hydroxy-5-methyl-4-isoxazole propionic acid receptors: a molecular determinant of selective vulnerability in amyotrophic lateral sclerosis. Ann Neurol., 42, 200-207.

Williamson, T.L. & Cleveland, D.W. (1999) Slowing of axonal transport is a very early event in the toxicity of ALS-linked SOD1 mutants to motor neurons. Nat Neurosci., 2, 50-6.

Wong, N.K., He, B.P. & Strong, M.J. (2000) Characterization of neuronal intermediate filament protein expression in cervical spinal motor neurons in sporadic amyotrophic lateral sclerosis (ALS). J Neuropathol Exp Neurol., 59, 972-982.

Wong, P.C., Pardo, C.A., Borchelt, D.R., Lee, M.K., Copeland, N.G., Jenkins, N.A., Sisodia, S.S., Cleveland, D.W. & Price, D.L. (1995) An adverse property of a familial ALS-linked SOD1 mutation causes motor neuron disease characterized by vacuolar degeneration of mitochondria. Neuron, 14, 1105-1116.

Wood, J.D., Beaujeux, T.P. & Shaw, P.J. (2003) Protein aggregation in motor neurone disorders. Neuropathol Appl Neurobiol., 29, 529-545.

Wu, D.C., Re, D.B., Nagai, M., Ischiropoulos, H. & Przedborski, S. (2006) The inflammatory NADPH oxidase enzyme modulates motor neuron degeneration in amyotrophic lateral sclerosis mice. Proc Natl Acad Sci USA., 103, 12132-12137.

Xu, Z.Q., de Vente, J., Steinbusch, H., Grillner, S. & Hökfelt, T. (1998) The NO-cGMP pathway in the rat locus coeruleus: electrophysiological, immunohistochemical and in situ hybridization studies. Eur J Neurosci., 10, 3508-16.

Yim, M.B., Chock, P.B. & Stadtman, E.R. (1990) Copper, zinc superoxide dismutase catalyzes hydroxyl radical production from hydrogen peroxide. Proc Natl Acad Sci USA., 87, 5006-5010.

Yim, M.B., Chock, P.B. & Stadtman, E.R. (1993) Enzyme function of copper, zinc superoxide dismutase as a free radical generator. J Biol Chem., 268, 4099-4105.

Yim, M.B., Kang, J.H., Yim, H.S., Kwak, H.S., Chock, P.B. & Stadtman, E.R. (1996) A gain-of-function of an amyotrophic lateral sclerosis-associated Cu,Zn-superoxide dismutase mutant: an enhancement of free radical formation due to a decrease in Km for hydrogen peroxide. Proc Natl Acad Sci USA., 93, 5709-5714.

Zabel, U., Kleinschnitz, C., Oh, P., Nedvetsky, P., Smolenski, A., Muller, H., Kronich, P., Kugler, P., Walter, U., Schnitzer, J.E. & Schmidt, H.H. (2002) Calcium-dependent membrane association sensitizes soluble guanylyl cyclase to nitric oxide. Nat Cell Biol., 4, 307-311.

Zagami, C.J., Beart, P.M., Wallis, N., Nagley, P. & O'Shea, R.D. (2009) Oxidative and excitotoxic insults exert differential effects on spinal motoneurons and astrocytic glutamate transporters: Implications for the role of astrogliosis in amyotrophic lateral sclerosis. Glia, 57, 119-35.

Zhang, B., Tu, P., Abtahian, F., Trojanowski, J.Q. & Lee, V.M. (1997) Neurofilaments and orthograde transport are reduced in ventral root axons of transgenic mice that express human SOD1 with a G93A mutation. J Cell Biol., 139, 1307-1315.

Zhao, W., Xie, W., Le, W., Beers, D.R., He, Y., Henkel, J.S., Simpson, E.P., Yen, A.A., Xiao, Q. & Appel, S.H. (2004) Activated microglia initiate motor neuron injury by a nitric oxide and glutamate-mediated mechanism. J Neuropathol Exp Neurol., 63, 964-977.

Zheng, Y. & Shen, X. (2005) H2O2 directly activates inositol 1,4,5-trisphosphate receptors in endothelial cells. Redox Rep., 10, 29-36.

Zhong, G., Masino, M.A. & Harris-Warrick, M.R. (2007) Persistent sodium currents participate in fictive locomotion generation in neonatal mouse spinal cord. J Neurosci., 27, 4507-4518.

Zhu, S., Stavrovskaya, I.G., Drozda, M., Kim, B.Y., Ona, V., Li, M., Sarang, S., Liu, A.S., Hartley, D.M., Wu, D.C., Gullans, S., Ferrante, R.J., Przedborski, S., Kristal, B.S. & Friedlander, R.M. (2002) Minocycline inhibits cytochrome c release and delays progression of amyotrophic lateral sclerosis in mice. Nature, 417, 74-78.

Zimmerman, M.C., Oberley, L.W. & Flanagan, S.W. (2007) Mutant SOD1-induced neuronal toxicity is mediated by increased mitochondrial superoxide levels. J Neurochem., 102, 609-618.

van Zundert, B., Peuscher, M.H., Hynynen, M., Chen, A., Neve, R.L., Brown, R.H. Jr., Constantine-Paton, M. & Bellingham, M.C. (2008) Neonatal neuronal circuitry shows hyperexcitable disturbance in a mouse model of the adult-onset neurodegenerative disease amyotrophic lateral sclerosis. J Neurosci., 28, 10864-74.